# Understanding the cryosphere and climate evolution from Pliocene to Plio-Pleistocene transition

Ning Tan

université PARIS-SACLAY

NNT : 2018SACLV032

Thèse de doctorat

UNIVERSITÉ DE VERSAILLES ST-QUENTIN-EN-YVELINES

université PARIS-SACLAY

# Understanding the cryosphere and climate evolution from Pliocene to Plio-Pleistocene transition

Thèse de doctorat de l'Université Paris-Saclay
préparée à
**l'Université de Versailles Saint-Quentin-en-Yvelines**

École doctorale n°129
Sciences de l'environnement d'Ile-de-France (SEIF)
Spécialité de doctorat:
**Météorologie, océanographie, physique de l'environnement**

Thèse présentée et soutenue à Saclay, le 25/4/2018, par

**Ning Tan**

Composition du Jury :

| | |
|---|---|
| Philippe Bousquet<br>Directeur de Recherche, (LSCE/CEA, France) | Président |
| Alan Haywood<br>Professeur, (University of Leeds, UK) | Rapporteur |
| Florence Colleoni<br>Chargé de Recherche, (CMCC, Italie) | Rapporteur |
| Zhongshi Zhang<br>Professeur, (Uni Research, Norvège) | Examinateur |
| Laurent Li<br>Directeur de Recherche, (LMD/IPSL, France) | Examinateur |
| Clara Bolton<br>Chargé de Recherche, (Cerege, France) | Examinateur |
| Gilles Ramstein<br>Directeur de Recherche, (LSCE/CEA, France) | Directeur de thèse |
| Christophe Dumas<br>Chargé de Recherche, (LSCE/CEA, France) | Co-Directeur de thèse |

université PARIS-SACLAY
ÉCOLE DOCTORALE
Sciences de l'environnement d'île-de-France (SEIF)

**Titre : Comprendre l'évolution de la cryosphère et du climat du Pliocène à la transition Plio-Pléistocène**

**Mots clés** : Modélisation du climat, MIS M2 glaciation, La période chaude du Plaisancien moyen, La transition du Plio-Pléistocène, les changements de détroits, les calottes groenlandaises

**Résumé :** Cette thèse est consacrée à l'étude de l'interaction cryosphère-climat depuis le milieu du Pliocène jusqu'au quaternaire pendant l'installation pérenne de la calotte groenlandaise. Nous étudions d'abord les causes du développement et de la disparition de l'importante mais courte glaciation qui a eu lieu pendant le stade isotopique marin M2 (MIS M2 3.264-¬3.312 Ma). Ensuite, dans le cadre du programme international sur la modélisation du Pliocène (PLIOMIP2), nous étudions le climat de la période chaude du Plaisancien moyen (MPWP, 3.3-3.0Ma). Enfin, la troisième période étudiée est la transition Plio-Pléistocène transition (PPT, 3.0-2.5Ma), que nous avons étudiée grâce à un couplage asynchrone entre un modèle de climat et un modèle de calotte. A travers ces différentes périodes, nous avons amélioré la connaissance des relations entre pCO2, tectonique et climat pendant la transition d'un monde chaud et riche en CO2 vers le monde bien plus froid et à faible pCO2 des glaciations quaternaires. Ce résultat montre l'importance de mieux comprendre les relations entre dynamique océanique, pCO2 et climat.

**Title : Understanding the cryosphere and climate evolution from Pliocene to Plio-Pleistocene transition**

**Keywords :** Climate modeling, MIS M2 glaciation, Mid Piacenzian warm period, Plio-Pleistocene transition, Seaway changes, Greenland ice sheet

**Abstract :** This thesis is devoted to understanding the interaction between cryosphere and climate from the mid Pliocene to the early Quaternary during the onset of Northern Hemisphere Glaciation (NHG).
Firstly, we investigate the causes for the development and decay of the large but short living glaciation that occurred during Marine Isotope Stage 2 (M2, 3.264-¬3.312 Ma); Secondly, in the framework of the international Pliocene Model Intercomparison Project (PLIOMIP2), we study the climate of Mid-Piacenzian Warm Period (MPWP, 3.3-3.0Ma). Thirdly, we explore the Plio-Pleistocene Transition (PPT, 3.0-2.5Ma) with an appropriate asynchronously coupled climate cryosphere model. Through these different periods, we provide a better understanding of the relationship between pCO2, tectonics and climat during the transition from a warm and high-CO2 world to the cold and low-CO2 Quaternary glaciations. This work also points out the necessity to further study the link between ocean dynamics, carbon cycle and climate.

**Université Paris-Saclay**
Espace Technologique / Immeuble Discovery
Route de l'Orme aux Merisiers RD 128 / 91190 Saint-Aubin, France

# Acknowledgments

Many people were involved in making this thesis possible. First of all I owe my deepest gratitude to my supervisor Mr Gilles Ramstein who suggested this topic to me and guided me into the world of paleoclimate. Without his continuous optimism concerning this work, enthusiasm, encouragement and support, this study would hardly have been completed. I also express my warmest gratitude to my other supervisor Mr Christophe Dumas, who helped me a lot to resolve the research problems during my thesis study and his guidance in experiment design and results analysis have been essential for my work.

I am deeply grateful to my colleagues Dr. Camille Contoux and Dr. Jean-Baptiste Ladant. Their suggestions and technical supports are really important for my thesis study. I also need to express my gratitude to Mr Olivier Marti, Mr Pierre Sepulchre and Ms Masa Kageyama for making it possible to carry out this work with IPSL model in LSCE laboratory. Many thanks to Ms Nada Caud and Ms Sarah Amram for their supports in the administrative process concerning my thesis study. I thank all my colleagues at LSCE who helped me in my work and adaptations in a new country.

I want to express my gratitude to all my thesis committee members for their support in my thesis defense. Thanks in particular to Prof. Alan Haywood, Prof. Florence Colleoni and Prof. Zhongshi Zhang for their constructive suggestions and precise revisions for my thesis work.

I need also to thank the OCCP project and all colleagues involved in this project in particular Prof.Stijn De Schepper, Prof.Eystein Jansen, Prof.Bjørg Risebrobakken, Dr. Paul Bachem and Prof. Kerim Nisancioglu for their help on thesis work.

The thesis could not be finished without the immense love of my family: my husband Xiangjun, my daughter Anne and my parents as well as my parents in law. Their supports are really important for me when I met problems in my study.

Three years were not only about research, but also about friendship. I'd like to thank

my friends who made this journey of great fun. Thanks in particular to Svetalana, Xin, Yong, Yating and to all other Chinese friends.

Finally, I honor LSCE and its foundation, which supported my entire Ph.D. study. The knowledge, friends, happiness, frustration and everything that you brought me shaped me to be me.

Ning TAN,

Laboratoire des Sciences du Climat et de l'Environnement,

Gif-sur-Yvette, March 2018

# Contents

# Summary

This thesis is devoted to understanding the interaction between cryosphere and climate from the mid Pliocene to the early Quaternary during the onset of Northern Hemisphere Glaciation (NHG). Firstly, we investigate the causes for the development and decay of the large but short living glaciation that occurred during Marine Isotope Stage 2 (M2, 3.264-¬3.312 Ma); Secondly, in the framework of the international Pliocene Model Intercomparison Project (PLIOMIP2), we study the climate of Mid-Piacenzian Warm Period (MPWP, 3.3-3.0Ma). Thirdly, we explore the Plio-Pleistocene Transition (PPT, 3.0-2.5Ma) with an appropriate asynchronously coupled climate cryosphere model. Through these different periods, we provide a better understanding of the relationship between pCO2, tectonics and climat during the transition from a warm and high-CO2 world to the cold and low-CO2 Quaternary glaciations.

Unlike the late Quaternary glaciations, the MIS M2 glaciation, corresponding to a 20-60m sea level drop only lasted 50 Kyrs and occurred under uncertain CO2 concentration (pCO2) (220–390 ppmv). The mechanisms causing the onset and termination of the M2 glaciation remain enigmatic, but a recent geological hypothesis suggests that the re-opening and closing of the shallow Central American Seaway (CAS) might have played a key role. However, through a series of modeling simulations, we show that re-opening of the shallow CAS cannot explain by itself the onset of the M2 glaciation. However, the large lowering of pCO2 as well as the internal feedback of vegetation and land ice are shown to be a major component in the M2 glaciation process. Finally, we demonstrate not only that the opening of a shallow CAS does not explain fully MIS-M2 glaciation but also that its closing plays a negligible role for the decay of MIS M2 ice sheet.

The MPWP following MIS M2 glaciation is well documented and simulated within PLIOMIP framework. Indeed its warming climate associated with similar-to-present pCO2 makes this period very appealing.This part of the thesis therefore contributes to the PLIOMIP

phase 2. We simulate this warm period with new boundary conditions. When comparing to the PlioMIP phase 1 (PlioMIP1) simulation with an identical model, our PlioMIP2 simulations show warmer conditions in high latitudes ocean and continent, and more precipitation in the tropics and monsoon regions. These differences mainly result from the new boundary conditions with changes in the high latitude seaways and land topography, which enables the ocean to transport more pole-ward energy and affect the local water vapor transport, respectively.

The Plio-Pleistocene transition (3.0-2.5 Ma) is an important tipping point in the Earth climate associated with perennial ice sheets in the Northern high latitudes. It is well known that the NHG establishment around 2.7Ma is associated with the long-term decreasing trends of pCO2 and sea surface temperatures. The Greenland ice sheet (GrIS) evolution during this transition is difficult to reconstruct due to the paucity of direct geological data and its light delta O18 signal in benthic foraminifera. Using a new asynchronously coupled climate cryosphere model, we apply the tri-interpolation method to simulate Greenland evolution during PPT. Our results show that lower than 280 ppmv pCO2 values are necessary for the inception of full GrIS. Moreover, pCO2 has to evolve in a narrow range to overcome the increase of insolation occurring after 2.7 Ma and to prevent GrIS melting during PPT. When confronting all simulated GrIS evolutions to the IRD records, we find that the most recently reconstructed pCO2 records can provide a better fit with the IRD data.

In summary, this thesis brings new constraints and understanding on the cryosphere and climate interaction from mid-Pliocene to the Quaternary glaciation. This result points out the necessity to further study the link between ocean dynamics, carbon cycle and climate.

# Résumé étendu

Cette thèse est consacrée à l'étude de l'interaction cryosphere-climat depuis le milieu du Pliocène jusqu'au quaternaire pendant l'installation pérenne de la calotte groenlandaise. Nous étudions d'abord les causes du développement et de la disparition de l'importante mais courte glaciation le stade isotopique marin M2 (MIS M2, 3.264-¬3.312 Ma). Ensuite, dans le cadre du programme international sur la modélisation du Pliocène (PLIOMIP2), nous étudions le climat de la période chaude du Plaisencien moyen (MPWP, 3.3-3.0Ma). Enfin, la troisième période étudiée est la transition du Plio-Pleistocèce (PPT, 3.0-2.5Ma), que nous avons étudiée grâce à un couplage asynchrone entre un modèle de climat et un modèle de calotte. A travers ces différentes périodes, nous avons amélioré la connaissance des relations entre pCO2, tectonique et climat pendant la transition d'un monde chaud et riche en CO2 vers le monde bien plus froid et à faible pCO2 des glaciations quaternaires.

Contrairement aux glaciations quaternaires, la glaciation du MIS-M2 ne correspond qu'à une baisse du niveau marin évaluée de 20 à 60 m et ne dure que 50 ka et se produit dans un contexte incertain quant à la pCO2 (220-390 ppmv). Les mécanismes produisant le développement et la fin de la glaciation du MIS M2 restent inexpliqués, mais une hypothèse géologique récente suggère que la réouverture de l'isthme de Panama peut avoir joué un rôle décisif. Cependant, grâce à une série de simulations numériques, nous avons montré que la réouverture même très peu profonde de la circulation dans l'isthme ne pouvait expliquer à elle seule le développement de la glaciation MIS-M2. Par contre, la baisse marquée du CO2 et les rétroactions liées à la végétation et au couvert neigeux sont des composantes majeures de la glaciation. Finalement, nous avons montré que d'une part l'ouverture de l'isthme n'expliquait pas la glaciation, et que d'autre part, sa fermeture joue un rôle négligeable dans la déglaciation.

La période (MPWP) est associé à une pCO2 similaire à l'actuelle, rend cette période

particulièrement intéressante. Nous avons simulé cette période avec de nouvelles conditions aux limites du PlioMIP phase 2. Par rapport aux simulations de la phase 1 (PLIOMIP1) avec le même modèle, nous simulons des températures plus chaudes aux hautes latitudes et des précipitations plus importantes dans les tropiques et les régions de mousson. Ces différences tiennent essentiellement aux nouvelles conditions aux limites, associées à des modifications dans les détroits et la paléogéographie, qui permettent à la circulation océanique de transférer plus d'énergie vers les pôles et d'affecter le cycle hydrologique à l'échelle régionale.

La PPT est une période charnière dans l'histoire de la Terre, correspondant à l'implantation d'une calotte pérenne aux hautes latitudes de l'hémisphère Nord. L'évolution de la calotte Groenlandaise (GrIS) pendant cette transition est difficile à reconstruire à cause de la pauvreté des données géologiques et au signal faible en O18 des formainifèeres benthiques. En utilisant un modèle couplé asynchrone climat-cryosphère, nous avons utilisé une méthode d'interpolation trilinéaire pour simuler l'évolution de la calotte groenlandaise pendant la PPT. Nos résultats montrent qu'il est nécessaire de passer sous une valeur seuil de 280 ppmv pour développer la GRIS. De plus, la pCO2 doit rester dans une étroite fenêtre pour compenser l'augmentation de l'insolation après 2.7 Ma et éviter la fonte du GRIS pendant la transition. Lorsqu'on confronte nos résultats de simulation aux données d'IRD, nous constatons que la reconstruction la plus récente de pCO2 est la plus cohérente.

En résumé, cette thèse apporte des contraintes nouvelles et de nouveaux éclairages sur les relations climat-cryosphère pendant la transition du Plio-Pleistocene. Ce résultat montre l'importance de mieux comprendre les relations entre dynamique océanique, pCO2 et climat.

# Chapter 1

# General introduction

## Contents

## 1.1 The climate evolution during late Pliocene

During the last 5 million years, sporadic Greenland glaciation occurred, but the real tipping point that will establish a perennial Greenland ice sheet only occurred 2.7 Ma ago (e.g., Maslin et al., 1998). Since 34 Ma, only Antarctic ice sheet developed and maintained through large dynamic evolution during Oligocene and Miocene (DeConto and Pollard, 2003; Ladant et al., 2014)(Colleoni et al., in prep). It is therefore at geological time scale a recent and infrequent context corresponding to ice sheets on both high latitude hemispheres. These evolution of cryosphere and climate took place during major paleogeographical changes (plate tectonics, orogenesis, seaways closing and opening) and are associated with a major tendency to atmospheric $CO_2$ decrease and global cooling (Pagani et al., 2005; Zachos et al., 2001). In this study, we focus on the cryosphere and climate interaction from Pliocene to the transition with Quaternary using state-of-the-art general circulation models for climate and ice sheet models for cryosphere simulations. Our major aim is to understand how during this period the climate and ice sheets evolved in a period which is tectonically close to present day and with similar $CO_2$ content. Late Pliocene (3.6 - 2.58 Ma) is indeed the most recent period of Neogene (Figure1.1). The average temperature of this period is studied to be higher than present level (Haywood and Valdes, 2004). The reconstructed $CO_2$ concentrations varies from 200ppmv to 450ppmv and with large uncertainties. For this long interval, the earth system presented relatively stable and warm conditions from 3.6 Ma - 3.0 Ma but also included several cooling perturbations. Following this period, the earth system entered to a shift stage highlighted by an increasing trend of positive benthic foraminiferal $\delta^{18}O$ (Lisiecki and Raymo, 2005), decreasing trends of $CO_2$ (e.g. Bartoli et al., 2011; Martínez-Botí et al., 2015; Seki et al., 2010) as well as sea surface temperatures (e.g. Lawrence et al., 2009). The large intensification of ice sheet in both Hemisphere likely took place around 2.7 Ma indicated by the appearance of remarkable IRD ((Flesche Kleiven et al., 2002, and references therein) and large sea-level estimate (e.g. Miller et al., 2012) (Figure1.2). The earth climate then stepped into a cyclic glacial-interglacial state with a 41-kyrs periodicity. Based on the numerous efforts of proxy data and modeling tools, the climate evolution of late Pliocene provides us a good history to study how the climate system function under both warm and cold conditions and also helps to understand the climate sensitivity to a near-present $pCO_2$ in a long-term period. The most representative intervals of this period are selected in this

thesis work and will be introduced in the subsection as following.

### 1.1.1 Mid-Piacenzian warm period

The mid-Piacenzian warm period (MPWP or mid-Pliocene warm period) represents an interval of warm and relatively stable climate between 3.264 and 3.025Ma (Dowsett et al., 2009; Haywood et al., 2010). During this warm phase, the $pCO_2$ records are estimated 50-150ppmv higher than pre-industrial level (280ppmv), the global annual mean temperature may have increased by more than 3 °C (e.g. Haywood and Valdes, 2004). The global extent of arid deserts decreased, and forests replaced tundra in the Northern Hemisphere high latitudes (Salzmann et al., 2008).The East Asian Summer Monsoon, as well as other monsoon systems, may have been enhanced (Zhang et al., 2013). Ice sheet of both hemispheres may have been largely retreated indicated by increased negative bethic foraminiferal $\delta^{18}O$ (Naish and Wilson, 2009) and other modeling studies(Lunt et al., 2008)(Hill, 2009)(Pollard and DeConto, 2009)(Dolan et al., 2015a). The sea-level is estimated to have been 22(+-10m) higher than modern(Miller et al., 2012). Sea surface temperatures (SSTs) were warmer than present level, especially in the higher latitudes and upwelling zones (Dekens et al., 2007; Dowsett et al., 2012). Accordingly,sea ice cover in the high latitudes is studied to be largely decreased, especially during warm seasons (Howell et al., 2016). During this period, the meridional SST gradients is largely decreased as the amplified warming in the high latitudes. The zonal SST gradients is much weaker than present day as the ocean warm pool extended over most of the tropics (Brierley et al., 2009). Thanks to the abundance of proxy data, the MPWP has become a focus for data/model comparisons that attempt to analyze the ability of climate models to reproduce a warm climate state in earth history.Furthermore, the MPWP has been proposed as an important interval to assess the sensitivity of climate to near-current concentrations of carbon dioxide ($CO_2$) in the long term (hundreds to thousands of years;(Lunt et al., 2010)). The Pliocene Model Intercomparison Project (PlioMIP) is a co-ordinated international climate modelling initiative to study and understand climate and environments of the Late Pliocene (MPWP), and their potential relevance in the context of future climate change. The first phase of PlioMIP (2008-2014) contributed a lot on modeling the climatic features of the MPWP by several groups of GCMs. However, nearly all models' results failed to simulate the amplified warming in the high latitudes. Now the on-going

PlioMIP second phase provides a new boundary conditions and focuses on a specific interglacial period (MIS KM5c, 3.205Ma) to improve the data-model comparison.

### 1.1.2 Glacial event of MIS M2

Just before the mid Piacenzian warm period, there was an interval with large excursion of $\delta^{18}O$ from benthic foraminifera (Lisiecki and Raymo, 2005) which indicating a large cooling state of the earth. This cooling interval is named as Marine isotope stage M2 (MIS M2). MIS M2 is thought to be a glacial comparable period associated with a huge but uncertain sea-level records of 20-60 m below the present level ((Naish and Wilson, 2009); 15 (+-5m); (Miller et al., 2012); 40 (+-10 m);(Dwyer and Chandler, 2008); 65m (+-15–25 m ). Direct and indirect proxy data indicate that the expansion of ice sheet during MIS M2 reside in Greenland and Svalbard/Barents Sea (Flesche Kleiven et al., 2002)(Knies et al., 2009)(Moran et al., 2006)(Sarnthein et al., 2009a) ,Iceland(Áslaug Geirsdóttir, 2011), Alaska, Canadian Rocky Mountain (Barendregt and Duk-Rodkin, 2011), and Antarctic region (Naish and Wilson, 2009)(Passchier, 2011). Atmospheric $CO_2$ values, varying among different reconstructed methods, were estimated to be within 220-390 ppmv. Each record has large uncertainty of 50 ppmv (Pagani et al., 2010)(Seki et al., 2010)(Bartoli et al., 2011)(Martínez-Botí et al., 2015). Unlike the well-known MPWP (mid-Pliocene warm period: 3.29 Ma - 2.97 Ma), M2 event is poorly known and remains an enigma in terms of possible scenarios for glaciation. The situation of M2 is relatively different from the Quaternary glacial periods in the following aspects: M2 took place during an interval of long warm stable periods; Atmospheric $CO_2$ concentration during M2 was relatively higher than the Quaternary glaciation period. Besides, reconstructed sea surface temperature in North Atlantic shows a relatively warm condition during M2. All these evidences suggest that the M2 event does not occur in typical glacial climate conditions. To explain this anomalous glaciation, geological forcing of brief shallow Panama reopening has been proposed by a recent study (De Schepper et al., 2013). By studying geochemical and palynological marine records from the Caribbean to the North Atlantic, they observed a decline in the strength of the North Atlantic current simultaneously to the existence of a Pacific-to-Atlantic through-flow via Central American Seaway (CAS)during this period. Upon that, this cold and fresh through-flow modulated the oceanic circulation and the related heat transport which help to favor the large ice sheet formation. Inversely, the

built-up of the large extent ice sheet could abase the global sea level and then close the shallow opening CAS.The closure of the CAS then brought about an opposite impact on the oceanic circulation and heat transport which help to melt the ice sheet then provide a way-out for M2 glaciation. However, this beautiful assumption has not yet been tested and the dominant factor for M2 glaciation still need to be surveyed.

### 1.1.3 Plio-Pleistocene Transition

After the MIS M2 glaciation, the earth kept in warming and stable conditions until the beginning of the major climate shift during the Pliocene Pleistocene transition from 3.2-3.0 Ma to 2.5 Ma. During this transition, the sea surface temperature(e.g. Lawrence et al., 2009) and the reconstructed $CO_2$ concentrations represent a slowly declining trend.Inversely, the ice sheet volume in both hemisphere progressively increased and got large expansion around 2.7 Main which can be highlighted by the benthic foraminiferal $\delta^{18}O$ (Lisiecki and Raymo, 2005)(Maslin et al., 1998)(Mudelsee and Raymo, 2005) and marine sedimentary records of ice rafted debris (IRDs) ((Bailey et al., 2013) and reference therein).This transition interval represent an important history of earth climatic system. A lot of studies have been contributed to seek the determinate factors and to understand the underlined mechanisms for the intensification of NHG during this period. These include studies linking to the tectonic events which help to modulate both atmospheric and oceanic circulation, the most popluar ideas focus on the uplift and erosion of the Tibetan-Himalayan plateau (Ruddiman et al., 1988)(Raymo, 1991), the deepening of the Bering Straits and/or the Greenland Scotland ridge (Wright and Miller, 1996), the restriction of the Indonesian seaway (Cane and Molnar, 2001), and the emergence of the Panama Isthmus (e.g. Haug and Tiedemann, 1998; KEIGWIN, 1982). However,these tectonic factors are proved by the modelling studies to be helpful but cannot be the major trigger for the large intensification of NHG (Lunt et al., 2008)(Brierley and Fedorov, 2016).Moreover, the timings for the tectonic phases have large uncertainties and are difficult to be constrained. Apart from the tectonic ideas, the role of decreasing $CO_2$ is the recently most approval factor. Lunt et al. (2008) highlighted the important role of large lowering of $pCO_2$ for the Greenland glaciation during the late Pliocene. However,Contoux et al. (2015a) based on their recent study prove that the Greenland glaciation might happen with a cumulative process during a long-term period rather than a rapid build-up. The evolution of Greenland ice sheet

is still unknown due to the paucity of geological data and its light signal in the estimated global sea-level changes. A transient simulation for the Greenland ice sheet evolution may provide an optimal way to resolve this puzzle.

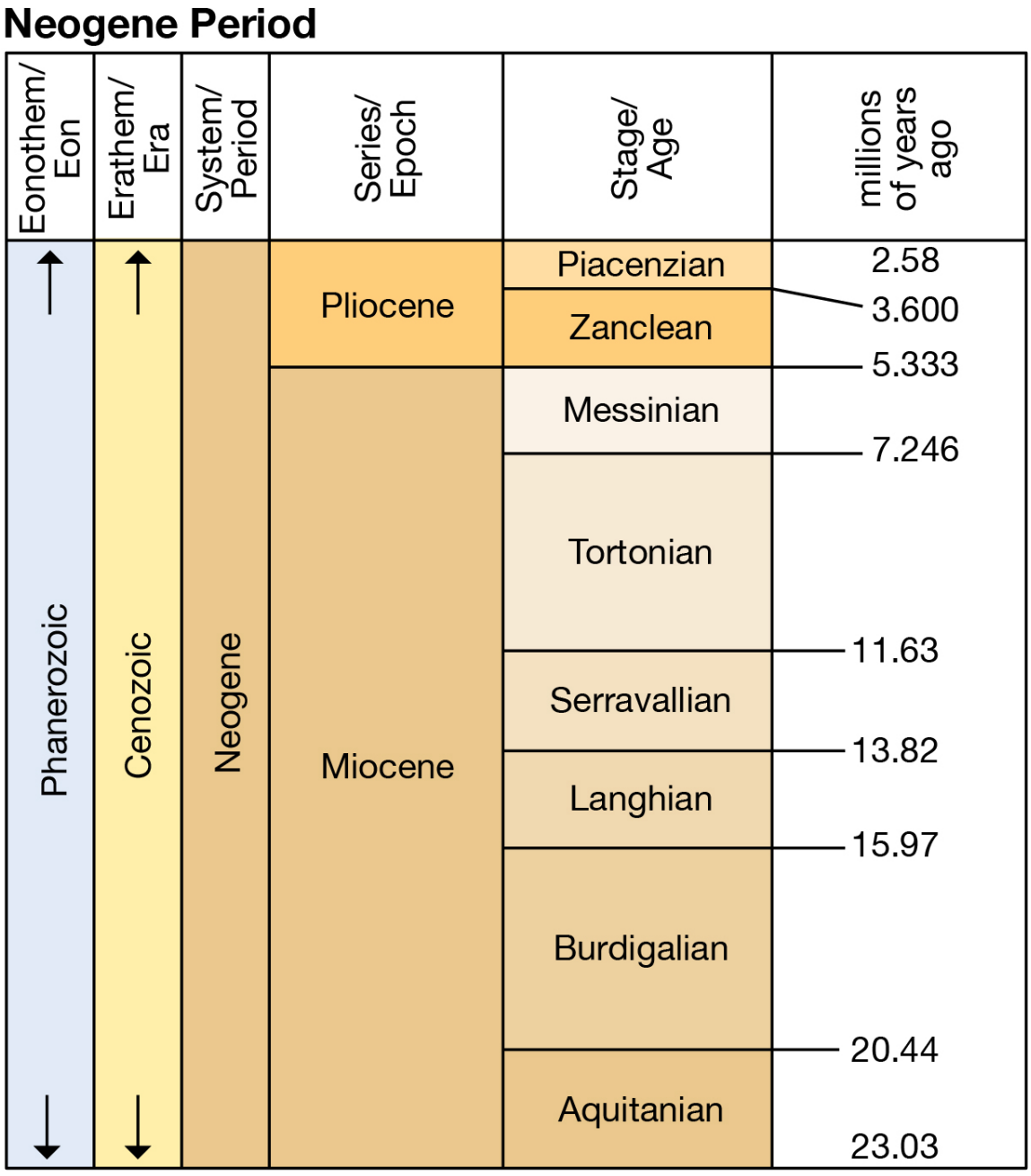


Figure 1.1 – The Neogene Period and its subdivisions.Figure after from 2015 International Commission on Stratigraphy (ICS)

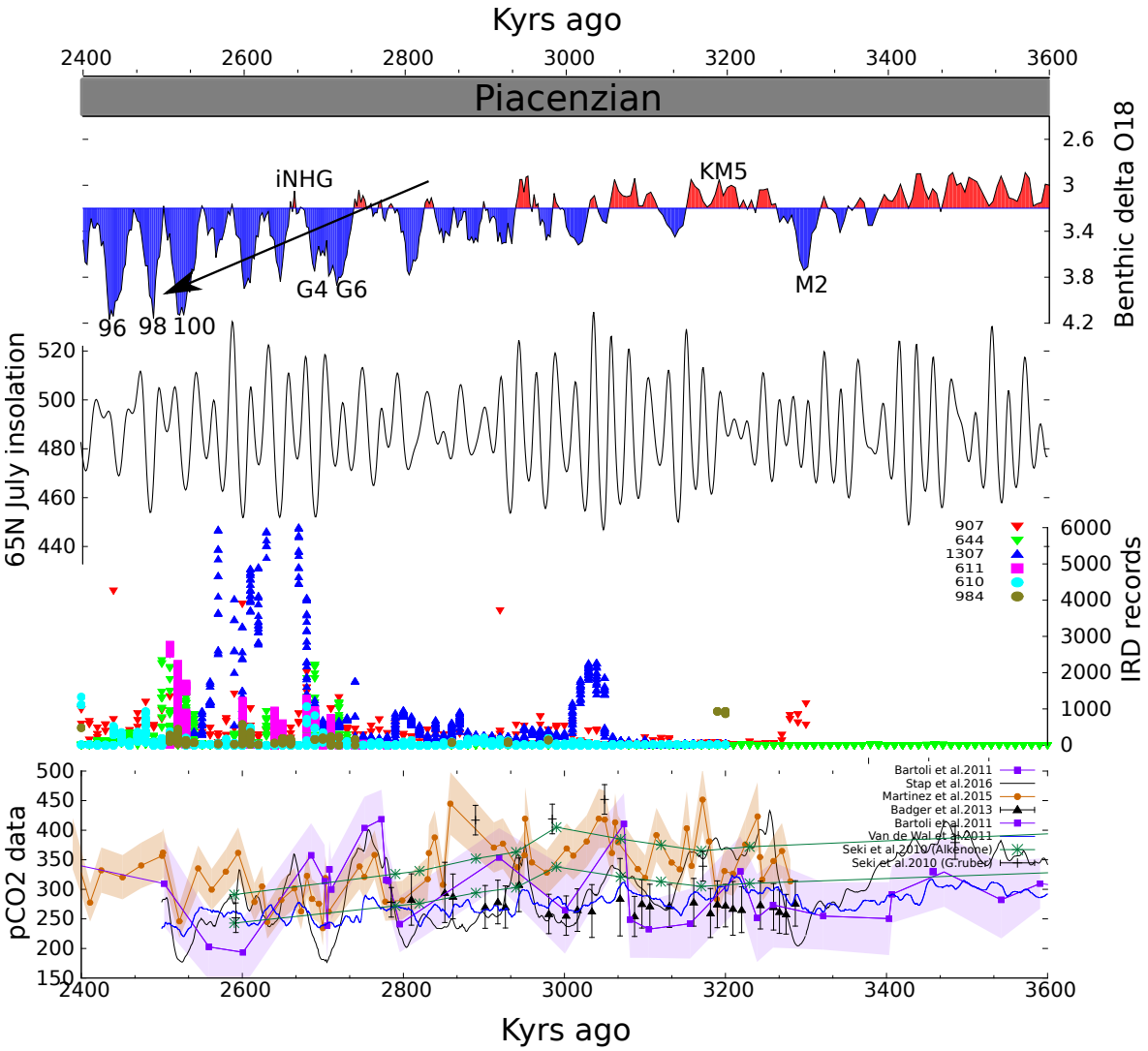


Figure 1.2 – A synthesis of Late Pliocene evolution. (a) LR04 benthic isotope stack (Lisiecki and Raymo, 2005); (b) July insolation at 65N (Laskar et al., 2004); (c) Ice rafted detritus (IRD) records from different studies (DSDP Site 610 (Flesche Kleiven et al., 2002), DSDP Site 611 (Bailey et al., 2013), ODP Site 644 (Jansen and Sjøholm, 1991), ODP Site 907 (Jansen et al., 2000), ODP Site 984 (Bartoli et al., 2011) and site U1307 (Sarnthein et al., 2009a); (d) Reconstructed $pCO_2$ records and model inverse data from different studies (Seki et al., 2010)(Bartoli et al., 2011) (Badger et al., 2013)(Martínez-Botí et al., 2015)(Van De Wal et al., 2011)(Stap et al., 2017)

## 1.2 Climate forcings and climate modeling

### 1.2.1 Climate forcings

The climate system is an interactive system consisting of five major components: the atmosphere, the hydrosphere, the cryosphere, the land surface and the biosphere (IPCC). This system is driven and affected by various forcing mechanisms which can be categorized into natural and anthropogenic factors. The natural forcings include the sun's energy output, change of orbital parameters and large volcanic eruptions which thrown great number of gases and dust particles in the atmosphere. Forcings due to human activities contains increased greenhouse gas concentrations produced by fossil fuel burning, aerosols,and changes in land use surface properties among other things. The imbalance of the incoming and outcoming energy at the top of the atmosphere, defined as "radiative forcing" by IPCC report, which is influenced by changes in individual forcing factors, drive directly the climate change.

In this study, two major forcing factors : orbital parameters and $CO_2$ concentrations are presented in the Figure1.2b,d. The orbital parameters are calculated based on the model of Laskar et al. (2004), which is relatively accurate. However, the $CO_2$ concentrations reconstructed based on different proxy data during the late Pliocene are highly uncertain. More studies are still urgently needed to constrain these uncertainties to provide more reliable deep paleoclimate modeling.

### 1.2.2 Climate modeling

It is largely accepted that the numerical modeling provide us the most effective way to represent paleoclimate and to predict the climate changes in the future. The key conception of any climate model is to represent processes that affect climate.A schematic of the processes that affected the climate system is shown in Figure1.3.The differences among climate models are generally from the extent of simplification in the processes, the resolution in time and space.Earth system models are currently the most comprehensive tools available for simulating past and future response of the climate system to external forcing, in which biogeochemical feedbacks play an important role.Atmosphere–Ocean General Circulation Models (AOGCMs) are the standard climate models in which the primary function is to understand the dynamics of the physical components of the climate

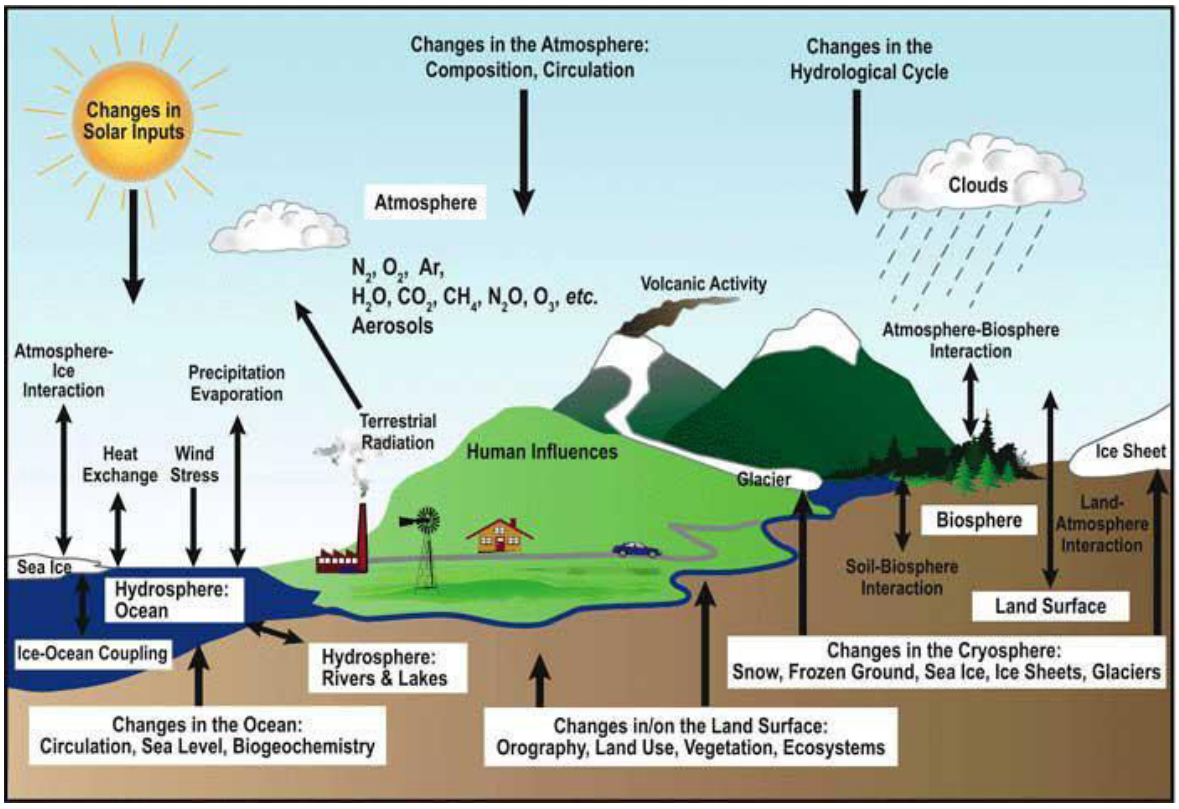


Figure 1.3 – Shematic for the processes that affected the climate in the earth system model.Figure modified from (Treut et al., 2007)

system (atmosphere, ocean, land and sea ice), and for making projections based on future greenhouse gas (GHG) and aerosol forcing. These models continue to be extensively used, and in particular are run (sometimes at higher resolution) for seasonal to decadal climate prediction applications in which biogeochemical feedbacks are not critical (Source: WG1AR5,Chapter09). In this study, we applied AOGCM of IPSL to accomplish all our numerical experiments. The details of this model will be introduced in Chapter 2

However, most existed climate models do not include the cryosphere component of climate system, since large ice sheets and caps require thousands of years to reach equilibrium state. Ice sheet models are generally designed to represent the dynamical and physical processes of ice sheets and ice shelves with different simplified and parameterized schemes. Although the ice sheet models have different complexities ,they are generally able to simulate the evolution of the ice over periods on an order of hundred thousand or a million year. However, due to the different timescale of functions, it is difficult to achieve a long-term coupled simulation GCM-ISM based on present computational technology. In my thesis, I used GRISLI model (Ritz et al., 2001) to do all the ice sheet modeling work. Moreover, as a part of my thesis work, I introduce a new methodology to

realize a long-term climate transient simulation for Greenland ice sheet during the Plio-Pleistocene transition, which will be introduced in Chapter 5 of this thesis.

## 1.3 Objectives and scientific issues in the thesis

As we know, the present projection of future climate are based on the understanding of the short-term impacts of the variations of the climate forcing in near-present era on climate, which is limited to provide a comprehensive understanding of the climate evolution. Therefore, paleoclimate provides a good means for us to better understand the mechanisms of on-going climate changes. This is why more and more climate models and modelers join in "paleoclimate modeling intercomparison programs (PMIP)", which aims to understand the mechanisms of long-term climate changes, to identify the different climatic factors that shape our environment and evaluate the capability of state-of-the-art models to reproduce different climates. The most recent phase of PMIP contains several specific paleoclimate periods like Mid-Holocene ( 6Ka), Last Glacial Maximum ( 21Ka), Last Millennium,Last interglacial (128Ka) and mid Pliocene warm Period ( 3.3-3.0Ma). Among these paleo histories, mid Pliocene warm period is the most suitable interval to study the climate warming under a present-like $pCO_2$ and insolation as introduced in the section 1.1.1. My thesis project started initially in the framework of the PlioMIP and now is already in the second phase as "PlioMIP phase 2". Thus one of my thesis goals is to complete core experiments required by PlioMIP phase 2 and to evaluate the ability of IPSL AOGCM in producing warming climate through the comparison with data and other models' outputs.

In addition to the study of this warm period of Late Pliocene, we also focus on the change of climate variability along Late Pliocene like the abrupt glacial event MIS M2 prior to MPWP; the progressively intensification of northern hemisphere glaciation during the Plio-Pleistocene.These intervals are of great interest for us to study the mechanisms of the climate change during cooling phases being different from the glaical-interglacial cycles of the late Pleistocene and to understand the interactions among atmospheric , oceanic and cryospheric and vegetation system during a long-term transition. Centered on these targets, three different parts of study have been carried out and will be introduced in this thesis with the order as follows:

1. The mechanism to explain the occurrence and termination of MIS M2 glacial event.
2. The Greenland ice sheet evolution during the Plio-Pleistocene
3. The Earth climatic features under mid-Piacezian warm Period.

Through these three objectives, we aims to address the major scientific questions as following:

1. What could have caused the MIS M2 glacial event and what was it like ?
2. What is the importance of palaeogeography in model simulations of global and regional climate change?
3. How was the Greenland ice sheet evolution during the PPT and how critical is atmospheric $CO_2$ concentration pathways to the Greenland ice sheet inception ?

# Chapter 2

# Description of the climate model used in this study

## Contents

## 2.1 Atmosphere-Ocean Global Circulation Model (AOGCM)

A very important issue in this thesis is that we perform our simulations with the same models that are currently used for Quaternary PMIP (6ka, 21ka) (Braconnot et al., 2007; Kageyama et al., 2013) and also for CMIP (Dufresne et al., 2013) future climate scenarios, as described in IPCC AR5. Therefore, from the modeling point of view, we may consider that our study is an important sensitivity test to understand how standard IPSL models respond to a slightly different tectonics context. In contrast, a major difference with modeling the last glacial-interglacial cycles of the Quaternary or future climates is the uncertainty on atmospheric CO2 reconstructions. Indeed, Antarctica ice sheet records describe very well the greenhouse gases content for the last 800 ka (Petit et al., 1999)(EPICA community members, 2004). For Pliocene periods, only indirect proxy reconstructions are available. Although they depict similar tendencies, the absolute values of reconstructed pC02 are different. Moreover, even if plate tectonics did not change drastically during these last three million years, recent orogenesis and seaways closing or opening (central American seaway, Indonesian through-flow) may impact atmospheric and oceanic circulation. These changes will drive climate and cryosphere evolutions. In the next three chapters, we will focus on three key periods of this evolution in different contexts.

To accomplish the modeling work, we employed two versions of Institut Pierre-Simon Laplace (IPSL) coupled atmosphere-ocean general circulation model (AOGCM):IPSL-CM5A and IPSL-CM5A2.1. IPSL-CM5A is a high resolution coupling model which has been applied in CMIP5 for historical and future simulations (Dufresne et al., 2013) as well as for Quaternary and Pliocene paleoclimatic studies (Contoux et al., 2012; Kageyama et al., 2013). The version of IPSL-CM5A2.1 is designed based on IPSL-CM5A with mainly tunning the cloud radiative effect to avoid the global cold bias in the model (Sepulchre et al.,2018 In prep). Moreover, the computational performance of IPSL-CM5A2.1 is improved by about 6 times ( 50 yrs/d) than that of IPSL-CM5A. We will shortly present the information of each components of the AOGCM as following.Figure2.1 show a shematic of IPSL earth system model. In our study, the Bio-geochemistry processes are not activated. More details can be referred (Dufresne et al., 2013).

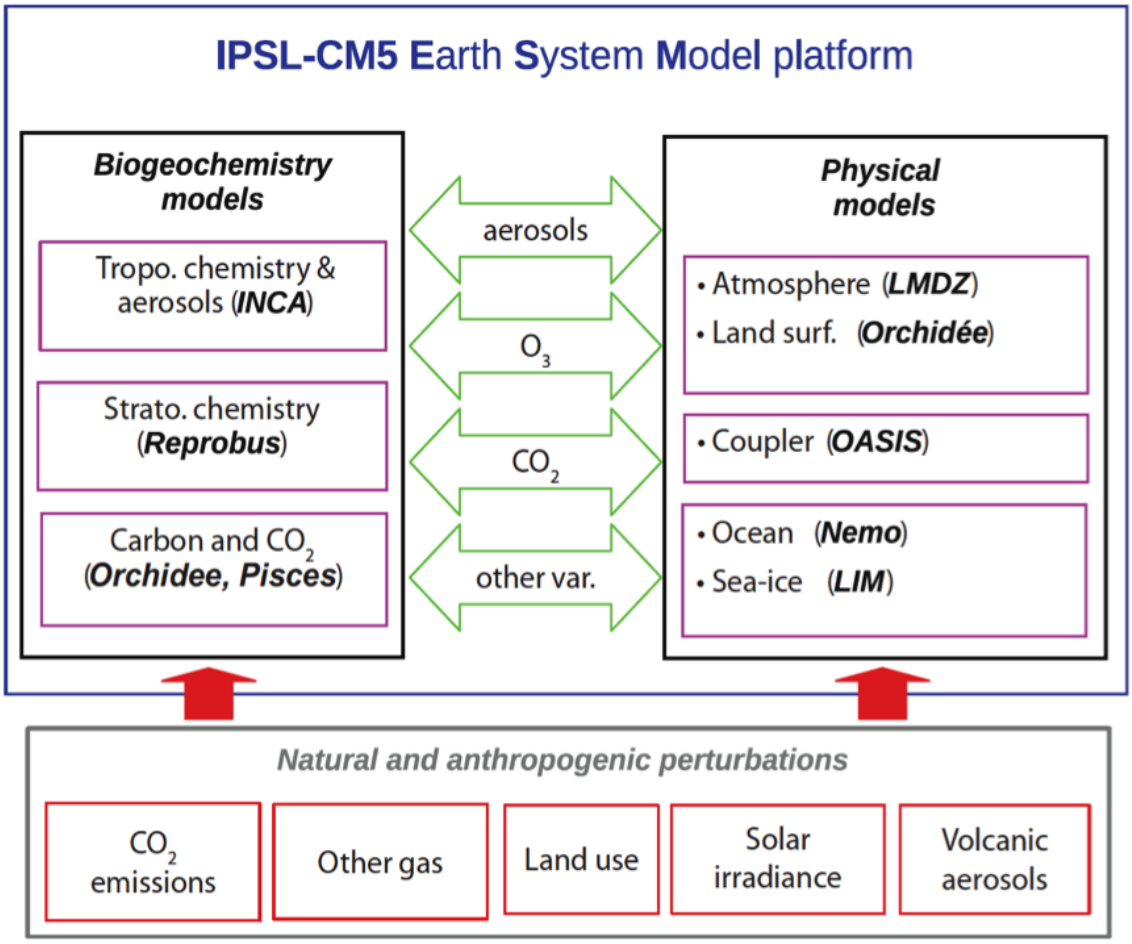


Figure 2.1 – Shematic for IPSL-CM5 earth system model.Figure after (Dufresne et al., 2013)

### 2.1.1 Atmosphere and Land

The atmosphere component of IPSL-CM5A is LMDZ model(Hourdin et al., 2013, 2006) developed at Laboratoire de Météorologie Dynamique in France. This is a complex model that incorporates many processes decomposed into a dynamic part, calculating the numerical solutions of general equations of atmospheric dynamics, and a physical part, calculating the details of the climate in each grid point and containing parameterizations processes such as the effects of clouds, convection, orography (LMD_Modelling_-Team, 2014). Atmosphere dynamics are represented by a finite-difference discretisation of the primitive equations of meteorology (e.g. Sadourny and Laval, 1984) on a longitude-latitude Arakawa C-grid(e.g. Kasahara, 1977). The chosen resolution of the model is 96x95x39, corresponding to an interval of 3.75 degrees in longitude and 1.9 degrees in latitude. There are 39 vertical levels, with around 15 levels above 20 km. This model has the specificity to be zoomed (the Z of LMDZ) if necessary on a specific region and then may be used for

regional studies (e.g. Jost et al., 2009).

The land component in IPSL-CM5A is ORCHIDEE (Organizing Carbon and Hydrology In Dynamic Ecosystems, (Krinner et al., 2005)) is composed of three modules: hydrology, carbon cycle and vegetation dynamics. The hydrological module, SECHIBA (Ducoudré et al., 1993), describes exchange of energy and water between atmosphere and biosphere, and the soil water budget(Krinner et al., 2005). The river routing scheme combines the river flow with a cascade of three reservoirs: the stream and two soil reservoirs with different time constants (Marti et al., 2010). Vegetation dynamics parametrisation is derived from the dynamic global vegetation model LPJ (Krinner et al., 2005; Sitch et al., 2003). The carbon cycle model simulates phenology and carbon dynamics of the terrestrial biosphere (Krinner et al., 2005). Vegetation distributions are described using 13 plant functional types (PFTs) including agricultural C3 and C4 plants, which are not used in the mPWP simulations, bringing down the number of PFTs to 11, including bare soil. In our case, hydrology and carbon modules are activated, but vegetation is prescribed as the same with Contoux et al. (2012), using 11 PFTs, derived from the PRISM3 vegetation dataset (Salzmann et al., 2008). Therefore, soil, litter, and vegetation carbon pools (including leaf mass and thus LAI) are calculated as a function of dynamic carbon allocation (Krinner et al., 2005).

### 2.1.2 Ocean and sea ice

The ocean model is NEMOv3.2 (Madec, 2008) which includes three principle modules: OPA (for the dynamics of the ocean), PISCES (for ocean biochemistry), and LIM (for sea ice dynamics and thermody- namics). The configuration of this model is ORCA2.3 (Madec and Imbard, 1996), which uses a tri-polar global grid and its associated physics. There are 31 unequally spaced vertical levels and a nominal resolution of 2° that is refined up to 0.5° in the equatorial area.Temperature and salinity advection is calculated by a total variance dissipation scheme (Lévy et al., 2001)(Cravatte et al., 2007). The mixed layer dynamics is parameterized using the Turbulent Kinetic Energy (TKE) closure scheme of Blanke and Delecluse (1993) improved by Madec (2008). The sea ice module LIM2 is a two-level thermodynamic-dynamic sea ice model (Fichefet and Morales Maqueda 1997, 1999). Sensible heat storage and vertical heat conduction within snow and ice are determined by a three-layer model. OASIS model plays as a coupler (Valcke, 2006) to interpo-

late and exchange the variables and to synchronize the models. This coupling and interpolation procedures ensure local energy and water conservation (Dufresne et al., 2013).

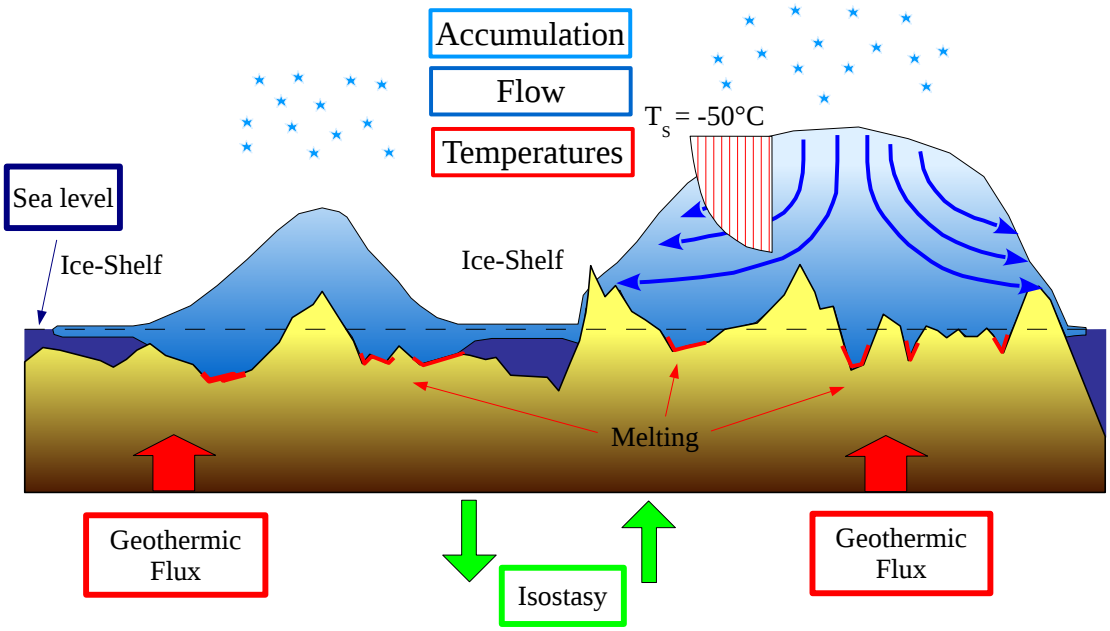


Figure 2.2 – Schematic design for GRISLI ice sheet model. Modified after Dumas (2002).

### 2.1.3 New AOGCM version :IPSL-CM5A2

IPSL-CM5A2 (for which a detailed description can be found in Sepulchre et al., in prep.) is an updated version of the CMIP5 IPSL-CM5A2 earth system model (ESM). The basics (LMDZ5A physics schemes, ORCHIDEE 2-level hydrology) and the resolutions of each components have been kept identical. However critical changes between the two ESMs include (i) technical developments to make IPSL-CM5A2 run faster, (ii) updates of different components and (iii) a retuning to correct IPSL-CM5A cold bias. On the technical side, IPSL-CM5A2 benefits from hybrid parallelization combining MPI parallelization on latitudinal bands for LMDZ-ORCHIDEE and shared memory parallel processing (OpenMP) on vertical levels, allowing the model to be run on more than 300 cores. Computation time has thus improved, switching from 8yrs per day in IPSL-CM5A to up to 62yrs perday in IPSL-CM5A2.

Regarding the different components, IPSL-CM5A2 uses recent (2017) version of each

compartment. NEMO v3.6 has been included in the model, with the vertical levels now discretized using the “partial steps“ scheme. ORCHIDEE has benefited from numerous bug corrections, especially on continental water fluxes, which conservation is now guaranteed. LMDz is rather similar to IPSL-CM5A version, modulo minor bug corrections. Re-tuning of the model has been done by altering the cloud radiative effect. The designated target was a pre-industrial temperature approaching 13.5°C with a null surface energy balance. Latest multi-millenia experiments with IPSL-CM5A2 provided a global 2-m temperature of 13.25°C, a value that Sepulchre et al. considered acceptable. Known biases of IPSL-CM5A-LR were not corrected: they include a double ITCZ structure over the Pacific ocean, underestimated precipitation over the Amazonian basin and the lack of deepwater formation in the Labrador sea. Still, tuning towards warmer temperatures improved the overall Atlantic Meridional Overturning Circulation by 2-3 Sv.

## 2.2 Ice sheet model

The ice sheet model used in this study is the GRenoble Ice-Shelf and Land-Ice model (GRISLI). GRISLI is a three-dimensional thermo-mechanical model that simulates the evolution of ice sheet geometry (extension and thickness) and the coupled temperature–velocity fields in response to climate forcing. A comprehensive description of the model can be found in Ritz et al. (2001) and (Peyaud et al., 2007). Figure2.2 represents a schematic design for the GRISLI ice sheet model. Over the grounded part of the ice sheet, the ice flow resulting from internal deformation is governed by the shallow-ice approximation (Morland, 1984). The model also deals with ice flow through ice shelves using the shallow-shelf approximation (MacAyeal, 1989) and predict the large-scale characteristics of ice streams using criteria based on the effective pressure and hydraulic load. At each time step, the velocity and vertical profiles of temperature in the ice are computed as well as the new geometry of the ice sheet. The isostatic adjustment of bedrock in response to ice load is governed by the flow of the asthenosphere, with a characteristic time constant of 3000 years, and by the rigidity of the lithosphere. The temperature field is computed both in the ice and in the bedrock by solving a time-dependent heat equation.The surface mass balance is defined as the sum between accumulation and ablation computed by the positive degree-day (PDD) method (Fausto et al., 2009).In this study, we use GRISLI on three different grids. Two 40km grids : one is for the Northern Hemisphere (Hereafter "GRISLI-

Table 2.1 – Major parameters applied in the GRISLI model

| | |
|---|---|
| Basal drag coefficient | 1500 m yr/Pa |
| Topographic lapse rate, annual | 6.0 °C/km |
| Precipitation ratio parameter | 0.07/°C |
| PDD standard deviation of daily temperature | 5.0 °C |
| PDD ice ablation coefficient | 8.0 mm/day°C |
| PDD snow ablation coefficient | 5.0 mm/day°C |

NH"), second is for Antarctica. Another refined cartesian grid (15kmx15km) was used on Greenland (Hereafter "GRISLI-Greenland").Table 2.1 show the standard parameters applied in the GRISLI model.

# Chapter 3

# Exploring the MIS M2 glaciation under a warm and high CO2 Pliocene climate

## Contents

## 3.1 Introduction

Prior to the perennial Greenland glaciation around 2.7 Ma, a large glaciation MIS M2 (3.312 – 3.264 Ma) took place locating in the interval between two warm periods. The estimated sea-level drops during this glaciation have large uncertainties and vary from 20 meters to 60 meters ((Dwyer and Chandler, 2009; Miller et al., 2012; Naish and Wilson, 2009), Figure3.3), which associated with likely large expanded land ice in both hemispheres ((De Schepper et al., 2014),Figure3.2). Moreover, the reconstructed pCO2 records during this event with the range of 220 - 405 ppmv(Bartoli et al., 2011; Martínez-Botí et al., 2015; Pagani et al., 2010; Seki et al., 2010) are much higher than that during Quaternary glaciation (Figure3.1). Unlike the mid Pliocene warm episode from 3.3 to 3.0 Myr ago, which is well documented from marine data (Dowsett et al., 2012), continental records (Salzmann et al., 2008) and model studies (Haywood et al., 2016), MIS M2 is poorly understood and there are few modeling studies focusing on the MIS M2 glaciation termination and decay. Only one recent work by Dolan et al. (2015b) studied M2 glaciations with discussing the likely extent of ice sheets during M2 glaciation by confronting the simulated climate conditions with different land ice scenarios to the available proxy data. Their study demonstrated the possibility of the existence of a larger-than-modern ice sheet during M2, but the driving factors were not discussed. The mechanism for M2 onset and decay remains still an enigma. Regarding the speculative features of M2, the classical forcing factors may not be enough to explain. Nevertheless, a recent geological hypothesis based on the marine proxy data invoked the specific role of re-opening and closing of shallow Central American Seaway (CAS) to explain the triggering and decay of M2 glaciation (details are represented in Section3.2.2. However, this hypothesis has not been validated by modeling studies. Therefore, in this study, we aim at exploring the mechanisms underlying M2 formation and termination. For this purpose, we firstly test this reasonable geological hypothesis,secondly discuss the roles of classical forcing factors and internal feedbacks and thirdly quantify the M2 glaciation extent with all favorable forcing factors. Since this work has been already published, A completed story about this work can be found in my paper included in Section3.3. Before going to the paper, I will give a brief review on the Central American Seaway issues in Section 3.2.2.

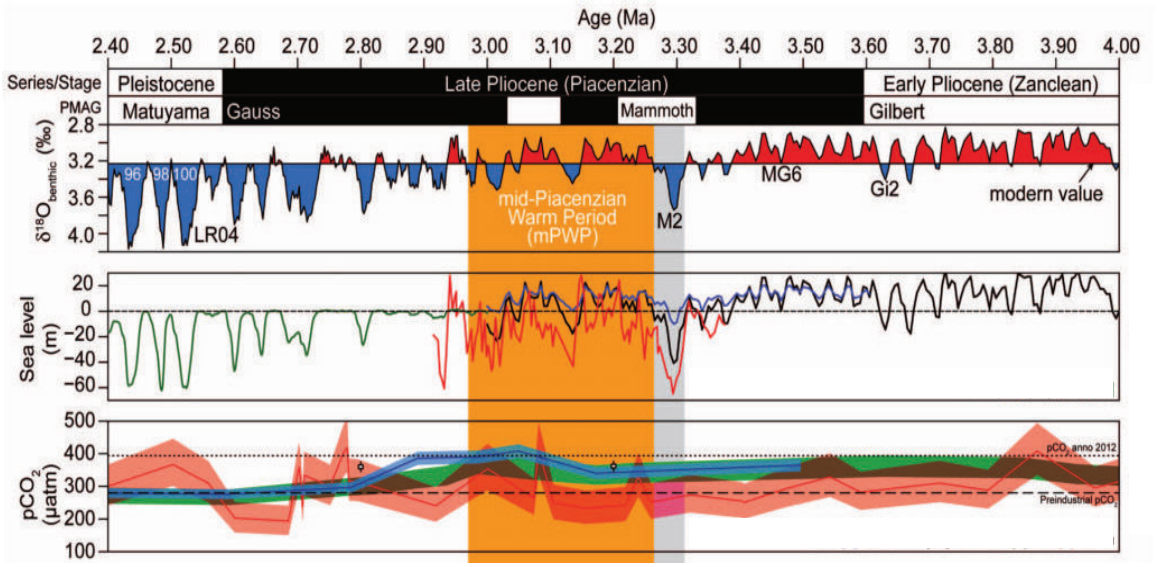


Figure 3.1 – Marine isotope stage M2 in the long-term climate evolution of the Pliocene. Figure modified from De Schepper et al.,2013

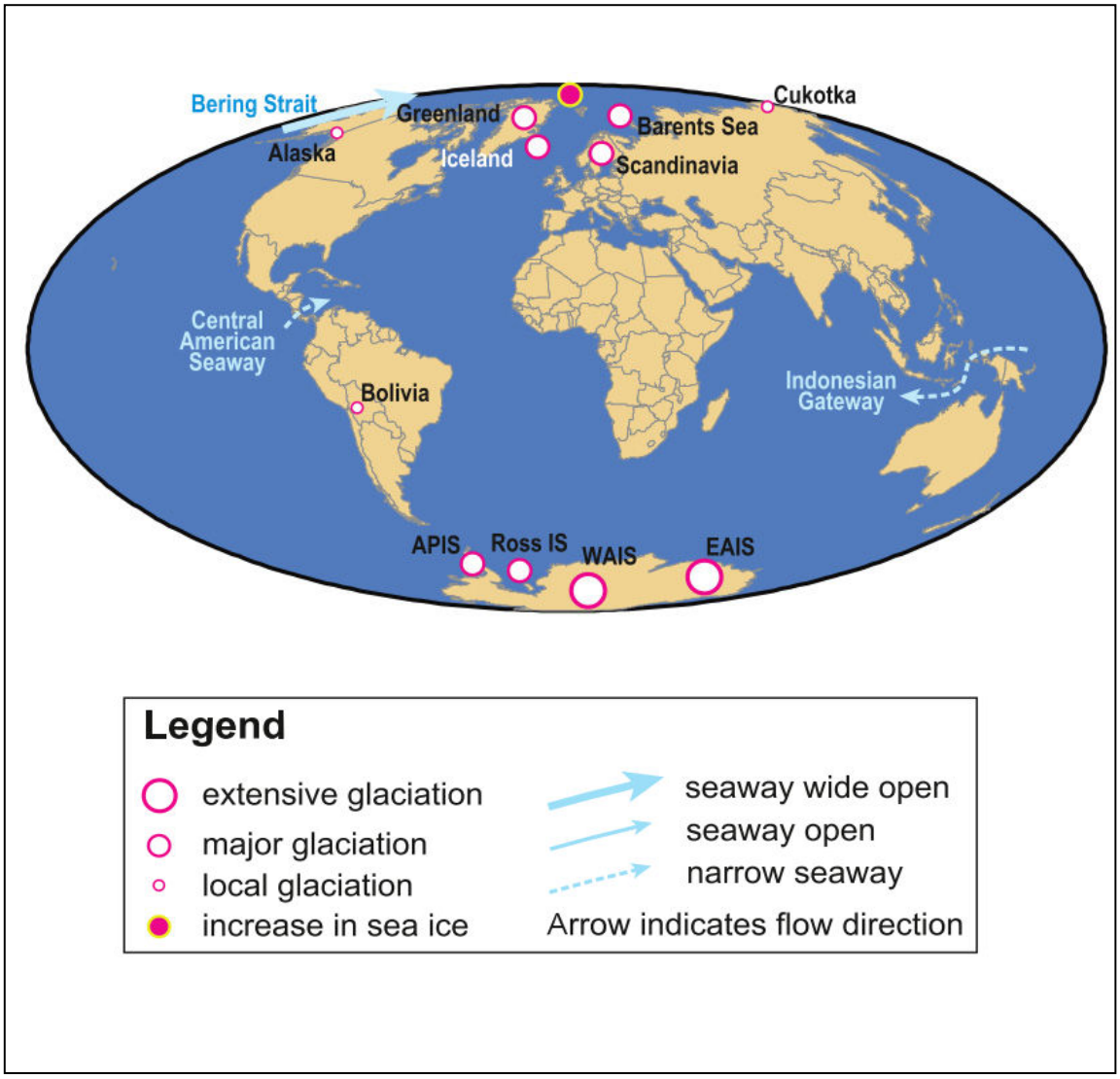


Figure 3.2 – The distribution of ice sheets at around 3.3Ma based on the marine and terrestrial records. Figure modified from De Schepper et al.,2014

## 3.2 The issue on Central American Seaway hypothesis

### 3.2.1 The classical CAS hypothesis

Under modern conditions, sea waters represent strong contrast in sea surface temperature (SST) and salinity (SAL) between East Pacific and Caribbean sea (Figure 3.3). However, these two sea waters deeply connected before the formation of the long peninsula connecting Panama to North America. Since the Early Miocene (ca.23–17 Ma), the Central American Seaway (CAS) constricted to a narrow range of 200 km (Montes et al.,2012a,2012b). Afterwards the marked uplift of the sill underwent and shut off deep-water flow across the isthmus between 12 to 10 Ma (Duque-Caro,1990). However, the shallow water exchange continued via CAS until the late Pliocene ((Molnar, 2008) and reference therein). While the actual timing of the final closure of the CAS is largely debated, studies based on biogeographical and paleoceanographical data have proved the early Pliocene to be the major period where underwent the progressively shoaling of the CAS (KEIGWIN, 1982)(Haug and Tiedemann, 1998).

Therefore, regarding the Pliocene period, one question of the particular interest is the closure or shoaling of the CAS. The impact of closure of the CAS on the high latitude climate has been extensively studied and remains largely debated. Theoretically, the closure or restriction of the CAS resulting in a cessation of fresher water transport from Pacific to the Caribbean sea, could affect the climate by enhancing the Atlantic meridional overturning circulation (AMOC) and modifying the heat and moisture transport. The classical 'Panama Hypothesis', first proposed by Keigwin(1982), stated that one of the effects of this change is to enhance evaporation rates in the North Atlantic, providing an enhanced moisture flux to northern high latitudes, increased precipitation and help to the inception or intensification of NHG beginning at 3 Ma (Haug and Tiedemann, 1998)

Numerous modeling studies have conducted to investigate the potential effects of the CAS closure or shoaling on the climate (Maier-Reimer et al. 1990; Mikolajewicz et al. 1993; Mikolajewicz and Crowley et al.,1997;Murdock et al. 1997; Nisancioglu et al. 2003; Prange and Schulz 2004; Klocker et al. 2005; von der Heydt and Dijkstra 2005; Schneider and Schmittner 2006;Brierley and Fedorov, 2016 and reference therein). Most of these studies demonstrate the role of the CAS closure in enhancing Atlantic thermohaline circulation associated with a strengthened North Atlantic Deep Water (NADW) formation result-

ing from the decreased fresher water transport from the Pacific into Atlantic, while few of these studies demonstrate the important role of CAS in the NHG reinforcement. As discussed before, the enhanced northward moisture transport that may help to increase NHG intensification (iNHG) is accompanied with the enhanced heat transport associated with the shoaling or closure of the CAS, which likely help to delay the iNHG. But the relative contributions of these two effects of the closure CAS is actually not very clear. Klocker et al.,(2005) demonstrate that the perennial snow cover decreased after the closure of the CAS, implying the doubtful role of the closure of CAS in the iNHG. Lunt et al., (2008) demonstrated that the closure of the CAS contributes little to the formation of the land ice in Greenland. Moreover, Brierley and Fedorov et al., 2016 compared three possible seaway changes during the Pliocene and demonstrated that both two tropical seaways (CAS and Indonesia Seaway) play much weaker roles in the high latitude climate than the high latitude seaway of Bering strait.

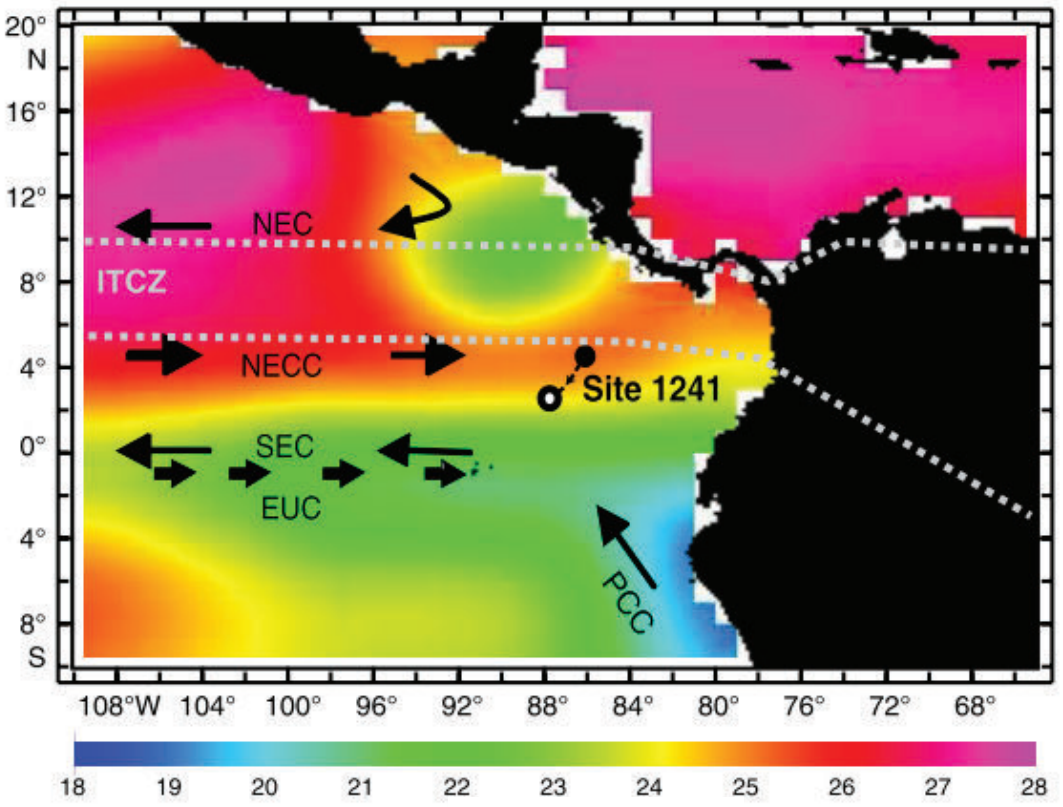


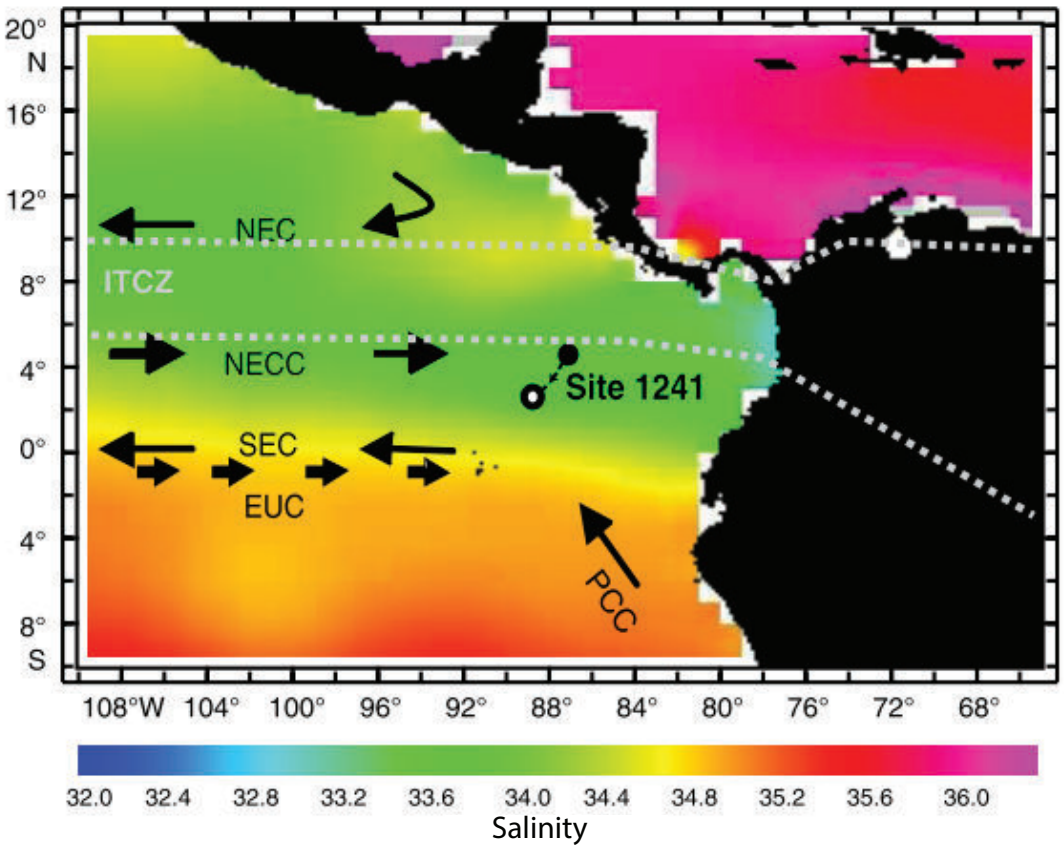


Figure 3.3 – Sea surface salinity and temperature distribution in the tropical eastern Pacific region with the major current.Figure modified from (Groeneveld et al., 2014)

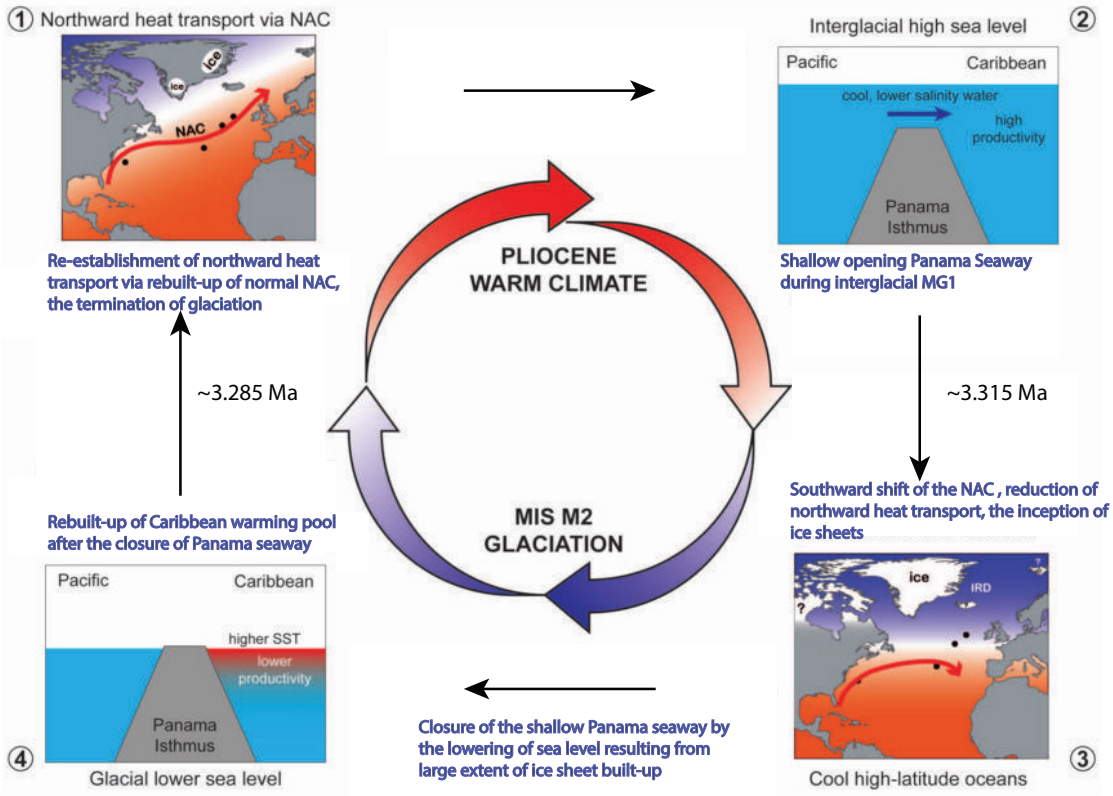


Figure 3.4 – The shematic for "shallow opening Panama Seaway" hypothesis. Figure modified from De Schepper et al.,2013

### 3.2.2 The “shallow re-opening CAS” hypothesis for MIS M2 glaciation

Although restriction of surface waters through the Central American Seaway might occur during the Early Pliocene (4.5–4.3 Ma) based on planktonic foraminifera data (e.g. Haug and Tiedemann, 1998), the final tectonic closure of the Central American Seaway might not occur until 2 Ma (Jackson et al., 1993). During this long interval, the exchange of surface waters was probably constrained up to a 100-meters sill depth and dynamically affected by the glacial induced sea-level change (Groeneveld et al., 2014). Even such shallow water exchange might have had influenced the Northern Hemisphere climate. A study of De Schepper et al. (2013) put forward the hypothesis that a re-opening and closing of the shallow CAS may have triggered the onset and the termination of the M2 glaciation. This hypothesis provides for the first time an explanation for the formation and decay of the NH ice sheets during M2 in relation to tectonic and glacio-eustatic change. Based on dinoflagellate cysts and geochemical proxy data from different Ocean

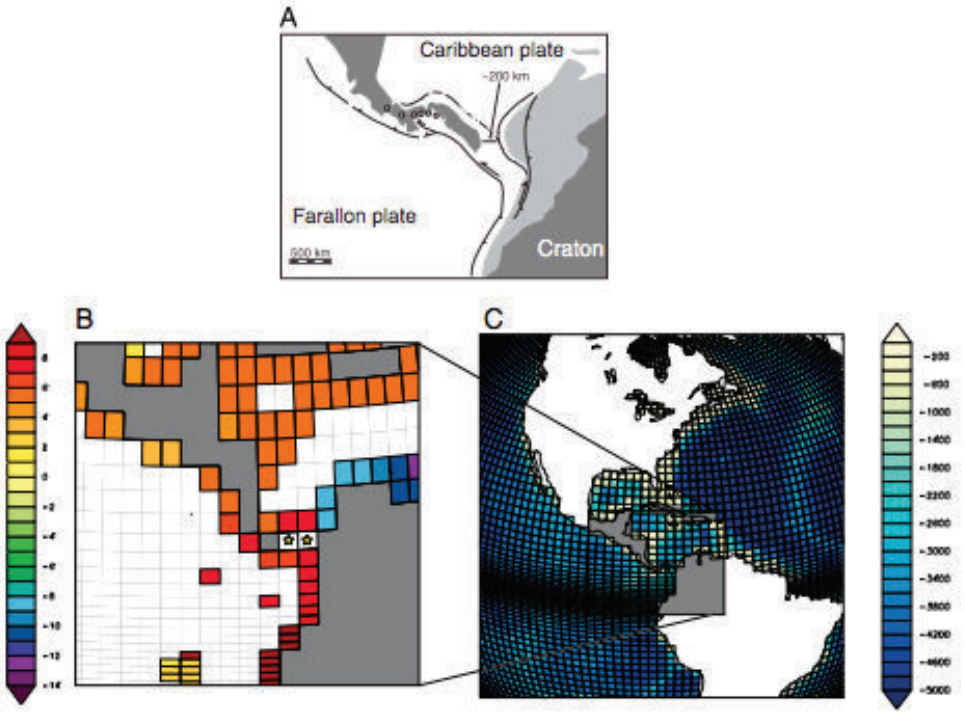


Figure 3.5 – The position of narrow Central American seaway since the early Miocene (a) and the related CAS location in the model (b and c). Figure modified from Sepulchre et al.,2014

Drilling Project sites, they conjecture that a re-opening of the shallow CAS occurring before and during the M2 event allowed seawaters flowing from the Pacific to the Atlantic. The fresher and cold inflow seawater helped to weaken the North Atlantic circulation and to cool the northern high latitudes. Then the cooling was gradually amplified by the positive sea ice albedo feedback, the adaptation of vegetation to colder climates and pCO2 changes, finally leading to substantial ice sheet growth in NH high latitudes (De Schepper et al., 2013). Inversely, the large ice volume accumulated over land would then produce a sea-level drop large enough to close the CAS. Following this glacio-eustatic closure, the ocean circulation shifted to its modern state and warmed the northern high latitudes, triggering the deglaciation. This hypothesis has gained a lot of attention because it provides an explanation both for the onset and the termination of the M2 glaciation. Moreover, this seaway hypothesis would better fit the short duration of the M2 glaciation comparing to other long-term geological processes and the glacio-eustatic closure corresponds well to the sea-level drop estimates (20–60 m)(Figure 3.4). However, this hypothesis is funda-

Table 3.1 – Results of the CAS opening in the model

| | CAS Width (km) | CAS Depth (m) | Eastward transport water flux via CAS (Sv) | Westward transport water flux via CAS (Sv) | AMOC (Sv) |
|---|---|---|---|---|---|
| PI | – | – | – | – | 11.4 |
| PlioMIP 1 | – | – | – | – | 11.7 |
| CAS50 | 440 | 50 | 1.2 | 0.0 | 11.5 |
| CAS500_Sepulchre | 440 | 512 | 12 | 5.9 | 3.9 |
| CAS50_Sepulchre | 440 | 55 | 0.09 | 3.5 | 2.5 |

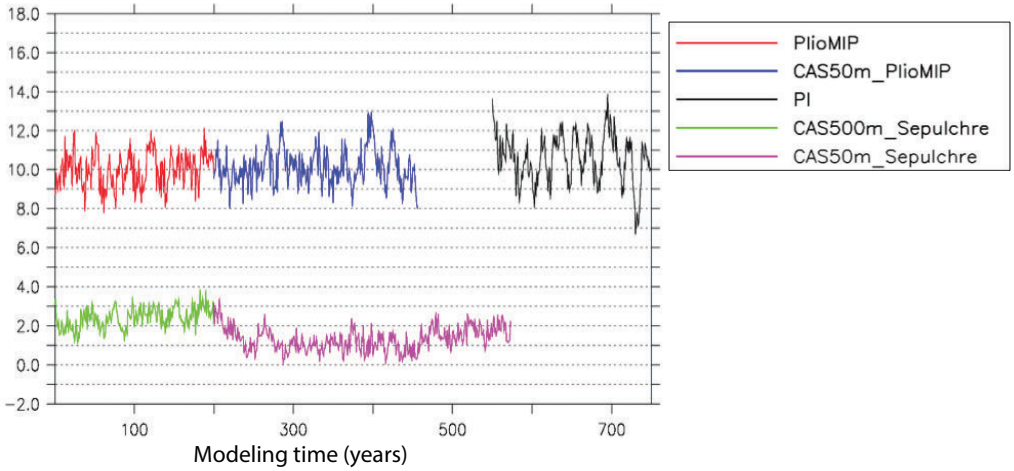


Figure 3.6 – Evolutions of AMOC index during the modeling time in each simulation that introduced in the table3.1

mentally different from the classical CAS hypothesis and it has not yet been tested. Thus in this study, we provide the first modeling effort to validate this assumption.

### 3.2.3 Sensitivity experiment with shallow opening CAS

#### The set-up of shallow opening CAS in the model

As discussed in the above, Montes et al. (2012a, 2012b) suggest that the CAS constriced to a narrow range of 200km (As showing in Figure 3.5a). However, the horizontal resolution in NEMO ocean model is 2 degrees in tropical region (see at chapter 2), which means the CAS width only takes up one grid in the model. Regarding the low sensibitlity to this one grid modification in our model, here we modify two grids of our model at 8N associated with 440km width to represent the narrow CAS and the location is consistent with the previous study of Sepulchre et al.(2014) (Figure 3.5). To take into account the glacio-eustatic closure of the CAS after M2, here we set-up a 50m sill depth for this narrow CAS in

the model. The sensitivity experiment with the openning CAS is carried out based on the PlioMIP 1 standard simulation of Contoux et al.,(2012), which show a present-comparable AMOC of ca.11x10$^6$ $m^3.s^{-1}$ (i.e., 11 Sverdrups, hereafter Sv).

**The modification on water current after CAS opening**

After opening this shallow and narrow CAS, we observed an expected eastward water transport of ca. 1.2 Sv via CAS (from Pacific ocean to Caribbean region ). This fresher water invasion reduces the SAL and SST in the Caribbean sea and further reduces the North Atlantic current. All the effects associated with the opening CAS are in good agreement with data observation (De Schepper et al.2013) except for the magnitude of each influences. More details can be found in section3.3.

Table3.1 represents a comparison work between our CAS50 experiment and the CAS simulations of Sepulchre et al.,(2014). However, with a similar sill depth of CAS (50meters), Sepulchre et al., (2014) (CAS50_sepulchre) observed an opposite water transport from Caribbean sea to Pacific region . The large difference can be attributed to the different initial states of AMOC in our experiment.In a theoretical study of Nof et al. (2003), they have shown how the circulation may change when different seaways are opened and closed, especially Bering straits, Drake passage and Central American seaway In particular, this study demonstrates that the water flow direction via the CAS highly depends on the initial North Atlantic Deep Water (NADW) state, when NADW is strong enough, the invasion of water is from Pacific to Atlantic, otherwise, water current is from Atlantic to Pacific. Accordingly, we find that the initial state of AMOC in CAS50_sepulchre is about 3.9 Sv, which is based on their CAS500 experiment (Figure 3.6). Nevertheless, our CAS50 experiment are based on PlioMIP 1 (Contoux et al., 2012), which show a much stronger AMOC (11.7 Sv). This results further demonstrate the sensitivity of the IPSL model to this narrow CAS set-up.

Regarding that our sensitivity experiment of CAS50 is carried out under a high pCO2 condition (405 ppmv), it is also necessary to test the CAS50 effects under a low pCO2 condition. Thus, based on the CAS50 experiment of 405ppmv, we carried out another CAS50 experiment with 280ppmv of pCO2. Then we find that, with a lower pCO2, the water current keep the same direction but get an increased water flux ( 2 Sv).More details are found in the next section.

## 3.3 Paper published in Earth Planetary Science Letters "Exploring the MIS M2 glaciation occurring during a warm and high atmosphere CO2 Pliocene background climate"

Earth and Planetary Science Letters 472 (2017) 266–276

Contents lists available at ScienceDirect

Earth and Planetary Science Letters

www.elsevier.com/locate/epsl

# Exploring the MIS M2 glaciation occurring during a warm and high atmospheric $CO_2$ Pliocene background climate

Ning Tan [a,*], Gilles Ramstein [a], Christophe Dumas [a], Camille Contoux [b], Jean-Baptiste Ladant [a], Pierre Sepulchre [a], Zhongshi Zhang [c,d,e], Stijn De Schepper [c]

[a] Laboratoire des Sciences du Climat et de l'Environnement, LSCE/IPSL, CEA-CNRS-UVSQ, Université Paris-Saclay, F-91191 Gif-sur-Yvette, France
[b] Aix-Marseille Université, CNRS, IRD, Collège de France, CEREGE UM34, Europôle de l'Arbois, 13545 Aix-en Provence, France
[c] Uni Research Climate, Bjerknes Centre for Climate Research, Nygårdsgaten 112-114, 5008 Bergen, Norway
[d] Department of Atmosphere Science, China University of Geoscience, 430074, Wuhan, China
[e] Nansen-Zhu International Research Center, Institute of Atmospheric Physics, Chinese Academy of Sciences, 100029, Beijing, China

ARTICLE INFO

*Article history:*
Received 23 July 2016
Received in revised form 27 April 2017
Accepted 28 April 2017
Available online 25 May 2017
Editor: M. Frank

*Keywords:*
glaciation
MIS M2
Central American Seaway
late Pliocene
warm climate
ice sheet modelling

ABSTRACT

Prior to the Northern Hemisphere glaciation around ~2.7 Ma, a large global glaciation corresponding to a 20 to 60 m sea-level drop occurred during Marine Isotope Stage (MIS) M2 (3.312–3.264 Ma), interrupted the period of global warmth and high $CO_2$ concentration (350–450 ppmv) of the mid Piacenzian. Unlike the late Quaternary glaciations, the M2 glaciation only lasted 50 kyrs and occurred under uncertain $CO_2$ concentration (220–390 ppmv). The mechanisms causing the onset and termination of the M2 glaciation remain enigmatic, but a recent geological hypothesis suggests that the re-opening and closing of the shallow Central American Seaway (CAS) might have played a key role. In this article, thanks to a series of climate simulations carried out using a fully coupled Atmosphere Ocean General Circulation Model (GCM) and a dynamic ice sheet model, we show that re-opening of the shallow CAS helps precondition the low-latitude oceanic circulation and affects the related northward energy transport, but cannot alone explain the onset of the M2 glaciation. The presence of a shallow open CAS, together with favourable orbital parameters, 220 ppmv of $CO_2$ concentration, and the related vegetation and ice sheet feedback, led to a global ice sheet build-up producing a global sea-level drop in the lowest range of proxy-derived estimates. More importantly, our results show that the simulated closure of the CAS has a negligible impact on the NH ice sheet melt and cannot explain the MIS M2 termination.



## 1. Introduction

Despite absolute differences, most atmospheric carbon dioxide proxies point towards a drastic decrease associated with large cooling from the Late Eocene to the Quaternary (Pagani et al., 2005; Zachos et al., 2001). The first major atmospheric $CO_2$ threshold for ice sheet build-up is reached around 34 Ma, when the Antarctic glaciation began under $CO_2$ levels equivalent to about three times those of the preindustrial concentrations (DeConto and Pollard, 2003; Ladant et al., 2014; Gasson et al., 2014). The onset of extensive Northern Hemisphere glaciation occurred approximately 30 million years later around 3.0–2.7 Ma (Lunt et al., 2008), ultimately leading to the glacial–interglacial cycles of the Quaternary (e.g. Ganopolski and Calov, 2011). However, prior to this glaciation, a major ephemeral glacial event took place, the Marine Isotope Stage (MIS) M2 (3.312–3.264 Ma), producing a ~0.5‰ shift of benthic foraminiferal $\delta^{18}O$ (Lisiecki and Raymo, 2005). The sea-level drop produced by this glacial event has been estimated at 20 to 60 m by different proxy estimates (Dwyer and Chandler, 2009; Miller et al., 2012; Naish and Wilson, 2009). As a comparison, 20–60 m sea level drop represents between one sixth and nearly half of the sea level drop during the Last Glacial Maximum. Therefore, the M2 ice sheets were not only confined to Greenland but must have spread over the Northern Hemisphere continents. Also, a contribution from an expanded Antarctic ice sheets is likely (detailed evidence for ice sheets during MIS M2 are summarised by De Schepper et al., 2014). Nevertheless, the M2 glaciation has some very peculiar characteristics with respect to Quaternary glaciations: first, this glacial event occurred in the interval of two long and stable warm periods and only lasted for ~50 kyr, which is half the duration of recent Quaternary glacial cycles (e.g. Ganopolski and Calov, 2011). In the southern Hemisphere, the East Antarctic ice sheets were present and lasted during the mid-Piacenzian warm period (Hill et al., 2007), whereas the West Antarctic ice

* Corresponding author.
*E-mail address:* ning.tan@lsce.ipsl.fr (N. Tan).

http://dx.doi.org/10.1016/j.epsl.2017.04.050
0012-821X/

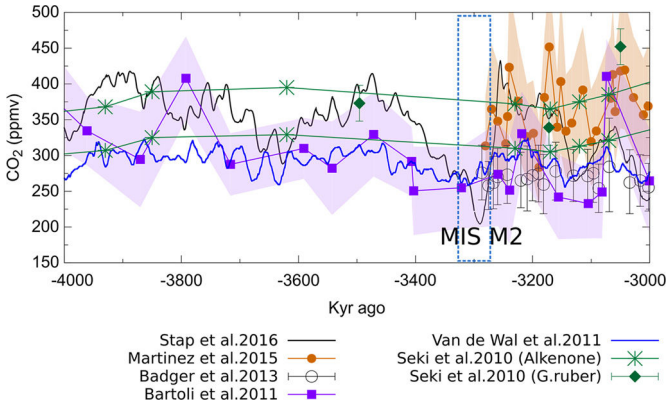


**Fig. 1.** Syntheses of reconstructed atmospheric $CO_2$ concentration from 4.0 to 3.0 Ma from different studies. The proxies from Martinez et al. (2015), Bartoli et al. (2011) and Seki et al. (2010) (green rhombus symbol) are boron-based data; The proxies from Badger et al. (2013) and Seki et al. (2010) (green asterisk symbol) are alkenone-based data. The reconstruction of Stap et al. (2016) and Van de Wal et al. (2011) are obtained by inversing benthic $\delta^{18}O$ routine with the climate and ice sheet model. (For interpretation of the references to colour in this figure legend, the reader is referred to the web version of this article.)

sheets experienced waning and waxing during and after M2 period, since it is much more sensitive to the change of climate in the adjacent ocean margin (Riesselman and Dunbar, 2013); second, the proxy records show that the M2 event might occur under $CO_2$ concentrations ranging between 220 and 390 ppmv (Fig. 1); third, the summer insolation over the high-latitudes of the Northern Hemisphere is not particularly favourable for ice sheet inception during the M2 period (Laskar et al., 2004) (Fig. A.1). Together, these three characteristics raise the question whether the classical forcing factors of low $CO_2$ concentrations and/or low high-latitude insolation are sufficient to explain the MIS M2 glaciation or whether other additional driving factors are needed.

The role of the closure of the CAS on changes in ocean circulation and climate change during the Pliocene remains heavily debated (e.g. Brierley and Fedorov, 2016; Lunt et al., 2008). Although restriction of surface waters through the Central American Seaway might occur during the Early Pliocene (4.5–4.3 Ma) based on planktonic foraminifera data (e.g. Haug and Tiedemann, 1998), the final tectonic closure of the Central American Seaway might not occur until ∼2 Ma (Jackson et al., 1993). During this long interval, the exchange of surface waters was probably constrained up to a 100-meters sill depth and dynamically affected by the glacial induced sea-level change (Groeneveld et al., 2014). Even such shallow water exchange might have had influenced the Northern Hemisphere climate. A study of De Schepper et al. (2013) put forward the hypothesis that a re-opening and closing of the shallow CAS may have triggered the onset and the termination of the M2 glaciation. This hypothesis provides for the first time an explanation for the formation and decay of the NH ice sheets during M2 in relation to tectonic and glacio-eustatic change. Based on dinoflagellate cysts and geochemical proxy data from different Ocean Drilling Project sites, they conjecture that a re-opening of the shallow CAS occurring before and during the M2 event allowed seawaters flowing from the Pacific to the Atlantic. The fresh and cold inflow seawater helped to weaken the North Atlantic circulation and to cool the northern high latitudes. Then the cooling was gradually amplified by the positive sea ice albedo feedback, the adaptation of vegetation to colder climates and $pCO_2$ changes, finally leading to substantial ice sheet growth in NH high latitudes De Schepper et al. (2013). Inversely, the large ice volume accumulated over land would then produce a sea-level drop large enough to close the CAS. Following this glacio-eustatic closure, the ocean circulation shifted to its modern state and warmed the northern high latitudes, triggering the deglaciation. This hypothesis has gained a lot of attention because it provides an explanation both for the onset and the termination of the M2 glaciation. Moreover, this seaway hypothesis would better fit the short duration of the M2 glaciation comparing to other long-term geological processes and the glacio-eustatic closure corresponds well to the sea-level drop estimates (20–60 m).

Unlike the mid-Pliocene Warm Period (ca. 3.3 to 3.0 Ma, mPWP), which is well documented in marine data (Dowsett et al., 2012), continental records (Salzmann et al., 2008) and model studies (Haywood et al., 2016 and reference therein), the M2 event is very poorly understood and suffers from a lack of modelling studies. Only the recent work of Dolan et al. (2015) study the M2 glaciation in a modelling framework. In their study, they implement plausible ice sheet configurations into a coupled atmosphere–ocean climate model to test whether larger-than-modern ice sheets in both hemispheres might exist during M2. They demonstrate that a larger-than-modern imposed ice sheets during the M2 period is more compatible with the marine proxy records, but they do not attempt to study the underlying mechanisms for M2 glaciation.

In this contribution, we performed a series of simulations using the IPSL-CM5A ocean/atmosphere GCM (Dufresne et al., 2013) and ice sheet model GRISLI (Ritz et al., 2001) (see Methods) first to explore whether the sole geological hypothesis of the re-opening and closure of the CAS can fully explain the M2 event, and second to quantify the maximum ice sheet scenario that our model can simulate for the M2 glaciation.

## 2. Method

### 2.1. Models

The climate model used in this study is the IPSL-CM5A atmosphere–ocean general circulation model (AOGCM). The atmosphere component is the LMDZ5A version of the LMDz model (including the ORCHIDEE land-surface model) with a resolution of $3.75° \times 1.875°$ and 39 vertical layers. More details about the physical parameterisation can be found in Hourdin et al. (2006). The ocean model is NEMOv3.2 including the ORCA2.3 ocean configuration (Madec, 2008), which uses a tri-polar global grid. There are 31 unequally spaced vertical levels and a nominal resolution of 2° that is refined up to 0.5° in the equatorial area. The atmosphere and ocean models are linked through the coupler OASIS, ensuring energy and water conservation. Additional details about the IPSL-CM5A model can be found in Dufresne et al. (2013). The IPSL-CM5A model has been used in the framework of CMIP5 for historical and future simulations (Dufresne et al., 2013) as well as for paleo-climate studies, like Quaternary (Kageyama et al., 2013) and Pliocene (Contoux et al., 2012) simulations.

The ice sheet model used in this study is the GRenoble Ice-Shelf and Land-Ice model (GRISLI). GRISLI is a three-dimensional thermo-mechanical model, which simulates the evolution of ice sheet geometry (extension and thickness) and the coupled temperature–velocity fields in response to climate forcing. A comprehensive description of the model can be found in Ritz et al. (2001). The equations are solved on a Cartesian grid (40 km × 40 km) and solved with a semi-implicit temporal scheme and a point relaxation method. The principle time step is 5 years, a short time step utilised for the mass-conservation equation is between 0.002 year and 1 year, which is adjustable and depends on the maximum velocity found over the whole domain. Over the grounded part of the ice sheet, the ice flow resulting from internal deformation is governed by the shallow-ice approximation. The model also deals with ice flow through ice shelves using the shallow-shelf approximation and predicts the large-scale characteristics of ice streams

using criteria based on the effective pressure and hydraulic load. At each time step, the velocity and vertical profiles of temperature in the ice are computed as well as the new geometry of the ice sheet. The isostatic adjustment of bedrock in response to ice load is governed by the flow of the asthenosphere, with a characteristic time constant of 3000 years, and by the rigidity of the lithosphere. The temperature field is computed in both the ice and bedrock by solving a time-dependent heat equation. The surface mass balance is defined as the sum between accumulation and ablation computed by the positive degree-day (PDD) method. Here, as the ice sheet model GRISLI is not synchronously coupled with the IPSL-CM5A model, temperature and precipitation fields are asynchronously passed from IPSL-CM5A to GRISLI.

### 2.2. Experiment design

#### 2.2.1. AOGCM experiments

To save computation resources, all AOGCM experiments are performed in succession in this study, which means an experiment always starts from the equilibrated state of the previous experiment. Boundary conditions and experiment configurations can be found in the Supplementary Table A.1. The control experiment used in our study is the IPSL-CM5A Pliocene standard experiment (named as "PlioMIP", Contoux et al., 2012). "PlioMIP" boundary conditions (atmospheric $CO_2$ level, paleotopography, ice sheets and vegetation) are derived from the United States Geological Survey (USGS) PRISM3D data set (Dowsett et al., 2012; Salzmann et al., 2008). The $pCO_2$ in this experiment is set to 405 ppmv. Initialised from the end of the equilibrated state of "PlioMIP" experiment, we first carry out a sensitivity experiment named "CAS50" to test the "shallow open Central American Seaway (CAS)" hypothesis (De Schepper et al., 2013). "CAS50" boundary conditions are equivalent to "PlioMIP" but with an open CAS (440 km width and 50 m depth). The position of CAS is the same as in Sepulchre et al. (2014). We prescribe here a 50 m sill depth in order to satisfy the glacio-eustatic closure of the CAS that would be produced by the approximate mean sea-level drop inferred from data (Dwyer and Chandler, 2009; Miller et al., 2012; Naish and Wilson, 2009). Initialised from the end of "CAS50", we carry out two other AOGCM experiments to explore the impact of astronomical parameters, greenhouse gases forcing and vegetation feedback. In these two experiments we choose a $CO_2$ concentration of 220 ppmv. This $CO_2$ concentration is the lowest value currently recorded around the M2 interval (Bartoli et al., 2011). Orbital parameters are taken as their 3.313 Ma values (Laskar et al., 2004), which provides the coldest boreal summer insolation of the M2 interval. In the first experiment, vegetation biomes are specified as in the baseline PlioMIP experiment ("M2-boreal") where boreal forests biomes dominate the northern high latitudes. In the second experiment, we impose an idealised tundra vegetation on the northern high latitudes: we replace boreal forest north of 50°N with tundra biomes ("M2-tundra") following the dynamical vegetation simulation by Koenig et al. (2011) in the context of a cold orbital forcing and low $CO_2$ concentration (map of vegetation distribution is shown in Fig. A.2). This vegetation configuration is in good agreement with pollen records showing dominant tundra biomes in Northeast Arctic Russia during M2 (Brigham-Grette et al., 2013). Moreover, Panitz et al. (2016) also show cool boreal forest and extensive peatlands in northern Norway around MIS M2. Other boundary conditions remain the same as "CAS50". From the "M2-tundra" experiment, successive regrowth experiments have been carried out (see the section 2.2.2), consisting of alternate use of the AOGCM and the ice sheet model (ISM). Finally, a closed CAS experiment is carried out ("M2-closeCAS"), based on the last "M2-tundra" regrowth simulation. More details can be found in the Supplementary Table A.1. In addition to discussing the CAS impact under lower $CO_2$ concentration and exploring the $CO_2$ threshold of 280 ppmv for the M2 glaciation, we perform two additional experiments: the first one named "CAS50p280" is similar to the sensitivity experiment "CAS50" but utilising 280 ppmv of $pCO_2$ instead of 405 ppmv; the second one named "M2-tundra-p280" is similar to "M2-tundra" but using 280 ppmv of $pCO_2$ instead of 220 ppmv. The results of these two experiments will be discussed in the Discussion section. All AOGCM experiments in this study have reached equilibrium for the atmosphere and the upper layer of the ocean.

#### 2.2.2. Ice sheet experiments

The ice sheet model GRISLI is forced with the monthly surface temperature at 2 meters and precipitation outputs from the IPSL-CM5A experiments. The initial bedrock topography and configuration of the NH ice sheets and Antarctic ice sheets in this study are from the PRISM3 dataset (Hill et al., 2007; Salzmann et al., 2008). All ice sheet experiments are run for 100 kyrs with constant insolation (one-way ice sheet simulations). Since the climate and ice sheet model are not synchronously coupled, the ice-sheet albedo feedback is not included in the climate model. For the M2-tundra experiment, we performed regrowth simulations to capture the ice sheet feedbacks, as this simulation generates the larger ice sheet in the one-way ice sheet experiment. The regrowth simulation is performed in three steps: first, we extracted the new ice sheet topography from the first-round ice sheet simulation; second, we imposed this new topography to the IPSL-CM5A model to continue the related AOGCM experiment; third, we extracted the new temperature and precipitation fields from the new AOGCM experiment to force another round of ice sheet simulation (Contoux et al., 2015). We repeated these steps in succession to reach an equilibrium state for the ice sheet. In the "M2-tundra" NH ice sheet experiment, we performed three regrowth simulations consisting of the alternation of 100 kyrs GRISLI runs to equilibrate the ice sheet and 100-yr IPSL-CM5A runs for the first and the second regrowth experiments, but 200-yr IPSL-CM5A runs for the third regrowth experiment (named M2-tundra-IS). After the 3rd regrowth experiment, the increase in ice volume was less than 10%. Then we stopped in the 3rd regrowth simulation due to the limit of computational resource.

In addition, in the Southern Hemisphere, the temperature and precipitation fields of M2-tundra-IS are used to explore whether the prescribed lower $CO_2$ concentration, orbital parameters and vegetation affect the Antarctic ice sheets (AIS). For comparison, we also carried out an AIS experiment by imposing the climatic fields of "PlioMIP" experiment. The basal melt rates in our AIS experiments are defined based on the standard basal melt rates in our model and also account for the impact of the ocean temperature anomaly between Pliocene conditions and pre-industrial condition. In detail, the definition of the basal melt rates in our study can be summarised as: $B_{\mathrm{AIS\_plio}} = B_{\mathrm{standard}} + \kappa * (T_{\mathrm{plio}} - T_{\mathrm{control}})$. "$B_{\mathrm{standard}}$" is the standard basal melt rates in GRISLI ice sheet model, which are defined separately for different regions. Kappa ($\kappa$) is set to 0.5 $\mathrm{myr}^{-1}\,\mathrm{K}^{-1}$ as in Álvarez-Solas et al. (2011); "$T_{\mathrm{plio}}$" means the ocean temperature at the depth of 300 m of the Pliocene simulation; "$T_{\mathrm{control}}$" means the ocean temperature at the depth of 300 m of the pre-industrial control simulation.

## 3. Results

### 3.1. The impact of shallow open CAS on M2 glaciation

In the CAS50 experiment, the CAS opening generates a reorganisation of the surface currents in the Caribbean region (Fig. 2). A colder and fresher water flux of ~1.2 Sv flows from the Pacific to the Atlantic, inducing a decrease in sea surface salinity (SSS) of

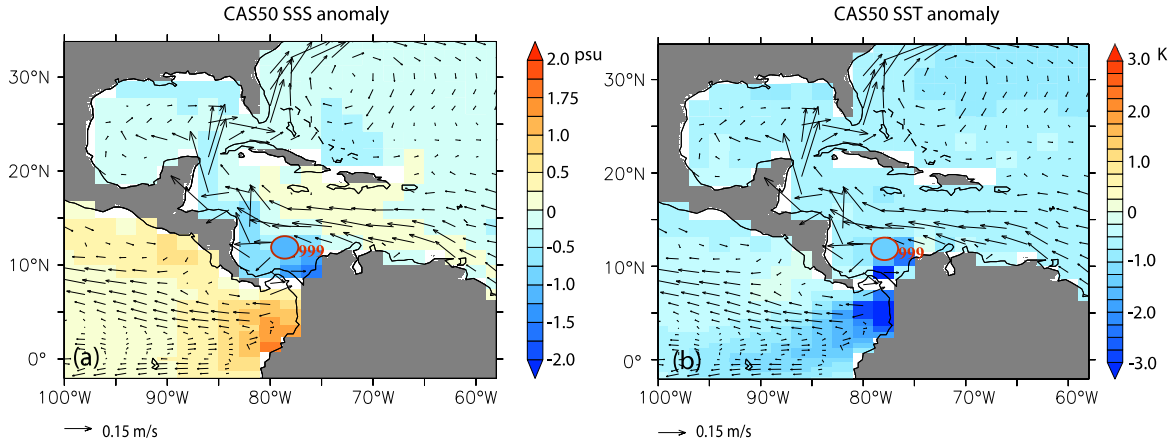


**Fig. 2.** Annual mean sea surface salinity (SSS) (a) and sea surface temperature (SST) anomalies (b) over Central America in the CAS50 experiment compared with the PlioMIP experiment. The vectors in both panels indicate the ocean currents above 50 m in CAS50 experiment. Red circles represent respectively the difference in reconstructed SSS and SST between M2 (3.3 Ma) and mid-Pliocene Warm Period (ca. 3.0–3.3 Ma) (data from De Schepper et al., 2013). (For interpretation of the colours in this figure, the reader is referred to the web version of this article.)

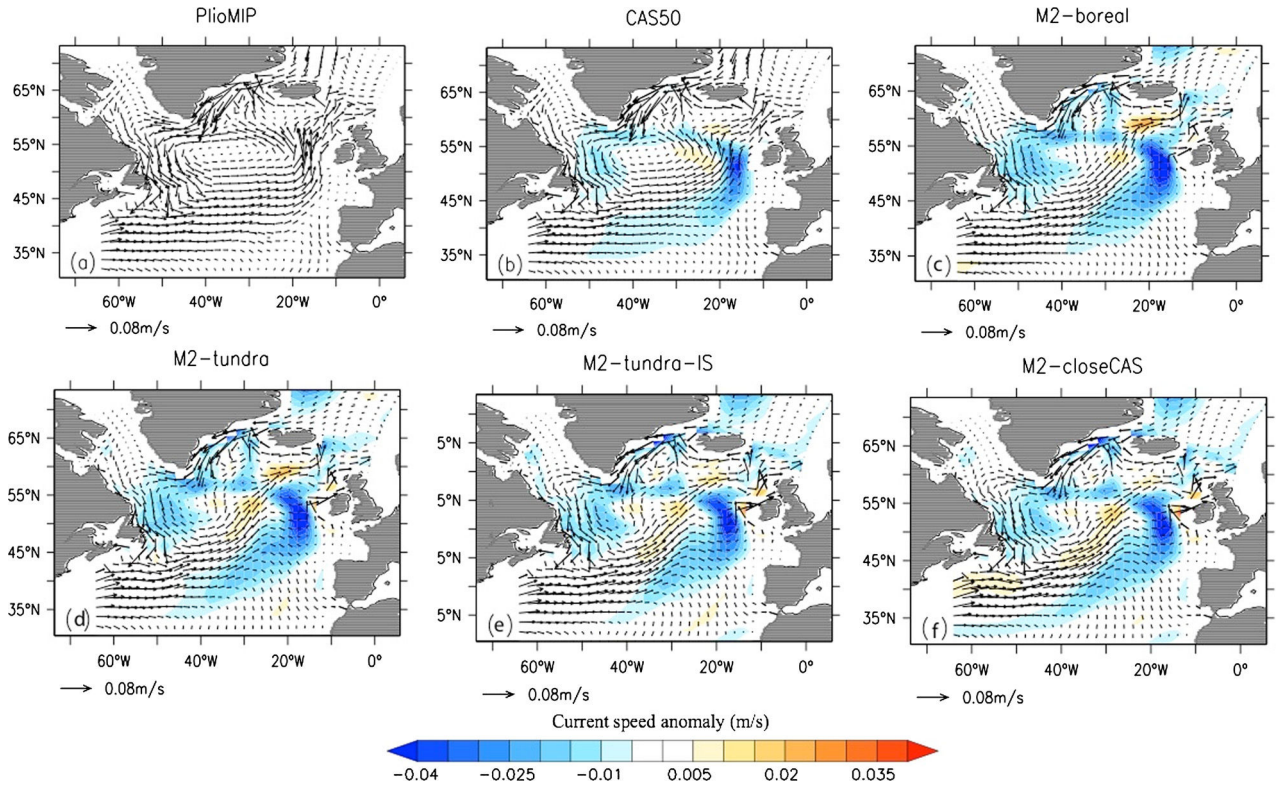


**Fig. 3.** Mean annual North Atlantic ocean current above 500 m (vectors); shaded colours are the current speed anomalies of each experiment in comparison to PlioMIP experiment.

up to 1 psu and a cooling of up to 0.5–0.75 °C in the Caribbean Sea with respect to the PlioMIP experiment. The magnitude of this freshening and cooling of the Caribbean Sea is in good agreement with data records at ODP Site 999 (De Schepper et al., 2013) (red circle in Fig. 2), obtained by comparing the reconstructed SSS and SST between M2 (3.3 Ma) and part of the mid-Pliocene Warm Period (3.0–3.3 Ma). This through-flow via the open CAS also affects the ocean circulation further north in the Atlantic. The North Atlantic Current strength decreases by ∼20% (NAC, Fig. 3b). The AMOC index after the CAS opening is not significantly different from the PlioMIP AMOC index and the Atlantic northward heat transport is reduced by up to 0.13 PW in the low latitudes North Atlantic (Fig. 4, red line). In contrast, a large AMOC decrease is observed in earlier CAS modelling studies when a deeper sill-depth was imposed (Sepulchre et al., 2014 and reference therein).

This change in ocean circulation after CAS opening leads to a small cooling over the Northern Hemisphere, predominantly over Eurasia continents, the North Atlantic Ocean and Arctic regions (Fig. 5a). In contrast to heat transport, the northward humidity transport is almost not affected by the CAS opening (Fig. A.3). Consequently, the simulated cooling only weakly increases the ice volume over Greenland by $0.25 \times 10^{15}$ m$^3$ (Fig. 6b) with respect to PlioMIP experiment (Fig. 6a), corresponding to a sea-level drop of about 1.5 m.

### 3.2. The impact of classic forcing factors on M2 glaciation

The CAS opening sensitivity experiment shows that the re-opening CAS alone cannot trigger the onset of the large M2 glaciation as it produces a small cooling in the northern high latitudes. The M2 glaciation has therefore to result from the synergy of many forcing factors rather than only from the CAS opening. To test the effect of forcing from $CO_2$, insolation and vegetation feedback, we designed the M2-tundra and M2-boreal experiments (for experiment set-up, see methods). The M2-tundra reveals a large cooling of up to ~8 °C (Fig. 5b) and a decrease in mean annual precipitation of 26% over the NH high latitudes (Fig. 5e), in response to the combination of lowered $CO_2$ concentration, weak solar insolation (Fig. A.4) and positive tundra-albedo feedback over northern high latitudes. The cooling and aridification over the northern high latitudes are also observed in M2-boreal (Figs. 5c, 5f), but are weaker than in M2-tundra. The tundra vegetation feedback is responsible for about 2 °C cooling (Fig. A.5) over northern high latitudes in comparison to boreal vegetation.

As a consequence of this cooling in M2-tundra, the ocean circulation significantly shifts with respect to PlioMIP: the NAC gets 30% weaker (Fig. 3d) and the AMOC strength index decreases by 1.2 Sv from 11–12 Sv (10% decrease), together with a decrease of northward heat transport in the regions of 0–30°N (−20%) and 40–80°N (−50%) (Fig. 4, blue line). However, the decrease of northward heat transport between 0–30°N of M2-tundra is comparable to the CAS50 experiment, i.e. a weakening by ca. −0.12 PW compared to the PlioMIP experiment, thereby suggesting that the CAS plays an important role in altering low latitude northward heat transport. In the M2-boreal experiment, the decrease in NAC speed (Fig. 3b) is comparable to the M2-tundra experiment. In response to ocean circulation change and surface air temperature cooling, the mean annual sea surface temperature (SST) in NH high latitudes decreases by an order of ~3 °C and 5 °C, accompanied by large extension of sea ice area of 36% and 48% (maximal sea-ice

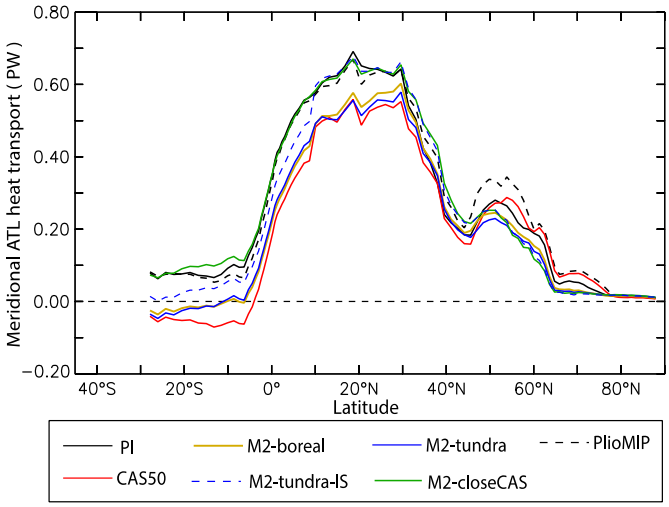


**Fig. 4.** Annual mean heat transport in Atlantic ocean (PW). (For interpretation of the colours in this figure, the reader is referred to the web version of this article.)

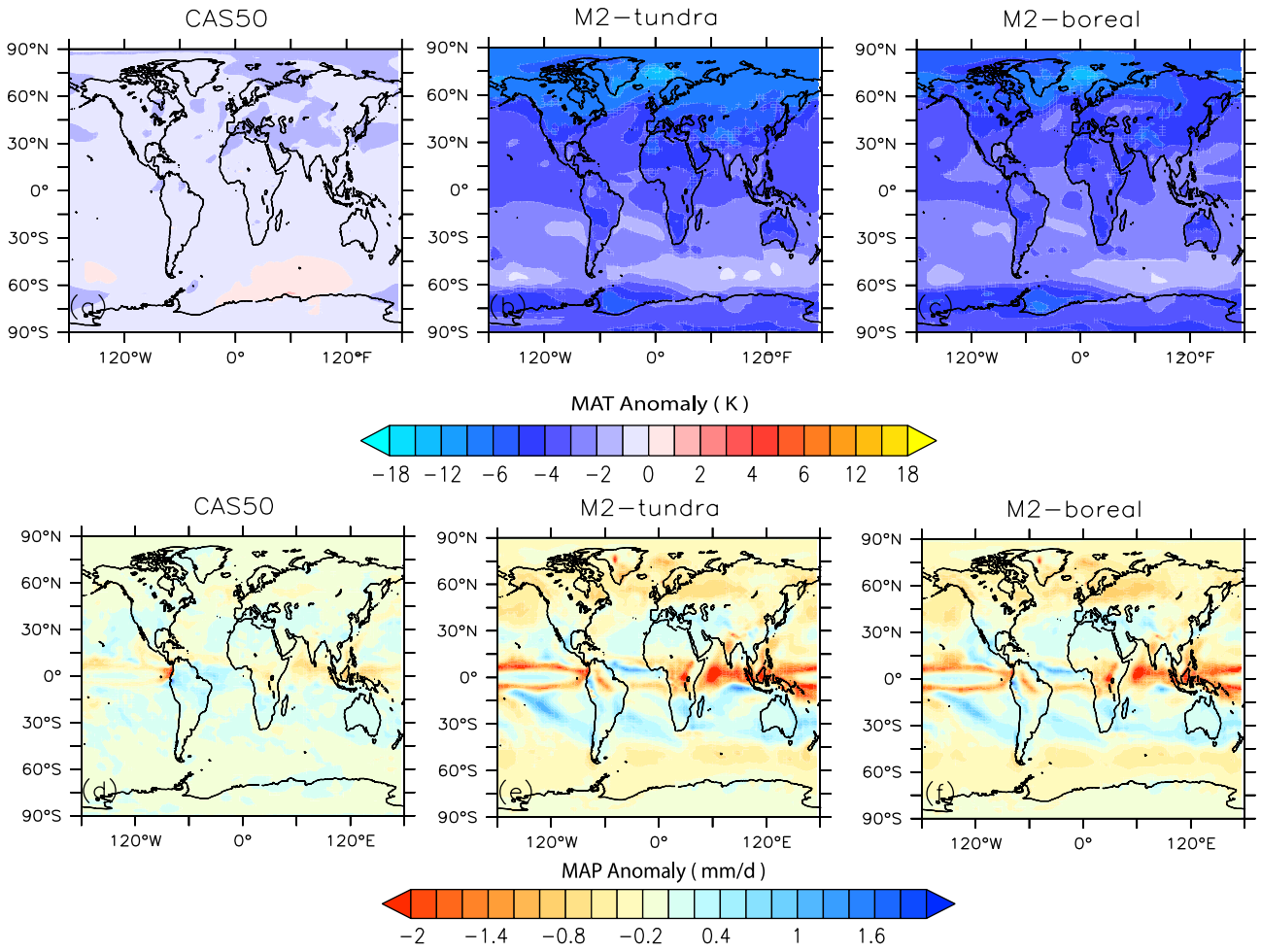


**Fig. 5.** Mean annual surface temperature (MAT) anomalies (a, b, c) and mean annual precipitation anomalies (d, e, f) in comparison to PlioMIP experiment.

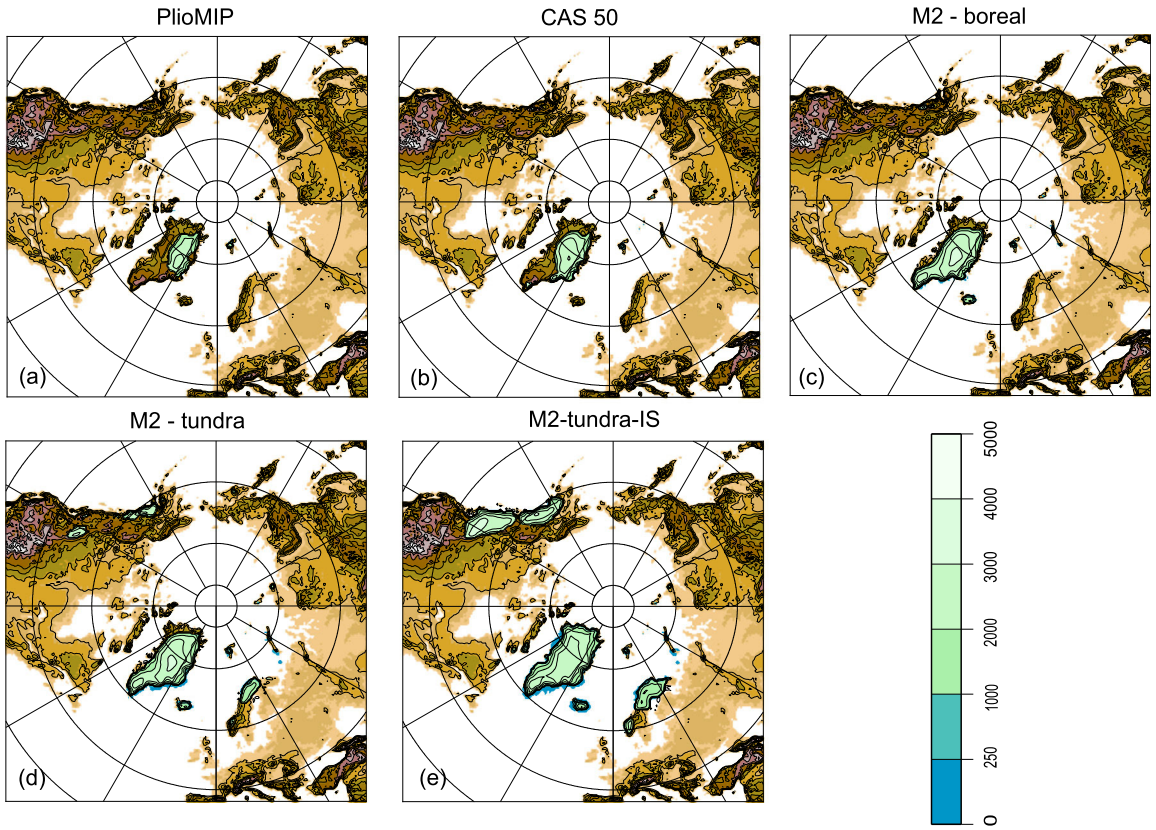


**Fig. 6.** Simulated Northern Hemisphere ice sheet overlain on the paleogeography. Colour bar depicts the ice sheet surface elevation (m) simulated by imposing climate fields of related climate experiments: a) PlioMIP experiment (Contoux et al., 2012), b) CAS50, c) M2-boreal; d) M2-tundra; e). M2-tundra-IS. (For interpretation of the colours in this figure, the reader is referred to the web version of this article.)

area) respectively in M2-boreal and M2-tundra experiments (not shown).

The simulated cooling in the "M2-tundra" experiment not only triggered a large expansion of the Greenland ice sheets but also favoured the nucleation of new ice caps over Alaskan Rockies and Scandinavia (Fig. 6d). In comparison, the boreal forest vegetation specified in the M2-boreal experiment prevents the expansion of an ice sheet outside Greenland (Fig. 6c). This highlights the important role of tundra-albedo feedback on Northern Hemisphere (NH) ice sheet inception, in good agreement with previous studies (De Noblet et al., 1996). The substantial expansion of the NH ice sheets in M2-tundra simulation may lead to positive feedbacks in local climate. We thus performed several "regrowth" experiments (offline coupling) to take into account these feedbacks ("M2-tundra-IS", see Methods). At the end of these steps, the total volume of Northern Hemisphere ice sheets reach $5.54 \times 10^{15}$ m$^3$ (Fig. 6e), corresponding to a sea-level drop of around 12 m, of which 44% is accounted for by Northern Hemisphere ice sheets located outside Greenland. Concerning the evolution of ice sheet volume in all ice sheet experiments, please refer to the Appendix A Fig. A.6.

In addition to the NH ice sheets, the possible contribution of the Antarctic ice sheets (AIS) on the global sea-level drop of M2 glaciation is also considered in this study. When compared to PlioMIP AIS (Fig. 7a), which show a collapse of West Antarctic ice sheets, the simulated MIS M2 AIS volume increases by $\sim 1.5 \times 10^{15}$ m$^3$ (+9%), with a substantial ice sheet expansion in West Antarctica and increased ice shelves both in West and East Antarctica (Fig. 7b), corresponding to a sea-level drop of ~4 m. Since the M2-tundra-IS orbital parameters generate a stronger summer insolation in the southern high latitudes (Fig. A.4), the West Antarctic ice sheet expansion is essentially driven by the lower $CO_2$ concentration comparing to PlioMIP conditions. The surface air temperature in West Antarctica is ~6 °C colder (Fig. A.7a) because of 1) the direct radiative contribution of the lowered atmospheric $CO_2$ and 2) an extended perennial snow cover which further amplifies the cooling by the positive albedo feedback (Fig. A.7b). In addition, the strong cooling in West Antarctic enhances the formation of sea ice (Fig. A.7c), which cools the sub-surface ocean temperatures (Fig. A.7d) and slows down the ice shelf basal melting. The 4 m sea-level drop produced by the additional AIS of M2 glaciation is lower than the data estimations (8–18 m; Naish and Wilson, 2009). However, in contrast to Northern Hemisphere ice sheets, the feedbacks associated with the ice height-mass change from the extended AIS on local and global climate is not taken into account but can favour additional expansion of the Antarctic ice sheets.

To summarise, the most favourable forcing factors for M2 glaciation generates the accumulation of a significant global ice volume of almost 16 m, which falls into the lower range of estimations of sea-level drop for this period (20–60 m), including a ~4 m contribution from the Antarctic ice sheets. The direct climatic impacts of the CAS opening barely contribute to this total volume (~9%) compared to the combined effects of the atmospheric $CO_2$ levels decrease, the favourable boreal summer insolation and the feedbacks of the tundra vegetation and the ice sheet.

### 3.3. The impact of CAS closure on M2 glaciation termination

The second part of the hypothesis of De Schepper et al. (2013) involves the closure of the CAS as a driver for the M2 deglaciation. They propose that the seaway closed following the large accumulation of ice on land. As a consequence, the warm and salty water pool in the Caribbean Sea could rebuild and strengthen the northward heat transport, thereby causing the deglaciation of the NH.

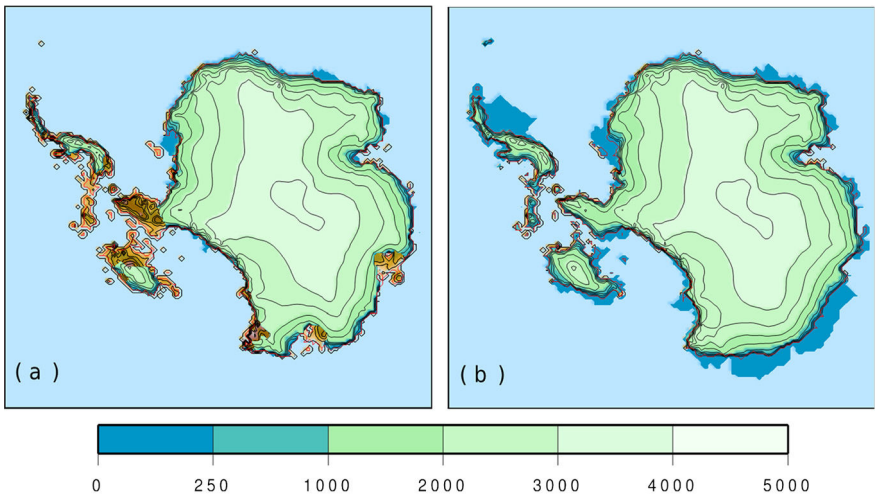


**Fig. 7.** Simulated Antarctic ice sheet overlain on the paleogeography of Antarctic. Colour bar depicts the ice sheet surface elevation (m) simulated by imposing climate fields of related climate experiments: (a) PlioMIP experiment (Contoux et al., 2012); (b) M2-tundra-IS.

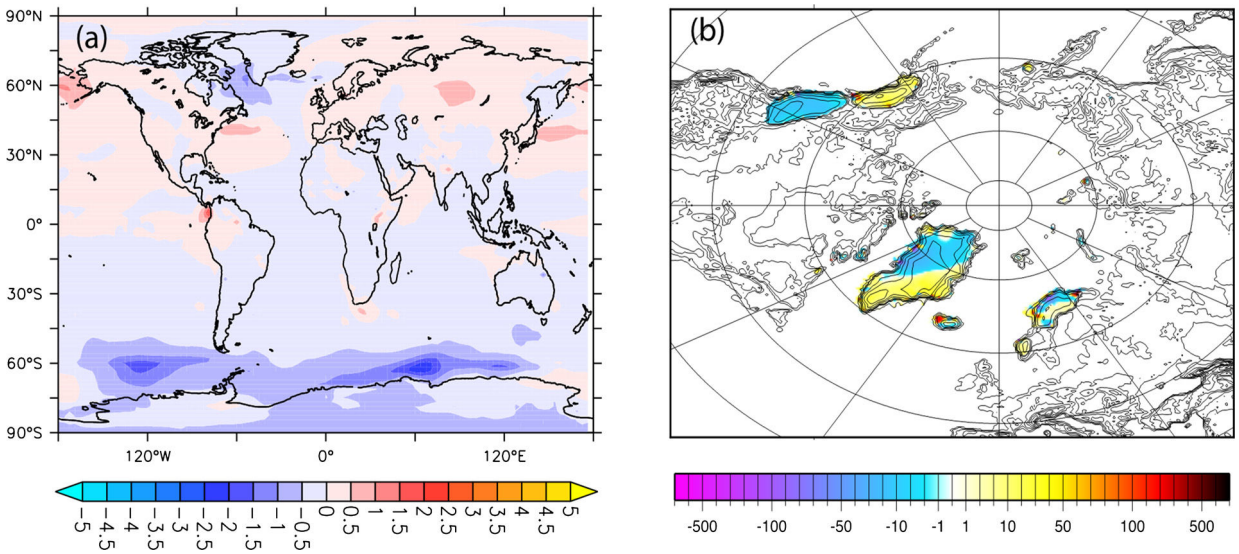


**Fig. 8.** (a) Mean annual surface temperature difference between M2-closeCAS and M2-tundra-IS experiment (K); (b) Simulated North Hemisphere ice sheet thickness difference between M2-closeCAS and M2-tundra-IS (m).

In our CAS closure experiment ("M2-closeCAS), there is a slight decrease of the Atlantic northward heat transport by ~9% south of 20°N but there is no large change in mid-to-high latitudes (Fig. 4, green line) when compared to M2-tundra-IS (Fig. 4, blue dash line). Note that both in M2-tundra-IS and M2-closeCAS, the Atlantic northward heat transport in low-to-mid latitudes is comparable to the pre-industrial level and the decrease magnitudes of NAC speeds relative to PlioMIP are smaller than in M2-tundra (Figs. 3e, 3f). This can be explained by the large ice sheet build-up in the Northern Hemisphere, which helps alter the AMOC strength (Gong et al., 2015). The CAS closure generates a small warming over the Northern Hemisphere, except over Greenland and the North Atlantic and Labrador Sea, where the surface air temperature is slightly colder than in M2-tundra-IS (Fig. 8a). The small impacts of the CAS closure are however not significant to alter the entire climatic state. When imposing this new climatic state in the ice sheet model, we observe both small growth and melt of the ice sheet in different regions, but the total Northern Hemisphere ice sheet volume remains almost unchanged when compared to M2-tundra-IS (Fig. 8b). The weak impact of CAS closure on Northern Hemisphere ice sheets in this study is in good agreement with the closed CAS experiment of Lunt et al. (2008), in which the authors only observe a decrease of the Greenland ice sheet volume of about 0.8 m of equivalent sea level (although with a different CAS configuration).

## 4. Discussion

After opening the CAS (CAS50 experiment), the flow of seawater from the Pacific into the Atlantic helps slow down the North Atlantic Current and decrease the northward heat transport. These features are well consistent with the proxy data (De Schepper et al., 2013). Moreover, the direction of the water flow through the shallow CAS in this study agrees with the findings of Nof and Van Gorder (2003), who demonstrated that the direction of water flow through an open Central American Seaway depends on the initial NADW state: when the NADW is strong enough, the inflow of water is from the Pacific to the Atlantic; in the other case, water flows from the Atlantic to the Pacific. In our CAS50 experiment, the initial NADW state (PlioMIP) is as strong as present-day condition in the model (11–12 Sv), thereby leading to a Pacific-to-Atlantic water flow. In contrast, the water flux through the CAS is reversed in the Sepulchre et al. (2014) shallow CAS experiment (55 m) realised

with an earlier version of the IPSL model, since their initial NADW is three times weaker than present-day.

The "re-opening of the shallow CAS hypothesis" for the glaciation during MIS M2 is an appealing mechanism, since it provides an explanation for both the onset and the termination of a major glaciation in a context of rather high atmospheric $CO_2$ concentrations in the Pliocene. The hypothesis proposes that an open CAS causes decreased ocean heat transport and leads to the expansion of Northern Hemisphere continental ice sheets. This is fundamentally different from the classical theory where the CAS closure leads to increased precipitation in the Northern Hemisphere high latitudes essential for ice sheet expansion (Haug and Tiedemann, 1998). Our study now shows that the sole impact of a shallow re-opening of the CAS on ocean circulation is too weak to trigger a large glaciation. It must be noted that this conclusion is based on the opening CAS with a rather high $CO_2$ concentration (405 ppmv). As presented in Fig. 1, $CO_2$ reconstructions show a large variability during the Pliocene. It is therefore is not clear whether the atmospheric $CO_2$ concentration was high (e.g. 405 ppmv), average or low (e.g. 280 ppmv) around MIS M2. To explore the impact of CAS opening under different greenhouse gases conditions, we also investigated the CAS opening at a lower $CO_2$ concentration (280 ppmv) in our "CAS50p280" experiment (details in Supplementary Table A.1, results in Fig. A.8). Under these conditions, $CO_2$ at 280 ppmv ("CAS50p280"), the impact of opening the CAS increases slightly, allowing ∼2 Sv surface waters from the Pacific to flow into Caribbean region instead of ∼1.2 Sv in "CAS50". As a consequence, the expansion of the NH ice sheets (Fig. 2b) increases with 20% compared to the CAS50 experiment at 405 ppmv $CO_2$. Such increase nevertheless remains too weak to produce a significant glaciation (Fig. A.8). This result, together with previous CAS modelling studies (Brierley and Fedorov, 2016 and reference therein) demonstrating that ice sheet inception is not triggered by CAS closure, suggest that the direct climatic impacts of a shallow CAS on Northern Hemisphere ice sheets development are limited. This view is backed up by a recent data study (Bell et al., 2015), which also suggests a weak impact of the progressive CAS shoaling on ocean circulation during the Early Pliocene. The authors find that the overall structure of the deep Atlantic was largely unaffected by the Early Pliocene CAS shoaling, the larger shift in NADW formation during early Pliocene occurred prior to the main shoaling phase of the CAS (4.2–4.7 Ma).

In addition to the CAS, two other important seaways underwent substantial changes during the Pliocene with potentially considerably effects on global climate: closing of the Indonesian seaway (Cane and Molnar, 2001; Karas et al., 2017 and reference therein) and opening of the Bering Strait (e.g. Horikawa et al., 2015). In the study of Cane and Molnar (2001), they demonstrate that the closure of the Indonesian seaway plays a crucial role in the East African aridification during the Late Pliocene and reduces the northward heat energy transport. The modelling study of Brierley and Fedorov (2016) demonstrates that the opening of the Bering Strait has a stronger climatic effect than CAS opening for glacial inception in the high northern latitudes. Northern Hemisphere cooling may have been amplified by the singular or combined effects of changes at the Indonesian seaway and Bering Strait together with the CAS before the M2 glaciation. However, the timing of these seaway changes are not very well constrained. For instance, the most recent reconstructed topography for the mid Late Pliocene (3.2 Ma) (Dowsett et al., 2016) shows a closed Bering Strait, while the gateway may have been open (occasionally) already from the Miocene to early Pliocene (e.g. Horikawa et al., 2015). In our study, we did not include these two gateway changes.

Our simulations, notably the "M2-tundra-IS" simulation taking into account other climatic forcing factors and ice sheet feedbacks, demonstrate that the prescription of a large $CO_2$ decrease is instrumental in triggering the M2 glaciation whereas the shallow CAS opening is not, although it remains a minor contributor to favourable conditions for ice sheet inception by modulating the ocean circulation. It is also interesting to note that summer insolation variations over northern high latitudes make the case for a large decrease in atmospheric $pCO_2$ during the M2 period. Indeed, the summer insolation minima at 65°N reached during M2 is larger than the three consecutive minima of summer insolation occurring around 2.7 Ma at the time of the onset of a perennial Greenland ice sheets (Fig. A.1). All else being equal, and based on the present study, a large decrease of atmospheric $CO_2$ levels to values below the Pre-industrial level would hence be necessary to compensate for the lower decrease of summer insolation and to contribute to ice sheet growth on both hemispheres. We demonstrate that using 220 ppmv may produce a large ice sheet development. Nevertheless this value corresponds to a large $pCO_2$ decrease. Therefore, we explore additionally a 280 ppmv of $pCO_2$ for "M2-tundra" experiment instead of 220 ppmv (here, we named it as "M2-tundra-p280", details can be found in Supplementary Table A.1, results are shown in Fig. A.8). In comparison with "M2-tundra", "M2-tundra-p280" leads to a decrease of NH ice sheets volume by 33%. More importantly, the extent of the ice sheet is almost completely restricted to Greenland. Although possibly model-dependant this result demonstrates that in order to allow nucleation of ice sheets outside Greenland $pCO_2$ levels are likely to have dropped under 280 ppmv during the MIS M2 glaciation. Further data and modelling studies are however needed to confirm this hypothesis that a large $CO_2$ decrease occurred during the M2 glaciation.

When accounting for all favourable forcing factors for the M2 inception (M2-tundra-IS experiment), we obtain an increased global ice volume of 16 m SLE (sea-level equivalent), which is at the lowest range of the different sea-level records. However, the simulated 16 m sea-level fall is likely to be underestimated in our experiment, since first we do not account for Antarctic ice sheets feedbacks, and second, the "regrowth" method remains an asynchronous coupling between GCM and ISM that may still underestimate the ice sheet growth. The proxy records used for sea-level reconstructions also have large uncertainties and differ among studies. Based on the combination of ostracod Mg/Ca deep ocean temperatures with benthic foraminiferal $\delta^{18}O$ data (Dwyer and Chandler, 2009), the largest estimation of sea-level drop during M2 is nearly half of LGM (∼60 m). Such a large sea-level drop is inconsistent with terrestrial records, which indicates that substantial ice expansion in North America was unlikely during the M2 period (Brigham-Grette et al., 2013). In terms of modelling experiments, Dolan et al. (2015) reveal that a ∼40 m SLE (34 m in NH and 6 m in SH) or a ∼60 m SLE (52 m in NH and 8 m in SH) of M2 glaciation are more consistent with marine proxy data. However, these large area ice sheets in their experiment may not reconcile with their boundary conditions, since these ice sheets are imposed in the model rather than simulated.

There are only a few sea surface temperature (SST) reconstructions available that depict North Atlantic cooling during MIS M2. SST records from five drilling sites in the North Atlantic and Caribbean Sea (shown in Fig. 9 and Table 1) are derived using planktonic foraminiferal Mg/Ca (De Schepper et al., 2013) and alkenones (Lawrence et al., 2009; Naafs et al., 2010; De Schepper et al., 2013). Fig. 9 shows a comparison between the interglacial (pre-M2; 3.332–3.305 Ma) and glacial (Full-M2; 3.305–3.285 Ma) SST anomaly and our simulated SST anomaly. In our modelling study, the "CAS50" experiment can be regarded as the "Pre-M2" condition and "M2-tundra-IS" experiment as "M2 full glaciation". At ODP Site 982 and DSDP Site 610 there is good agreement between model results and data reconstructions (Table 1). At IODP Site U1308, both proxies depict a larger cooling than our model

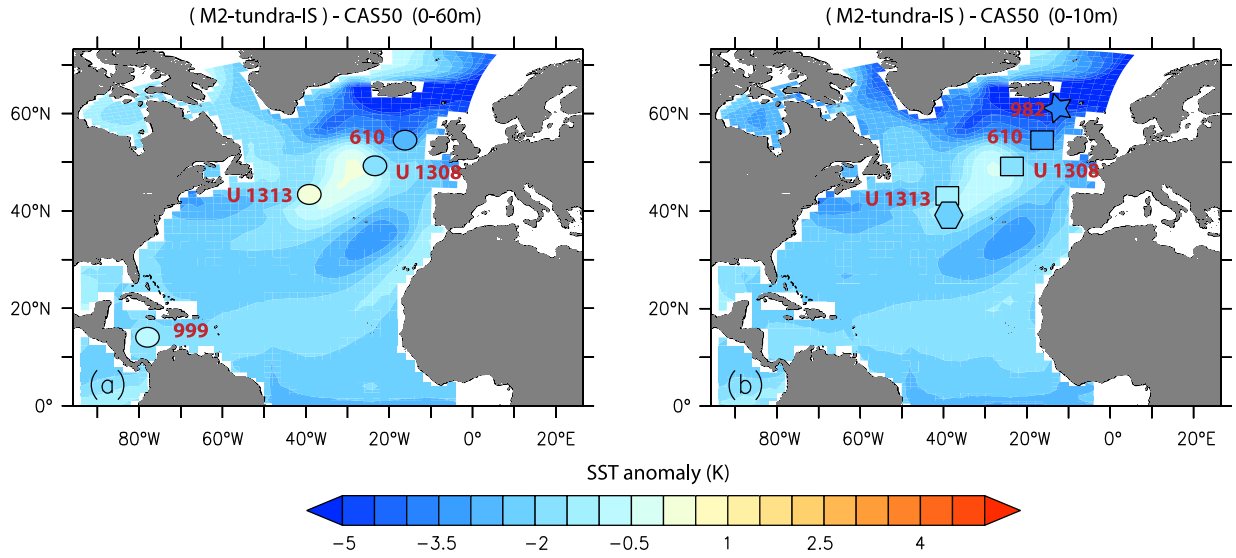


**Fig. 9.** Sea surface temperature (SST) anomaly between "M2 full glaciation" (3.305–3.285 Ma) and "Pre-M2" (3.332–3.305 Ma). The shaded symbols in the figure indicate the proxy data anomalies: the circles are the Mg/Ca-based records (0–60 m, a) from De Schepper et al. (2013); the squares (De Schepper et al., 2013), star (Lawrence et al., 2009) and polygone (Naafs et al., 2010) are the alkenones-based records (0–10 m, b). The background shaded regions represent the anomalies of the model results by comparing the SST (March to August) of "M2-tundra-IS" with that of "CAS50" simulation. The specific values in each ODP sites are shown in Table 1.

**Table 1**
Sea surface temperature (SST) anomaly between "M2 full glaciation" (3.305–3.285 Ma) and "Pre-M2" (3.332–3.305 Ma). Positions of each ODP sites are shown in Fig. 9. The model results are the difference in SST (March to August) between "M2-tundra-IS" and "CAS50" simulation. Indice (1) means data from Lawrence et al. (2009); (2) data are from De Schepper et al. (2013); (3) means data from Naafs et al. (2010).

| DSDP, ODP, IODP sites | Mg/Ca based records (0–60 m) | Model results (0–60 m) | Alkenone based records (0–10 m) | Model results (0–10 m) |
|---|---|---|---|---|
| 982 | – | – | $\Delta T_{(1)} = -3.5\,^{\circ}C$ | $\Delta T = -4.6\,^{\circ}C$ |
| 610 | $\Delta T_{(2)} = -2.5\,^{\circ}C$ | $\Delta T = -2.7\,^{\circ}C$ | $\Delta T_{(2)} = -3.2\,^{\circ}C$ | $\Delta T = -2.8\,^{\circ}C$ |
| U1308 | $\Delta T_{(2)} = -2.3\,^{\circ}C$ | $\Delta T = -0.6\,^{\circ}C$ | $\Delta T_{(2)} = -2.3\,^{\circ}C$ | $\Delta T = -1.0\,^{\circ}C$ |
| U1313 | $\Delta T_{(2)} = 0.8\,^{\circ}C$ | $\Delta T = -0.5\,^{\circ}C$ | $\frac{\Delta T_{(2)} = -1.6\,^{\circ}C}{\Delta T_{(3)} = -2.4\,^{\circ}C}$ | $\Delta T = -0.9\,^{\circ}C$ |
| 999 | $\Delta T_{(2)} = -0.3\,^{\circ}C$ | $\Delta T = -1.9\,^{\circ}C$ | – | – |

results by 1.5 °C. At the IODP Site U1313, there is a large spread between data reconstructions, even using the same proxy. Nevertheless our model results underestimate the cooling in IODP Site U1313 when compared to the alkenones-based reconstructions. In the Caribbean Sea ODP Site 999, our model overestimates the cooling anomaly by ∼1.5 °C. Accounting for the location of this site near from the CAS, this may be attributed to the uncertain timing of CAS open and closing in the data. Considering uncertainties on the timing of the records during MIS M2, the proxies reconstructions accuracy and model variability, the comparison between model results and data reconstructions for MIS M2 cooling draws a rather consistent picture.

In our study, we also show that the M2 glacial termination is not linked to the CAS closure, since the NH ice sheet volume remains almost unchanged (M2-closeCAS experiment) after the CAS closure. The short duration of M2 glaciation may rather result from the weak boreal summer insolation variability during M2. As discussed by Haug and Tiedemann (1998), the low amplitude obliquity during 4.5–3.1 Ma cannot produce cold enough summers to prevent the ice sheet from melting, thus glaciations during this period are hard to develop into large and long-term glaciations.

## 5. Conclusions

The glaciation (3.312–3.264 Ma, MIS M2) occurring just prior to the well-known mid-Pliocene Warm Period (mPWP, ca. 3.3 to 3.0 Ma; Haywood et al., 2016) has always been thought to be enigmatic, since it took place in a warm and high-$CO_2$ climate. Yet the related studies for M2 glaciation are rare (Dolan et al., 2015) and no modelling studies discuss the mechanism of the onset and termination of M2 glaciation. A recent geological hypothesis suggesting the crucial role of re-opening and closing (glacio-eustatic induced) of the shallow Central American Seaway (CAS) (De Schepper et al., 2013) to explain the onset and termination of MIS M2 glaciation has been tested here with a set of modelling experiments.

Here, for the first time, we have investigated the mechanism of the onset of M2 glaciation based on the shallow CAS hypothesis and also accounted for principal forcing factors by using a fully coupled atmosphere ocean general circulation model and dynamic ice sheet model. Our results show that even with the most favourable conditions and all the feedbacks associated, we can only achieve a sea level drop of 16 m corresponding to the lowest estimates, including a 4 m contribution from Antarctica. More importantly, the closing of the CAS does not induce any important melting. Our major finding is therefore the crucial role of $pCO_2$ changes. Future studies should first bring more constrain on carbon climate interaction during MIS M2 and more modelling efforts should be done to simulate this glaciation, notably by exploring potential synergistic effects between the CAS, Bering Strait and Indonesian Seaway.

**Author contributions:** N.T. and G.R. conceived this study. C.D. helped running the ice sheet model. C.C. provided the initial

PlioMIP simulation and helped with the model design. J.B.L., P.S. and Z.S.Z. helped for interpretation of the results. S.D.S. provided the proxy records. All the authors contributed to the preparation of the manuscript.

## Acknowledgements

We thank Oliver Marti for his help with providing the land-sea mask settings. Many thanks to Masa Kageyama, Dider Paillard, Aurelien Quiquet for their help with the model and related discussion. We thank Céline Ramstein for the help with polishing the language. We must thank two anonymous reviewers and the editor for their constructive comments that greatly improved an earlier version of this manuscript. This work was performed using HPC resources from GENCI-TGCC (Grant 2016-GENCI t2016012212) and supported by the French project LEFE "ComPreNdrE" (AO2016-992936), French State Program Investissements d'Avenir (managed by ANR) and the Norwegian Project "OCCP" (NFR project number 221712).

## Appendix A. Supplementary material

Supplementary material related to this article can be found online at http://dx.doi.org/10.1016/j.epsl.2017.04.050.

## References

Álvarez-Solas, J., et al., 2011. Heinrich event 1: an example of dynamical ice-sheet reaction to oceanic changes. Clim. Past 7, 1297–1306. http://dx.doi.org/10.5194/cp-7-1297-2011.

Badger, M.P.S., Schmidt, D.N., Mackensen, A., Pancost, R.D., 2013. High resolution alkenone palaeobarometry indicates relatively stable $pCO_2$ during the Pliocene (3.3 to 2.8 Ma). Philos. Trans. R. Soc. A 371, 20130094.

Bartoli, G., Honisch, B., Zeebe, R.E., 2011. Atmospheric $CO_2$ decline during the Pliocene intensification of Northern Hemisphere glaciations. Paleoceanography 26. http://dx.doi.org/10.1029/2010PA002055.

Bell, D.B., Jung, S.J.A., Kroon, D., Hodell, D.A., Lourens, L.J., Raymo, M.E., 2015. Atlantic deep-water response to the Early Pliocene shoaling of the Central American Seaway. Sci. Rep. 5, 12252. http://dx.doi.org/10.1038/srep12252.

Brierley, C.M., Fedorov, A.V., 2016. Comparing the impacts of Miocene–Pliocene changes in inter-ocean gateways on climate: Central American Seaway, Bering Strait and Indonesia. Earth Planet. Sci. Lett. 444, 116–130. http://dx.doi.org/10.1016/j.epsl.2016.03.010.

Brigham-Grette, J., Melles, M., Minyuk, P., Andreev, A., Tarasov, P., DeConto, R., Koenig, S., Nowaczyk, N., Wennrich, V., Rosen, P., Haltia, E., Cook, T., Gebhardt, C., Meyer-Jacob, C., Snyder, J., Herzschuh, U., 2013. Pliocene warmth, polar amplification, and stepped Pleistocene cooling recorded in NE Arctic Russia. Science 80 (340), 1421–1427. http://dx.doi.org/10.1126/science.1233137.

Cane, M.a, Molnar, P., 2001. Closing of the Indonesian seaway as a precursor to east African aridification around 3±4 million years ago. Nature 411, 157–162. http://dx.doi.org/10.1038/35075500.

Contoux, C., Dumas, C., Ramstein, G., Jost, A., Dolan, A.M., 2015. Modelling Greenland ice sheet inception and sustainability during the Late Pliocene. Earth Planet. Sci. Lett. 424, 295–305. http://dx.doi.org/10.1016/j.epsl.2015.05.018.

Contoux, C., Ramstein, G., Jost, A., 2012. Modelling the mid-Pliocene warm period climate with the IPSL coupled model and its atmospheric component LMDZ5A. Geosci. Model Dev. 5, 903–917. http://dx.doi.org/10.5194/gmd-5-903-2012.

De Noblet, N.I., Prentice, I.C., Joussaume, S., Texier, D., Botta, A., Haxeltine, A., 1996. Possible role of atmosphere–biosphere interactions in triggering the Last Glaciation. Geophys. Res. Lett. 23, 3191. http://dx.doi.org/10.1029/96GL03004.

De Schepper, S., Gibbard, P.L., Salzmann, U., Ehlers, J., 2014. A global synthesis of the marine and terrestrial evidence for glaciation during the Pliocene Epoch. Earth-Sci. Rev. 135, 83–102. http://dx.doi.org/10.1016/j.earscirev.2014.04.003.

De Schepper, S., Groeneveld, J., Naafs, B.D.a, Van Renterghem, C., Hennissen, J., Head, M.J., Louwye, S., Fabian, K., 2013. Northern hemisphere glaciation during the globally warm early Late Pliocene. PLoS ONE 8, e81508. http://dx.doi.org/10.1371/journal.pone.0081508.

DeConto, R.M., Pollard, D., 2003. Rapid Cenozoic glaciation of Antarctica induced by declining atmospheric $CO_2$. Nature 421, 245–249. http://dx.doi.org/10.1038/nature01290.

Dolan, A.M., Haywood, A.M., Hunter, S.J., Tindall, J.C., Dowsett, H.J., Hill, D.J., Pickering, S.J., 2015. Modelling the enigmatic Late Pliocene Glacial Event – Marine Isotope Stage M2. Glob. Planet. Change 128, 47–60. http://dx.doi.org/10.1016/j.gloplacha.2015.02.001.

Dowsett, H.J., et al., 2012. Assessing confidence in Pliocene sea surface temperatures to evaluate predictive models. Nat. Clim. Change 2, 365–371. http://dx.doi.org/10.1038/nclimate1455.

Dowsett, H., et al., 2016. The PRISM4 (mid-Piacenzian) palaeoenvironmental reconstruction. Clim. Past Discuss. 4, 1–39. http://dx.doi.org/10.5194/cp-2016-33.

Dufresne, J.L., et al.. Climate change projections using the IPSL-CM5 Earth System Model: from CMIP3 to CMIP5. Clim. Dyn. (2013). http://dx.doi.org/10.1007/s00382-012-1636-1.

Dwyer, G.S., Chandler, M.a, 2009. Mid-Pliocene sea level and continental ice volume based on coupled benthic Mg/Ca palaeotemperatures and oxygen isotopes. Philos. Trans. R. Soc., Math. Phys. Eng. Sci. 367, 157–168. http://dx.doi.org/10.1098/rsta.2008.0222.

Ganopolski, a., Calov, R., 2011. The role of orbital forcing, carbon dioxide and regolith in 100 kyr glacial cycles. Clim. Past 7, 1415–1425. http://dx.doi.org/10.5194/cp-7-1415-2011.

Gasson, E., et al., 2014. Uncertainties in the modelled $CO_2$ threshold for Antarctic glaciation. Clim. Past 10, 451–466. http://dx.doi.org/10.5194/cp-10-451-2014.

Gong, X., Zhang, X., Lohmann, G., Wei, W., Zhang, X., Pfeiffer, M., 2015. Higher Laurentide and Greenland ice sheets strengthen the North Atlantic ocean circulation. Clim. Dyn. 45, 139–150. http://dx.doi.org/10.1007/s00382-015-2502-8.

Groeneveld, J., Hathorne, E.C., Steinke, S., DeBey, H., Mackensen, A., Tiedemann, R., 2014. Glacial induced closure of the Panamanian Gateway during Marine Isotope Stages (MIS) 95–100 (∼2.5 Ma). Earth Planet. Sci. Lett. 404, 296–306.

Haug, G.H., Tiedemann, R., 1998. Effect of the formation of the Isthmus of Panama on Atlantic Ocean thermohaline circulation. Nature 393, 673–676. http://dx.doi.org/10.1038/31447.

Haywood, A.M., Dowsett, H.J., Dolan, A.M., 2016. Integrating geological archives and climate models for the mid-Pliocene warm period. Nat. Commun. 7, 10646. http://dx.doi.org/10.1038/ncomms10646.

Hill, D.J., Haywood, A.M., Hindmarsh, R.C.A., Valdes, P.J., 2007. Characterizing Ice Sheets During the Pliocene: Evidence from Data and Models. Geological Society of London.

Horikawa, K., Martin, E.E., Basak, C., Onodera, J., Seki, O., Sakamoto, T., Ikehara, M., Sakai, S., Kawamura, K., 2015. Pliocene cooling enhanced by flow of low-salinity Bering Sea water to the Arctic Ocean. Nat. Commun. 6, 7587. http://dx.doi.org/10.1038/ncomms8587.

Hourdin, F., et al., 2006. The LMDZ4 general circulation model: climate performance and sensitivity to parametrized physics with emphasis on tropical convection. Clim. Dyn. 27, 787–813. http://dx.doi.org/10.1007/s00382-006-0158-0.

Jackson, J.B., Jung, P., Coates, A.G., Collins, L.S., 1993. Diversity and extinction of tropical American mollusks and emergence of the Isthmus of Panama. Science 260, 1624–1626.

Kageyama, M., Braconnot, P., Bopp, L., Caubel, A., Foujols, M.-A., Guilyardi, E., Khodri, M., Lloyd, J., Lombard, F., Mariotti, V., Marti, O., Roy, T., Woillez, M.-N., 2013. Mid-Holocene and Last Glacial Maximum climate simulations with the IPSL model—part I: comparing IPSL_CM5A to IPSL_CM4. Clim. Dyn. 40, 2447–2468. http://dx.doi.org/10.1007/s00382-012-1488-8.

Karas, C., et al., 2017. Pliocene oceanic seaways and global climate. Sci. Rep. 7, 39842. http://dx.doi.org/10.1038/srep39842.

Koenig, S.J., DeConto, R.M., Pollard, D., 2011. Late Pliocene to Pleistocene sensitivity of the Greenland Ice Sheet in response to external forcing and internal feedbacks. Clim. Dyn. 37, 1247–1268. http://dx.doi.org/10.1007/s00382-011-1050-0.

Ladant, J.-B., Donnadieu, Y., Lefebvre, V., Dumas, C., 2014. The respective role of atmospheric carbon dioxide and orbital parameters on ice sheet evolution at the Eocene–Oligocene transition. Paleoceanography 29, 810–823. http://dx.doi.org/10.1002/2013PA002593.

Laskar, J., Robutel, P., Joutel, F., Gastineau, M., Correia, a.C.M., Levrard, B., 2004. A long-term numerical solution for the insolation quantities of the Earth. Astron. Astrophys. 428, 261–285. http://dx.doi.org/10.1051/0004-6361:20041335.

Lawrence, K.T., Herbert, T.D., Brown, C.M., Raymo, M.E., Haywood, A.M., 2009. High-amplitude variations in North Atlantic sea surface temperature during the early Pliocene warm period. Paleoceanography 24, 1–15. http://dx.doi.org/10.1029/2008PA001669.

Lisiecki, L.E., Raymo, M.E., 2005. A Pliocene–Pleistocene stack of 57 globally distributed benthic $\delta^{18}O$ records. Paleoceanography 20. http://dx.doi.org/10.1029/2004PA001071.

Lunt, D.J., Foster, G.L., Haywood, A.M., Stone, E.J., 2008. Late Pliocene Greenland glaciation controlled by a decline in atmospheric $CO_2$ levels. Nature 454, 1102–1105. http://dx.doi.org/10.1038/nature07223.

Madec, G., 2008. NEMOocean engine. Technical note. IPSL. Available at: http://www.nemo-ocean.eu/About-NEMO/Reference-manuals, NEMO book v3 4.pdf (last accessed 22 May 2012).

Martínez-Botí, M.A., Foster, G.L, Chalk, T.B., Rohling, E.J., Sexton, P.F., Lunt, D.J., Pancost, R.D., Badger, M.P.S., Schmidt, D.N., 2015. Plio-Pleistocene climate sensitivity evaluated using high-resolution $CO_2$ records. Nature 518, 49–54. http://dx.doi.org/10.1038/nature14145.

Miller, K.G., Wright, J.D., Browning, J.V., Kulpecz, A., Kominz, M., Naish, T.R., Cramer, B.S., Rosenthal, Y., Peltier, W.R., Sosdian, S., 2012. High tide of the warm Pliocene: implications of global sea level for Antarctic deglaciation. Geology 40, 407–410. http://dx.doi.org/10.1130/G32869.1.

Naafs, B.D.A., Stein, R., Hefter, J., Khélifi, N., De Schepper, S., Haug, G.H., 2010. Late Pliocene changes in the North Atlantic Current. Earth Planet. Sci. Lett. 298, 434–442. http://dx.doi.org/10.1016/j.epsl.2010.08.023.

Naish, T.R., Wilson, G.S., 2009. Constraints on the amplitude of Mid-Pliocene (3.6–2.4 Ma) eustatic sea-level fluctuations from the New Zealand shallow-marine sediment record. Philos. Trans. R. Soc., Math. Phys. Eng. Sci. 367, 169–187. http://dx.doi.org/10.1098/rsta.2008.0223.

Nof, D., Van Gorder, S., 2003. Did an open Panama Isthmus correspond to an invasion of Pacific water into the Atlantic? J. Phys. Oceanogr. 33, 1324–1336. http://dx.doi.org/10.1175/1520-0485(2003)033<1324:DAOPIC>2.0.CO;2.

Pagani, M., Zachos, J.C., Freeman, K.H., Tripple, B., Bohaty, S., 2005. Marked decline in atmospheric carbon dioxide concentrations during the Paleocene. Science 309 (5734), 600–603. http://dx.doi.org/10.1126/science.1110063.

Panitz, S., Salzmann, U., Risebrobakken, B., De Schepper, S., Pound, M.J., 2016. Climate variability and long-term expansion of peatlands in Arctic Norway during the late Pliocene (ODP Site 642, Norwegian Sea). Clim. Past 12, 1043–1060. http://dx.doi.org/10.5194/cp-12-1043-2016.

Riesselman, C.R., Dunbar, R.B., 2013. Diatom evidence for the onset of Pliocene cooling from AND-1B, McMurdo Sound, Antarctica. Palaeogeogr. Palaeoclimatol. Palaeoecol. 369, 136–153. http://dx.doi.org/10.1016/j.palaeo.2012.10.014.

Ritz, C., Rommelaere, V., Dumas, C., 2001. Modeling the evolution of Antarctic ice sheet over the last 420,000 years: implications for altitude changes in the Vostok region. J. Geophys. Res. 106, 31943. http://dx.doi.org/10.1029/2001JD900232.

Salzmann, U., Haywood, A.M., Lunt, D.J., Valdes, P.J., Hill, D.J., 2008. A new global biome reconstruction and data-model comparison for the Middle Pliocene. Glob. Ecol. Biogeogr. 17, 432–447. http://dx.doi.org/10.1111/j.1466-8238.2008.00381.x.

Seki, O., Foster, G.L., Schmidt, D.N., Mackensen, A., Kawamura, K., Pancost, R.D., 2010. Alkenone and boron-based Pliocene $pCO_2$ records. Earth Planet. Sci. Lett. 292, 201–211. http://dx.doi.org/10.1016/j.epsl.2010.01.037.

Sepulchre, P., et al., 2014. Consequences of shoaling of the Central American Seaway determined from modeling Nd isotopes. Paleoceanography 29, 176–189. http://dx.doi.org/10.1002/2013PA002501.

Stap, L.B., de Boer, B., Ziegler, M., Bintanja, R., Lourens, L.J., van de Wal, R.S.W., 2016. $CO_2$ over the past 5 million years: continuous simulation and new $\delta^{11}$B-based proxy data. Earth Planet. Sci. Lett. 439, 1–10. http://dx.doi.org/10.1016/j.epsl.2016.01.022.

Van De Wal, R.S.W., De Boer, B., Lourens, L.J., Köhler, P., Bintanja, R., 2011. Reconstruction of a continuous high-resolution $CO_2$ record over the past 20 million years. Clim. Past 7, 1459–1469. http://dx.doi.org/10.5194/cp-7-1459-2011.

Zachos, J., Pagani, M., Sloan, L., Thomas, E., Billups, K., 2001. Trends, rhythms, and aberrations in global climate 65 Ma to present. Science 292 (5517), 686–693. http://dx.doi.org/10.1126/science.1059412.

## Appendix A. Supplementary material

The following is the Supplementary material related to the article.

**Table A.1** Boundary conditions in the experiments.

| Experiment | CO2 (ppmv) | Orbital parameters | Topography & Initial ice sheet | Vegetation | CAS | Length of AOGCM simulations | Length of ice sheet simulations |
|---|---|---|---|---|---|---|---|
| **PlioMIP**[28] | 405 | Pre-industrial | PRISM3 | PRISM3 | close | 650 yrs | 100 kyrs |
| **CAS50** | 405 | Pre-industrial | PRISM3 | PRISM3 | open | 400 yrs | 100 kyrs |
| CAS50p280 | 280 | Pre-industrial | PRISM3 | PRISM3 | open | 250 yrs | 100 kyrs |
| **M2-tundra** | 220 | 3.313 Ma | PRISM3 | Modified PRISM3** | open | 200 yrs | 100 kyrs |
| M2-tundra-p280 | 280 | 3.313 Ma | PRISM3 | Modified PRISM3** | open | 200 yrs | 100 kyrs |
| **M2-boreal** | 220 | 3.313 Ma | PRISM3 | PRISM3 | open | 200 yrs | 100 kyrs |
| **M2-tundra-IS** | 220 | 3.313 Ma | PRISM3* | Modified PRISM3** | open | 200 yrs | 100 kyrs |
| **M2-closeCAS** | 220 | 3.313 Ma | PRISM3* | Modified PRISM3** | close | 400 yrs | 100 kyrs |

More details about PRISM3 data can be found in (Dowsett et al., 2012; Salzmann et al., 2008)

* Topography is kept align with PRISM3 except of the ice sheet regions, where ice sheet and topography are derived from the second climate-ice regrowth simulation of M2-tundra.

** Replace boreal biomes north of 50°N with tundra biomes based on the PRISM3D vegetation map

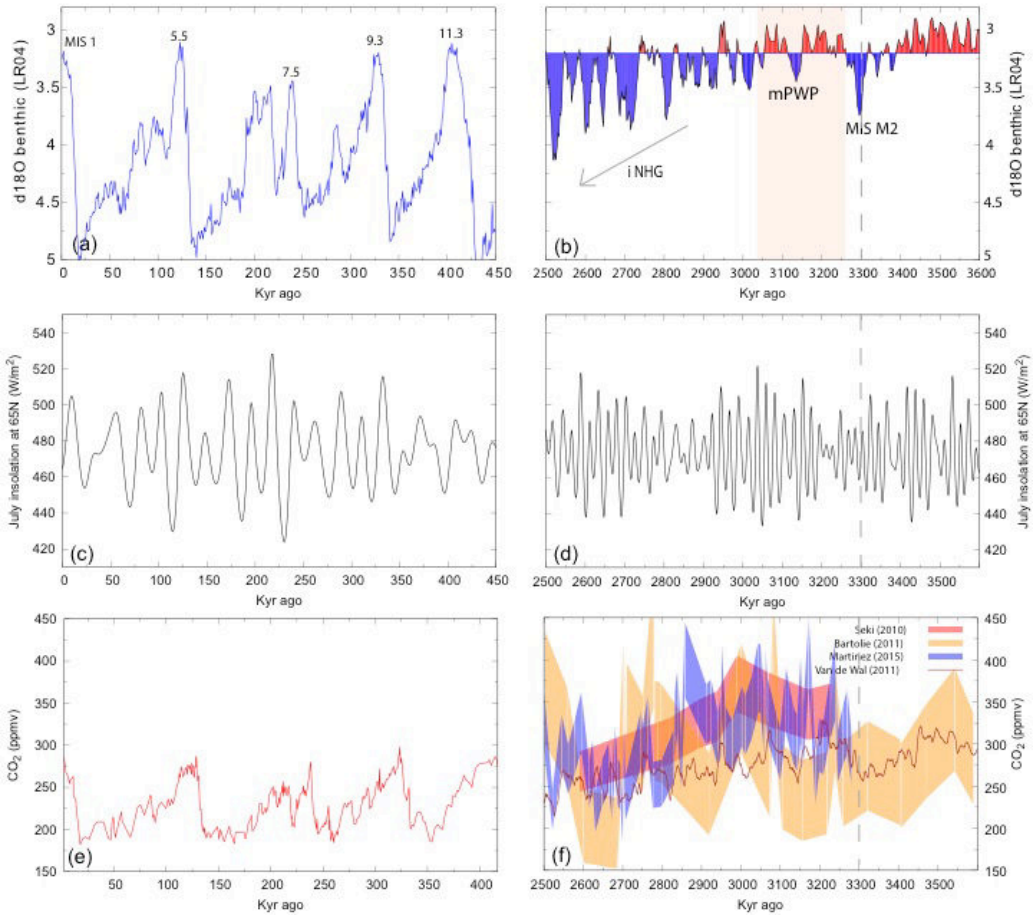


**Figure. A.1**. The comparison between Piacenzian (3.6-2.58 Ma) and the past 420,000 years in terms of Benthic $\delta^{18}O$ (a, b) (Lisiecki and Raymo, 2005); July solar radiation at 65 °N (Laskar et al., 2004) (c,d; W/m$^2$) and Reconstructed atmospheric$CO_2$ concentration (e; Petit et al., 1999 ), (f ; Bartoli et al., 2011; Martínez-Botí et al., 2015; Seki et al., 2010; Van De Wal et al., 2011)

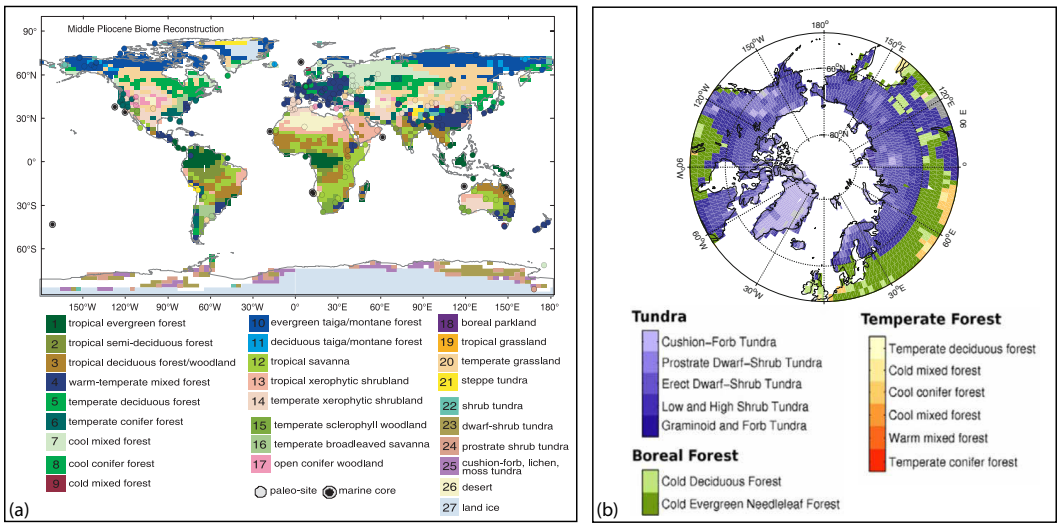


**Figure. A.2** Vegetation distribution in PRISM3 (a; modified after Salzmann et al. 2008); Dynamical vegetation model simulated tundra distribution north of 50N in response to cold orbit and 200ppmv of pCO2 (b; modified after Koenig et al. 2011)

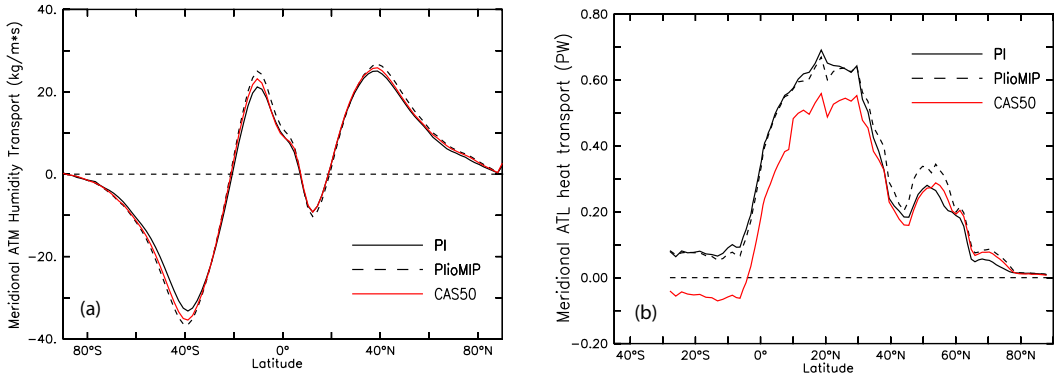


**Figure. A.3** (a) Meridional humidity transport in Atmosphere and (b) Meridional heat transport in the Atlantic Ocean.

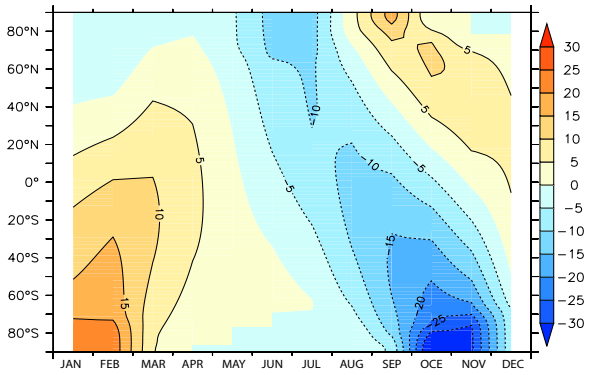


**Figure. A.4** Difference in incoming solar radiation at the top of atmosphere between 3.313 Ma and Pre-industrial level ($W/m^2$).

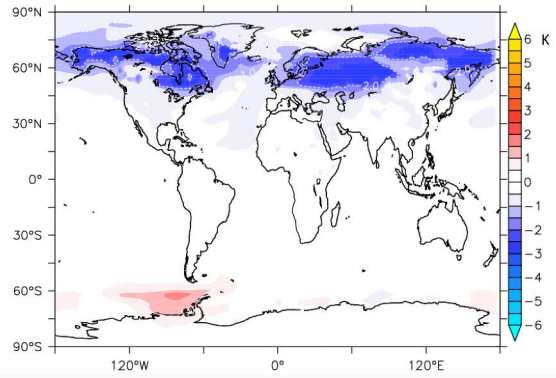


**Figure. A.5** Difference in mean annual surface temperature between M2-tundra and M2-boreal experiment.

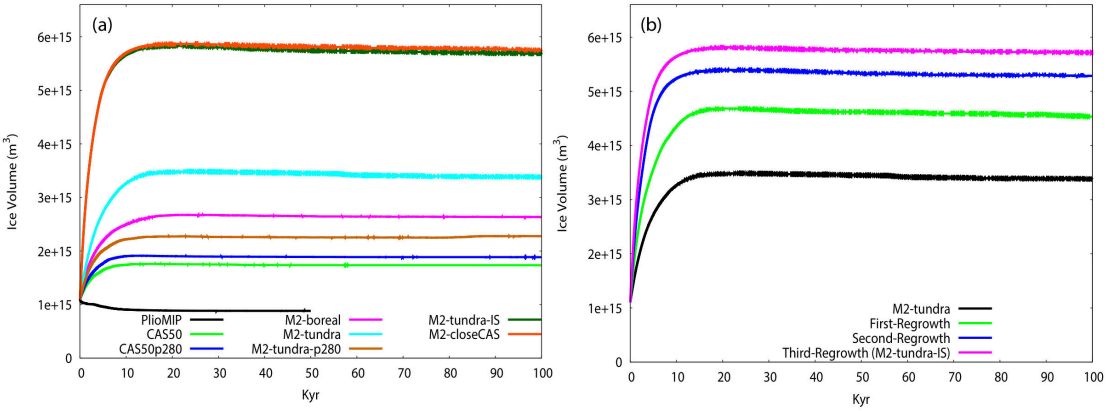

**Figure. A.6** Simulated NH ice sheet evolution for all principle experiments (a); Simulated NH ice sheet evolution for regrowth experiments (b)

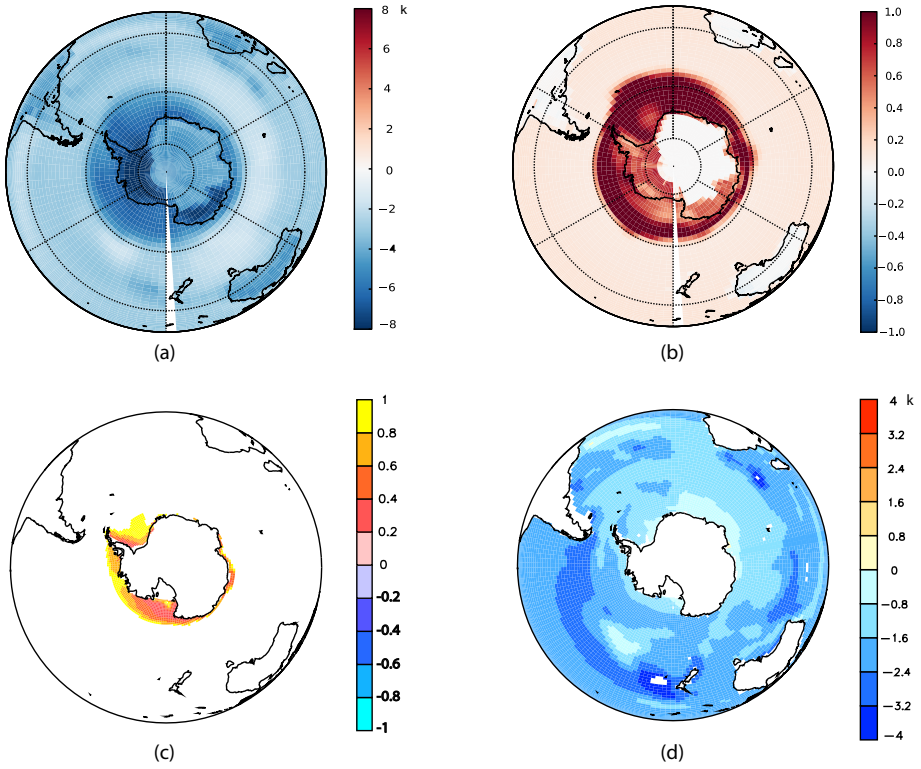


**Figure. A.7** Differences between M2-tundra-IS and PlioMIP in mean annual air surface temperature at 2 meters (a); in mean annual surface albedo (ratio) (b); in mean annual sea ice fraction (ratio) (c); in mean annual ocean temperature at the depth of 300 meters (d).

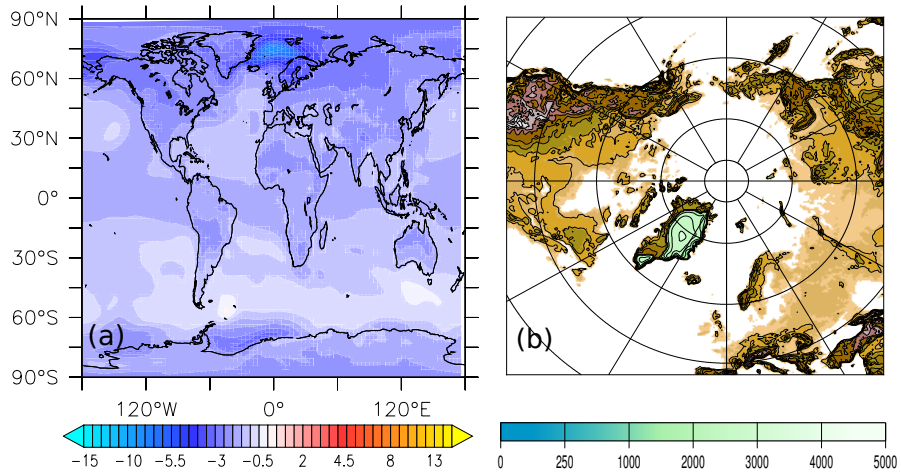


**Figure. A.8** Mean annual temperature difference between CAS50 and CAS50p280 (a); simulated northern hemisphere ice sheet with the climate of CAS50p280 (b).

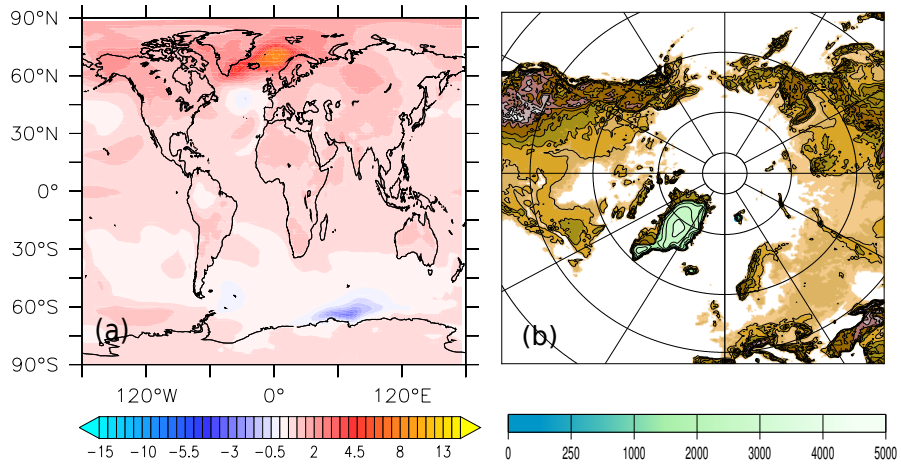


**Figure. A.9** Mean annual temperature difference between M2-tundra-p280 and M2-tundra(a); simulated northern hemisphere ice sheet with the climate of M2-tundra-p280 (b).

## References

Bartoli, G., Hönisch, B., Zeebe, R.E., 2011. Atmospheric CO2 decline during the Pliocene intensification of Northern Hemisphere glaciations. Paleoceanography 26. doi:10.1029/2010PA002055

Dowsett, H.J., Robinson, M.M., Haywood, A.M., Hill, D.J., Dolan, A.M., Stoll, D.K., Chan, W.-L., Abe-Ouchi, A., Chandler, M.A., Rosenbloom, N.A., Otto-Bliesner, B.L., Bragg, F.J., Lunt, D.J., Foley, K.M., Riesselman, C.R.,

2012. Assessing confidence in Pliocene sea surface temperatures to evaluate predictive models. Nat. Clim. Chang. 2, 365–371. doi:10.1038/nclimate1455

Koenig, S.J., DeConto, R.M., Pollard, D., 2011. Late Pliocene to Pleistocene sensitivity of the Greenland Ice Sheet in response to external forcing and internal feedbacks. Clim. Dyn. 37, 1247–1268. doi:10.1007/s00382-011-1050-0

Laskar, J., Robutel, P., Joutel, F., Gastineau, M., Correia, a. C.M., Levrard, B., 2004. A long-term numerical solution for the insolation quantities of the Earth. Astron. Astrophys. 428, 261–285. doi:10.1051/0004-6361:20041335

Lisiecki, L.E., Raymo, M.E., 2005. A Pliocene-Pleistocene stack of 57 globally distributed benthic δ 18 O records. Paleoceanography 20, n/a–n/a. doi:10.1029/2004PA001071

Martínez-Botí, M. a., Foster, G.L., Chalk, T.B., Rohling, E.J., Sexton, P.F., Lunt, D.J., Pancost, R.D., Badger, M.P.S., Schmidt, D.N., 2015. Plio-Pleistocene climate sensitivity evaluated using high-resolution CO2 records. Nature 518, 49–54. doi:10.1038/nature14145

Salzmann, U., Haywood, A.M., Lunt, D.J., Valdes, P.J., Hill, D.J., 2008. A new global biome reconstruction and data-model comparison for the Middle Pliocene. Glob. Ecol. Biogeogr. 17, 432–447. doi:10.1111/j.1466-8238.2008.00381.x

Seki, O., Foster, G.L., Schmidt, D.N., Mackensen, A., Kawamura, K., Pancost, R.D., 2010. Alkenone and boron-based Pliocene pCO2 records. Earth Planet. Sci. Lett. 292, 201–211. doi:10.1016/j.epsl.2010.01.037

Van De Wal, R.S.W., De Boer, B., Lourens, L.J., Köhler, P., Bintanja, R., 2011. Reconstruction of a continuous high-resolution CO 2 record over the past 20 million years. Clim. Past 7, 1459–1469. doi:10.5194/cp-7-1459-2011

## 3.4 Summary

The Marine Isotope Stage M2 (3.264-3.312 Ma) occurred just prior to the well documented warm mid-Pliocene (mPWP). With a 0.5‰benthic foraminiferal $\delta^{18}O$ shift (Lisiecki and Raymo, 2005), MIS M2 is thought to be a glacial comparable period associated with huge but uncertain sea-level records of 2060m below present level (Naish et al. 2009; Miller et al. 2012; Dwyer et al. 2009). However, the mechanism of M2 initiation and termination are still an enigma, since CO2 records were relatively higher than the Quaternary glaciation period and the minima summer insolation during M2 was stronger than other glacial periods. By inferring from marine proxy data, De Schepper (2013) proposed that the shallow open Central American Seaway (CAS) observed during M2 could play as a trigger in M2 initiation, then the closure of this shallow CAS resulted from M2 large ice sheet buildup terminates this glacial period. But this assumption has not been tested by the model.

In this study, we apply IPSL-CM5A Atmosphere-Ocean coupled General Circulation Model (AOGCM) and GRISLI ice sheet model to investigate mechanisms of M2 initiation and termination. We firstly investigate the role of "shallow opening CAS" (De Schepper et al. 2013) on M2 initiation. In the mean time we also take into account the main forcing during M2, which includes astronomical parameters, Greenhouse gases and vegetation. Our results show that shallow opening CAS plays an important role in reducing northward heat transport in Atlantic low latitudes by 0.05-0.1 PW, but it is not a key factor in NH ice sheet build-up; Astronomical parameters and low pCO2 concentration are essential to create a basic global cooling environment for M2 (cooling by about 3.65 K than mPWP); Cold vegetation replacement amplifies the cooling in north high latitudes by about 8 K, which finally allows large ice sheet building up in Northern Hemisphere (12.25 m sea level drop is simulated with considering ice sheet feedback on the climate) and a large expansion in West Antarctic ice sheet which provides about 4m sea level drop. The simulated ice sheet locations and areas correspond well to the terrestrial ice evidence. The diagnostics in the Atlantic Ocean also suggest a better agreement with data especially in terms of sea surface temperature and North Atlantic Current change. Finally, to explore the relationship between M2 termination and the closure of shallow CAS, we close CAS based on the simulation with large ice sheet built-up scenario. However, after the closure of this shallow CAS, we observed a small change in NH ice sheet which is in the agreement with

previous CAS studies (Lunt et al. 2008). Our major finding in this study is therefore the crucial role of pCO2 changes.Future studies should first bring more constrain on carbon climate interaction during MIS M2 and more modeling efforts should be done to simulate this glaciation, notably by exploring potential synergistic effects between the CAS, Bering Strait and Indonesian Seaway.

# Chapter 4

# Simulating Mid-Piacenzian Warm Period

## Contents

## 4.1 Introduction

The MPWP (3.264 to 3.025 Ma, Figure.4.1) following MIS M2 glaciation is well studied and discussed due to its warmer-than-present climate and its similar-to-present pCO2. Studies on this period enable us to better understand the mechanism under warm condition and to know the models' abilities in simulating warm climate. Most of these studies are in the frame of Pliocene Model Intercomparison Project (PlioMIP) and Pliocene Research Interpretation and Synoptic Mapping project (PRISM). In this chapter, I will introduce our modeling study on the MPWP involved in the PlioMIP phase 2 project. A paper has been prepared for this study which is shown in the second section of this chapter. Before going to the paper, I will provide a short review of the PlioMIP projects and its related results as following.

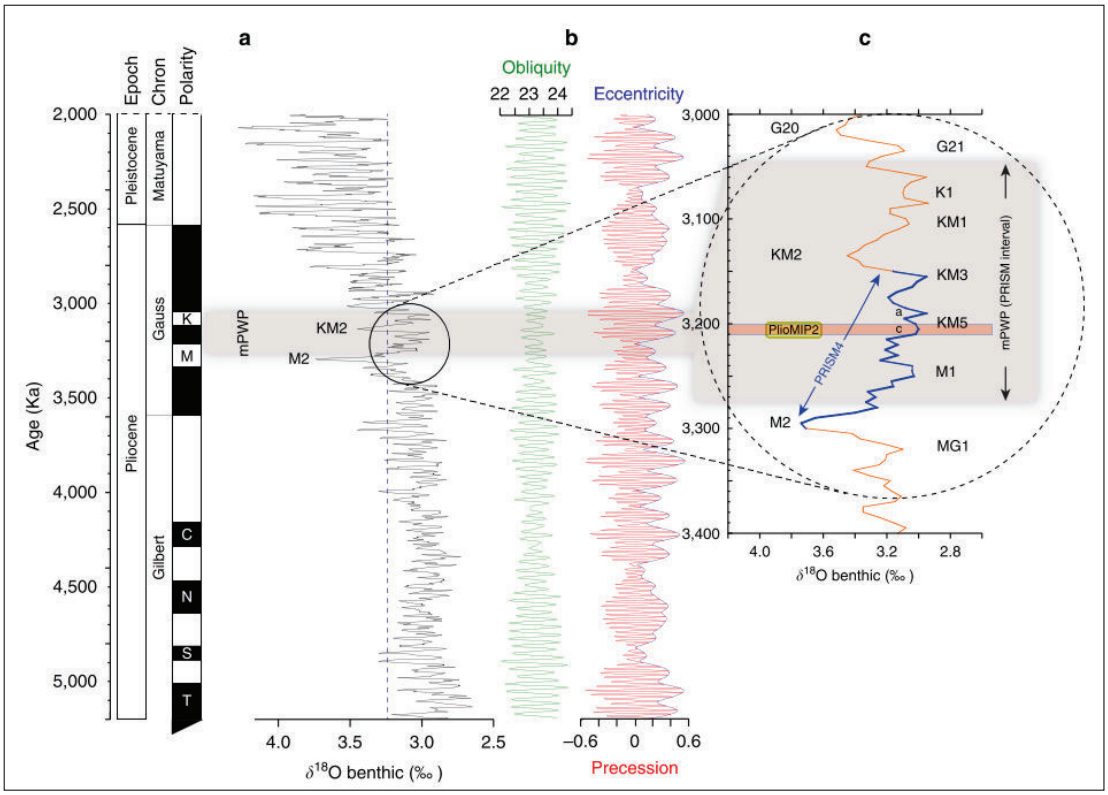


Figure 4.1 – The LR04 benthic oxygen isotope stack (Lisiecki and Raymo, 2005) and Orbital parameters (Laskar et al., 2004) for the Pliocene interval. Figure after (Haywood et al., 2016)

## 4.2 PlioMIP and PRISM project

The Pliocene Model Intercomparison Project (PlioMIP) initiated in 2008 is a co-ordinated international climate modelling initiative to study and understand climate and environments of the Late Pliocene (MPWP), and their potential relevance in the context of future climate change. PlioMIP operates under the umbrella of the Palaeoclimate Modelling Intercomparison Project (PMIP), which examines multiple intervals in Earth history, the consistency of model predictions in simulating these intervals and their ability to reproduce geological climate archives. The PlioMIP is closely aligned with the US Geological Survey Initiative known as PRISM (Pliocene Research Interpretation and Synoptic Mapping), which has for more than 20 years focused on the reconstruction and understanding of mid-Pliocene climate ( 3.3 to 3 million years ago), as well as the production of boundary condition data sets suitable for use with numerical climate model simulations.(from: $https://geology.er.usgs.gov/egpsc/prism/7_pliomip2.html$)

The MPWP is always considered to be an analogue for the future climate change, which is the initial reason for the PlioMIP project. But along with the recognition of the

climate equilibrium, the "analogue" concept is denied. Since the MPWP is an equilibrate state but the modern climate is non-equilibrium due to the continuous change of the forcing factors. Thus the purpose of the PlioMIP turns to better understand the MPWP itself and to study the mechanism under warm climate. Moreover the model intercomparison work enable to know how the model abilities in simulating warm climate. All these objectives can still serve the future climate projections as well as improve the model competences.

The PlioMIP project now has two phases linking to the updating of boundary conditions provided by PRISM project. The PlioMIP phase 1 (PlioMIP1) commenced at 2008 associated with PRISM3(D) is already finished. The PlioMIP phase 2 (PlioMIP2) corresponding to PRISM4 has been launched since 2014.Tens of modeling groups from the world have been participated in this project.The major results of PlioMIP1 and the objectives of PlioMIP2 will be introduced in the next section.

### 4.2.1 Major Results of PlioMIP1 and the objective of PlioMIP 2

In PlioMIP1, the simulated global annual mean surface temperatures increased by 1.84-3.6°C (Fig.4.2, (Haywood et al., 2013)).The IPSL model represented a warming by 2.07°C in the AOGCMs result (Contoux et al., 2012). The simulated gloal annual mean surface temperatures across models show consistency in the tropics but lack of consistency in high latitudes. The modeled Atlantic Meridional Overturning Circulation (AMOC) was predicted as present conditions, which did not support enhanced AMOC as well as enhanced pole-ward heat transport during the MPWP.The predicted AMOC in IPSL is about 11 Sv representing a relatively weaker AMOC than other models(Zhang et al., 2013). The albedo feedback, majorly associated with landice and snow cover and Greenhouse gases were identified to be important roles in high latitude climate for the MPWP. Regionally, the simulated weakened East Asian winter winds in north monsoon China and intensified East Asian summer winds in monsoon China agreed well with geological reconstructions (Zhang et al., 2013). The simulated tropical overturning circulations in the MPWP were weaker than preindustrial circulations, just as they are projected to be in future climate change (Corvec and Fletcher, 2017) The weakening HC response is consistent with future projections, and its strength is strongly related to the meridional gradient of sea surface warming between the tropical and subtropical oceans. However, the data-model compar-

ison show that the models' results underestimated the magnitude of polar amplification (Dowsett et al., 2013; Salzmann et al., 2011) (Fig.4.3).

PlioMIP1 was the first attempt to provide the framework for modeling warmer than pre-industrial climate with higher pCO2 values. Many GCMs provided simulations for intercomparison studies associated with many publications (e.g.,Haywood et al.,2016 and reference therein). However the weaknesses of this phase are majorly attributed to unrealistic boundary conditions and the concept of "average" warm period.Therefore, PlioMIP2 is launched with choosing a specific interglacial period (MIS KM5c,3.205),which has an orbital forcing similar to present and largely retains many warm conditions on which the PlioMIP1 focused. Accordingly, new boundary conditions (PRISM4) are updated for the PlioMIP2 experiments.Comparing to the PRISM3, the PRISM4 (Fig.4.4,(Dowsett et al., 2016)) provides a new topography and bathymetry in which the Bering strait and Canadian Archipelago seaway are closed, the Greenland ice sheet reduce by 50% and the topography is more near modern conditions. Moreover, in PRISM4, the maps of reconstructed soil types and paleolakes are provided, but the sea surface temperatures and vegetation are kept the same as in the PlioMIP1. Meanwhile,the data scientists in the PRISM community are working on reconstructing high time-resolution proxy data focusing on the key regions which is important for understanding the MPWP warmth. These new proxy-data are more appropriate for the data-model comparison.Standard time series data will also provided to better understand the climate variability(Haywood et al., 2015).This study is involved in the PlioMIP2 project. More details can be found in the next section.

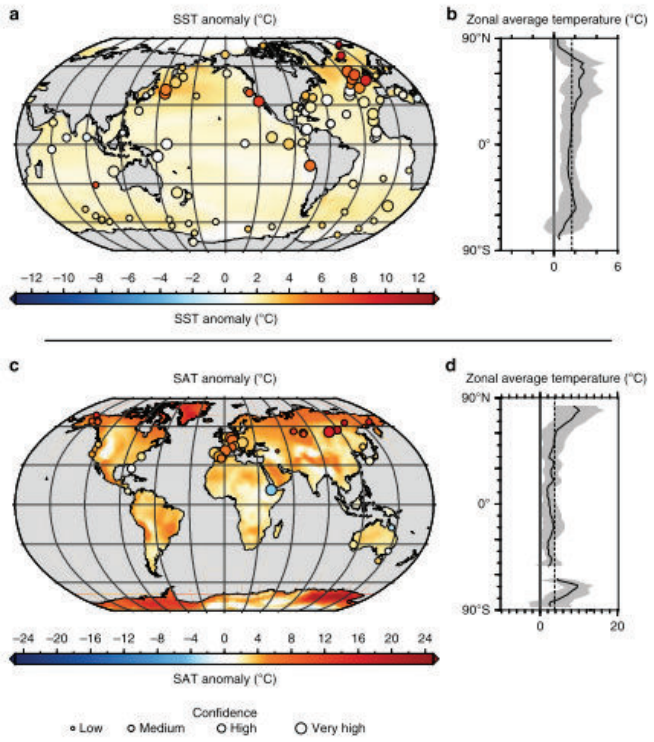


Figure 4.2 – Simulated global mean annual surface temperatures and sea surface temperature in the PlioMIP 1. Circles are the data from PRISM3. Figure after (Haywood et al., 2016)

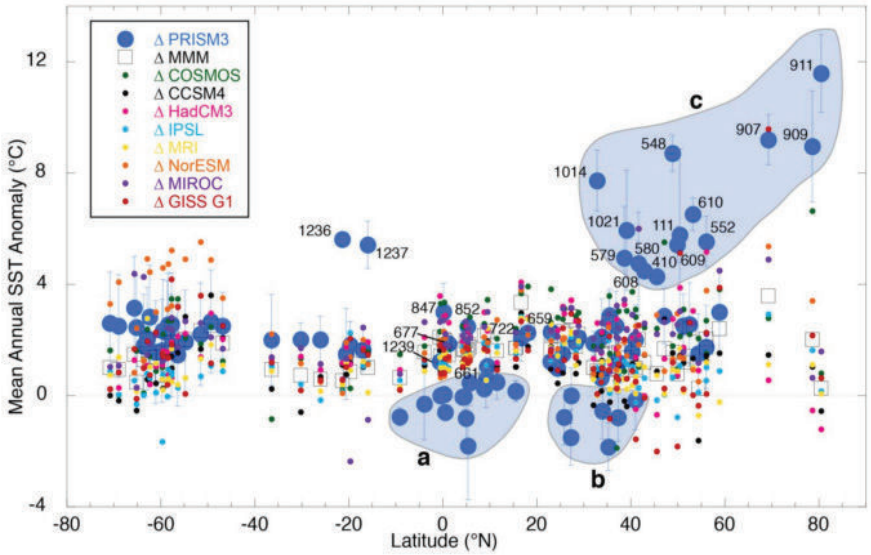


Figure 4.3 – Data model comparison in zonally averaged surface temperatures.Figure after (Dowsett et al., 2013)

Along with the studies on the MPWP, the discord between model and data is considered to majorly result from the uncertainties associated with the derivation of the proxy-data sets used to assess the climate models(Haywood et al., 2015). The MPWP is simply considered to be an warm period for the PlioMIP1 and this concept determinate the approach of the reconstruction of data and related boundary conditions. However, climate variation within the MPWP is very important, the average approach is not appropriate for the interpretation of data reconstruction. Therefore, PlioMIP2 is launched with choosing a specific interglacial period (MIS KM5c,3.205),which has a orbital forcing similar to present and largely retains many warm conditions on which the PlioMIP1 focused. Accordingly, new boundary conditions (PRISM4) are updated for the PlioMIP2 experiments.Comparing to the PRISM3, the PRISM4 (Fig.4.4,(Dowsett et al., 2016)) provides a new topography and bathymetry in which the Bering strait and Canadian Archipelago seaway are closed, the Greenland ice sheet reduce by 50% and the topography is more near modern conditions. Moreover, in PRISM4, the maps of reconstructed soil types and paleolakes are provided, but the sea surface temperatures and vegetation are kept the same as in the PlioMIP1. Meanwhile,the data scientists in the PRISM community are working on reconstructing high time-resolution proxy data focusing on the key regions which is important for understanding the MPWP warmth. These new proxy-data are more appropriate for the data-model comparison.Standard time series data will also provided to better understand the climate variability(Haywood et al., 2015).This study is involved in the PlioMIP2 project. More details can be found in the next section.

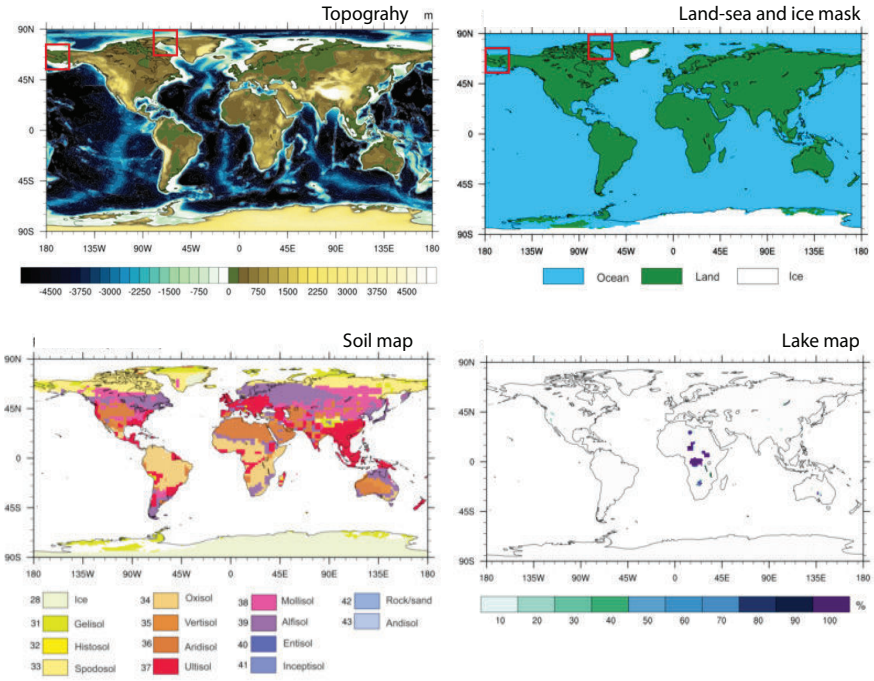


Figure 4.4 – New boundary conditions in PRISM4 .Figure modified from (Haywood et al., 2015)

## 4.3 Paper in preparation for Climate of the Past:Study on the MIS KM5c warm period using IPSL coupling model under PlioMIP phase 2 project

### 4.3.1 Abstract

The mid-Piacenzian warm period (MPWP; 3.264 to 3.025 Ma) is the most recent geological period with a present-like pCO2 concentration and exhibiting significant warmth relative to present conditions. This interval has been intensively studied during the last three decades due to its potential relevance for future climate change. Most of these studies are in the framework of Pliocene Model Intercomparison project (PlioMIP) and the US Geological Survey Initiative known as PRISM (Pliocene Research Interpretation and Synoptic Mapping). With the advanced understanding of the climate variability of this interval, a specific interglacial (marine isotope stage KM5c, 3.205 Ma) is selected and new boundary conditions (PRISM4) are updated for better understanding this warming period in the PlioMIP phase 2 (PlioMIP2) based on the previous PlioMIP phase 1 project (PlioMIP1). In this study, we carried out series of the MPWP experiments designed by the PlioMIP2 with adapting PRISM4 boundary conditions into IPSL Atmosphere-Ocean Coupled General Circulation Model (AOGCM), IPSL-CM5A and IPSL-CM5A2.1.The simulated global PlioMIP2 climate is warmer by 2.2-2.3°C than pre-industrial conditions and warmer by 0.1-0.2°C than PlioMIP1 by the identical model. In comparison with PlioMIP1, the modified orography in PlioMIP2 enhances Atlantic meridional overturning circulation that associated with a stronger poleward heat transport. Therefore PlioMIP2 represents a stronger warming in mid-to-high latitudes relative to PlioMIP1 and produce a better fit with proxy data. However the warming amplification in high latitudes is still underestimated. Besides, pCO2 uncertainties (+-50 ppmv) have a strong impact on the modeled warm conditions, especially on the high latitude climate. When augmenting/lowering pCO2 by 50ppmv, the climate increase/decrease by about 1°C in the high latitudes and the impact of lowering pCO2 is more important.

### 4.3.2 Introduction

The mid-Piacenzian warm period (MPWP; 3.264 to 3.025 Ma) is the most recent geological period with a present-like $pCO_2$ concentration and exhibiting significant warmth relative to today. This interval has been intensively studied during the last three decades as it is generally considered to be a potential guide for future warming. Most of these studies are in the frame work of these two projects: one is US Geological Survey Initiative known as PRISM (Pliocene Research Interpretation and Synoptic Mapping) which is responsible for the data reconstructions, the other is the Pliocene Model Intercomparison Project (PlioMIP) that focuses on the climate modeling and model intercomparison.Thanks to the PRISM project, an abundance of marine and terrestrial data are provided to represent the ocean/land temperatures, soil and vegetation conditions. Generally, the MPWP is studied to be globally warmer by 2-4°C than present level (e.g., Dowsett et al., 2009). A large warming amplification of 7-15°C is estimated in arctic regions derived from terrestrial proxies from the arctic lake El'gygytgyn in NE arctic Russia (Brigham-Grette et al., 2013) and Ellesmere Island in North Arctic circle (Rybczynski et al., 2013). Associated with this strong warmth, the reconstructed eustatic sea level is estimated to be 22(+-10m) higher (between 2.7 and 3.2 Ma) than present (e.g., Miller et al., 2012) which might link to a large melting of Greenland ice sheet and a significant collapse of West Antarctic Ice sheet as well as unstable regions of East Antarctic (Dolan et al., 2015b; Hill, 2009; Koenig et al., 2015).The reconstructed $pCO_2$ data during MPWP ranged from 350 to 450 ppmv (Bartoli et al., 2011; Martínez-Botí et al., 2015; Pagani et al., 2010; Seki et al., 2010), which are similar to present level.The distribution of vegetation is different from nowadays that northward shift of boreal forest takes place of the tundra regions due to the warming conditions (Salzmann et al., 2008).

The initial purpose of study on this period is to learn its relevance for the future climate change. However, considering the non-equilibrium state of the present climate due to the continuous change of forcing factors, the simulated stabilized MPWP may not be directly regarded as an analogue for future warming. The importance of the MPWP studies now is to know how the abilities of climate models to produce warm climate and to study the respective roles of forcing factors and feedback of internal climate components under warm conditions, which can also serve future climate projections.In PlioMIP phase 1 (PlioMIP1), there are 11 models participating to conduct the MPWP experiments.

Among these results,there exists consistency in surface temperature change across models in the tropics and lack of consistency identified in model responses at high latitudes as well as total precipitation rate in the tropics(Haywood et al., 2013). The modelled Atlantic Meridional Overturning Circulation and Ocean heat transport for this interval in different models are likely unchanged relative to modern conditions(Zhang et al., 2013). However, when comparing to data proxies of sea surface and air surface temperature, climate models uniformly underestimate the warming in the high latitudes(Dowsett et al., 2012)(e.g., Haywood et al., 2016).Reasons for this discord between data and model results are complex, but they are generally thought to be attributed to three main aspects:boundary conditions uncertainty, modeling uncertainty and data uncertainty(Haywood et al., 2013).In PlioMIP1, the MPWP is regarded simply as a stable interval despite of the climate variability exhibiting over a 300-kyrs time slab, thus the boundary conditions and data proxies interpretation are made as an averaged conditions over this long interval, which is now considered as the main contributor to this data-model discrepancy(Haywood et al., 2015). Therefore, the ongoing PlioMIP phase 2 (PlioMIP2) changes the strategy with choosing a representative interglacial of marine isotope stage KM5c (MIS KM5c;3.205 Ma) during the MPWP interval. This fixed time slice can help to improve the resolution in data proxies and to better constrain the boundary conditions. Therefore, new boundary conditions (known as PRISM4;(Dowsett et al., 2016)) are updated for PlioMIP2 which include a new palaeogeography reconstruction containing ocean bathymetry and land/ice surface topography, which represent closure of Bering Strait and North Canadian Archipelago region and a shrunk of Greenland ice sheet by 50% in comprison to PlioMIP1. Besides, extra information of lake distribution and soil types(Pound et al., 2014) are also provided in this new boundary conditions.

This study is conducted in the framework of PlioMIP2, hence we will employ the new boundary conditions of PRISM4 to conduct the MPWP experiments by using two versions of French AOGCM models (IPSL-CM5A and IPSL-CM5A2.1). The purpose of this study is to better understand the warm climate of the MPWP and also to study the sensitivity of IPSL AOGCM model to the change of boundary conditions and forcing factors. As IPSL AOGCM model has been participated in PlioMIP1 by (Contoux et al., 2012), we will also compare the modeling results of PlioMIP2 with those of PlioMIP phase 1.

### 4.3.3 Model Description

To accomplish the modeling work, we employed two versions of Institute Pierre-Simon Laplace (IPSL) coupled atmosphere-ocean general circulation model (AOGCM):IPSL-CM5A and IPSL-CM5A2.1. IPSL-CM5A is a high resolution coupling model which has been applied in CMIP5 for historical and future simulations (Dufresne et al., 2013) as well as for Quaternary and Pliocene paleoclimate studies (Contoux et al., 2012; Kageyama et al., 2013). The version of IPSL-CM5A2.1 is designed based on IPSL-CM5A with mainly tuning the cloud radiative effect to avoid the global cold bias in the model(Sepulchre et al.,in prep). Moreover, the computational performance of IPSL-CM5A2.1 is improved by about 6 times ( 50 yrs/d) than that of IPSL-CM5A. For the purpose of comparison with PlioMIP1 Contoux et al. (2012), we launched PlioMIP2 core experiment with IPSL-CM5A, and we also conducted PlioMIP2 core experiment and tire experiments with IPSL-CM5A2.1 to save the computational cost. Components of these models are shortly presented as following. More details can be referred to Dufresne et al. (2013) and Chapter 2.

### 4.3.4 Experiment Design

This section describes the boundary and the initial conditions imposed in our experiments. Here, the experiment names are consistent with the design of PlioMIP2 by Haywood et al. (2015) which are referred by an abbreviated form E$x^c$, where c is the concentration of atmospheric $CO_2$ in ppmv and x represents boundary conditions that have been changed from the pre-industrial (PI) such that x can be absent (for cases in which no boundary conditions have been modified) or it can be "o" for a change in orography and/or "i" for a change in land ice configuration.

#### Pre-industrial experiments

The pre-industrial control simulation in IPSL-CM5A was performed as required by CMIP5/PMIP3 by the LSCE modelling group. It is a 2800-years simulation which already started from equilibrium conditions.The pre-industrial control simulation in IPSL-CM5A2.1 was conducted by Sepulchre et al., (in prep) forced by CMIP5 pre-industrial boundary conditions and has 3000-years integration length.

**Pliocene experiments**

We conducted five AOGCM experiments for the PlioMIP2 study, they are respectively core experiment E$oi^{400}$ with IPSL-CM5A model and core experiment E$oi^{400}$_v2.1 and three tire experiments E$oi^{450}$_v2.1 , E$oi^{350}$_v2.1 , E$o^{400}$_v2.1 with IPSL-CM5A2.1 model.Although a standard $pCO_2$ of 400ppmv is selected for the Pliocene core experiments, the $pCO_2$ records during this interval mostly range from 350 to 450 ppmv. Thus the tire experiments E$oi^{450}$_v2.1 and E$oi^{350}$_v2.1 are conducted to learn the impact of $pCO_2$ uncertainties on the modeled Pliocene warm climate. The tire experiment E$o^{400}$_v2.1 is conducted to study the importance of ice sheet configurations in simulating the warming period. As defined by the abbreviated form, $CO_2$ concentration imposed in each simulation can be refereed to the number of the experiment's name.Other greenhouse gases and orbital forcing are kept the same as IPSL pi control run (Table4.1).

Vegetation scenarios are kept the same as PlioMIP1 AOGCM simulation by Contoux et al. (2012). River routing and soil patterns are not changed in this study. Land sea mask in these experiments are modified based on present level with closing Bering Strait, North Canada Archipelago region,and augmenting the topography in Hudson Bay (Figure4.5). Ice sheet mask are referred to PRISM4 dataset ((Dowsett et al., 2016)),except for E$o^{400}$_-v2.1 experiment, which is imposed with modern ice sheet. Topography in these five experiments are calculated based on modern topography used in IPSL model by superimposing on the anomaly between PRISM4 reconstructed topography and modern topography provided by PlioMIP2 database (Haywood et al., 2015). When the new topography was lower than zero, absolute PRISM4 topography was implemented.Figure4.5 shows the new resulting topography in our PlioMIP2 experiments and topography anomaly between PlioMIP2 and PlioMIP1 experiments.

The initial sea surface temperature and sea ice in E$oi^{400}$ and E$o^{400}$_v2.1 are derived from IPSL PlioMIP1 AOGCM simulation (Contoux et al., 2012).E$oi^{400}$ is conducted based on the equilibrium state of PlioMIP1 experiment ((Contoux et al., 2012),with 650 years of integration length) and integrated for 800 years,while E$oi^{400}$_v2.1 has 1500-years integration length.Average climatologies for these two experiments are calculated over the last 50 years. Three tire experiments: E$oi^{450}$_v2.1 , E$oi^{350}$_v2.1 , E$o^{400}$_v2.1 are conducted based on the equilibrium state of E$oi^{400}$_v2.1 core experiment and have 400 years of integration length. Average climatologies for these three experiments are calculated over the last 30

years. Table4.2 gives a summary for the experiments settings.

Table 4.1 – Configuration common to all experiments described in this paper.

| | |
|---|---|
| $CH_4$ | 760 ppb |
| $N_2O$ | 270 ppb |
| $O_3$ | Local modern |
| CFCs | 0 |
| Solar constant | 1365 W/m$^2$ |
| Eccentricity | 0.016715 |
| Obliquity | 23.441 |
| Perihelion | 102.7 |
| Dynamic vegetation | Off |
| Soil types and lakes | Local Modern |

Table 4.2 – Details of experimental settings

| Exp names | Models | $CO_2$(ppmv) | Integration length | Climatologies |
|---|---|---|---|---|
| Eoi400 | IPSL-CM5A | 400 | 650+800 yrs | Last 50yrs |
| Eoi400_v2.1 | IPSL-CM5A2.1 | 400 | 1500 yrs | Last 50yrs |
| Eoi450_v2.1 | IPSL-CM5A2.1 | 450 | 1500+400yrs | Last 30yrs |
| Eoi350_v2.1 | IPSL-CM5A2.1 | 350 | 1500+400yrs | Last 30yrs |
| Eo400_v2.1 | IPSL-CM5A2.1 | 400 | 1500+400yrs | Last 30yrs |

### 4.3.5 Results and Discussion

In this section, We will present the results of core experiments (E$oi^{400}$ and E$oi^{400}$_v2.1) conducted respectively with IPSL-CM5A and IPSL-CM5A2.1. We will compare E$oi^{400}$ with the PlioMIP1 (Contoux et al., 2012) with the identical model to understand the impact of boundary conditions change on the warm climate. We will also discuss the impacts of $pCO_2$ uncertainties and the ice sheet configurations on the Pliocene warm climate.Finally, we will compare our simulated climate with the available data to learn the competence of IPSL coupling model in simulating warm climate. Table4.3 gives the general diagnostics for each experiments.

#### Pliocene runs with IPSL-CM5A

Results in the Atmosphere

Figure4.6 show the anomalies of global mean annual surface air temperature (SAT),precipitation rate and sea surface temperature (SST) between Pliocene experiments and pre-industrial control with IPSL-CM5A.The global mean annual SAT in E$oi^{400}$ experiment is about 14.4°C, which is 2.3°C warmer than that of pre-industrial.The warming in high latitude (4.2°C) is larger than that in the tropics (1.8°C). The warming extent of E$oi^{400}$ is slightly larger than that of PlioMIP1 experiment which show a global warming by 2.1°C.The major

Table 4.3 – Diagnostics for each experiment

| Exp Names | MA SAT & PRECIP (Anomaly) (units: °C & mm/d) | | | MA SST (Anomaly) (units: °C) | AMOC index (absolut (units: Sv) |
|---|---|---|---|---|---|
| | Global | Tropics | High Latitudes(NH) | | |
| PlioMIP1 | 2.1&0.13 | 1.7&0.17 | 3.9&0.21 | 1.4 | 10.8 |
| Eoi400 | 2.3&0.14 | 1.8&0.20 | 4.2&0.28 | 1.7 | 15.7 |
| Eoi400_v2.1 | 2.2&0.13 | 1.6&0.19 | 3.8&0.23 | 1.6 | 17.9 |
| Eoi450_v2.1 | 2.6&0.15 | 2.1&0.23 | 4.5&0.27 | 1.9 | 17.4 |
| Eoi350_v2.1 | 1.5&0.09 | 1.0&0.13 | 2.5&0.14 | 1.2 | 17.6 |
| Eo400_v2.1 | 2.0&0.13 | 1.5&0.18 | 3.0&0.20 | 1.2 | 18.3 |

differences in SAT between E$oi^{400}$ and PlioMIP1 are found respectively in mid-latitude Eurasian and arctic regions due to the change of regional topography and high latitude seaways as well as the reduced Greenland ice sheet.The global mean annual precipitation rate increases by 0.14 mm/d in E$oi^{400}$,the major increase locates in the monsoon regions and tropical oceans. Although the increased global mean precipitation rate in E$oi^{400}$ is similar to that in PlioMIP1,regional differences still exist that the precipitation rates in E$oi^{400}$ in the tropics and NH high latitudes are higher than those of PlioMIP1 by 0.03 - 0.05 mm/d.Regionally, the PlioMIP2 simulates an intensified precipitation in East Africa than the PlioMIP1, which is better consistent with proxy data from East Africa inferring a wetter vegetation condition and hydrological systems during this period (Drapeau et al.,). The regional difference in topography between PlioMIP2 and PlioMIP1 may considered to be a major influence. Further sensitivity studies are needed to verify it.

Results in the Ocean

Accordingly, The global mean annual SST of E$oi^{400}$ increases by 1.7°C than present day,which is 0.3°C warmer than PlioMIP1 and this warming majorly locates in the mid to high latitude oceans of NH. The warming in E$oi^{400}$ relative to PlioMIP1 may attribute to the closure of Bering Strait,Canadian Archipelago which are the major difference between these two experiments. In control run, the water flux through Bering strait is about 1.0 Sv transporting much fresher and warmer water from the North Pacific to the Arctic ocean. In E$oi^{400}$, as showing in Figure4.8, the water currents from the North Pacific to the Arctic through the Bering Strait and from the Arctic to the Baffin Bay are shut down. Consequently, the Arctic sea water gets much denser, then the wind-drived Beaufort gyre and transpolar drift get weakened that further reduce the associated East Greenland current and the Labrador current, hence lead to a saltier condition in these adjacent regions which can help to increase the convection and the formation of North Atlantic Deep Wa-

ter. Accordingly, we observe a strengthened gulf stream and North Atlantic currents as well as enhanced sub-polar gyre which can transport more heat energy to high latitudes and may link to a stronger convection. Consequently, an enhanced and shallowed AMOC by 4.9Sv is observed in E$oi^{400}$, while AMOC in PlioMIP1 is not from present level Figure4.9. The increased AMOC resulting from the closure of Bering Strait and Archipelagos is likely consistent with previous studies of Hu et al., (2015), Kamae et al., (2016) and Chandan et al.,(2016). However, the magnitude of AMOC strength change in our PlioMIP2 simulation is much larger other models. Hu et al.,(2015) using CCSM3 and CCSM2 with different climate backgrounds show that the AMOC responses to the closure of the Bering strait are about 2-3 Sv. Chandan et al.,(2016) show an increased AMOC strength by 2 Sv after closing the Bering strait in the CCSM4 model. In the study of Kamae et al.,(2016), they present a much stronger AMOC in their PlioMIP2 than their pre-industrial level. However, they use different flux adjustment in their PlioMIP2 simulation and their pre-industrial simulation, the AMOCs in these two simulations cannot be directly compared. In fact, the simulated AMOC largely depends upon the vertical mixing schemes (Zhang et al., 2013b). Thus it is expected to see variations of simulated AMOC across models. Although we observe a largely increased AMOC (4.9Sv) in our PlioMIP2 simulation with IPSL-CM5A, it should be noted that the simulated modern AMOC (11 Sv) with this model is weaker than the observations (17.2Sv , McCarthy et al.,2015) and the simulated AMOC in this model is always weaker than other models (Zhang et al.,2013b).

The warming condition in E$oi^{400}$ is unfavorable for the sea ice formation for both hemisphere,especially during the cold season. In Figure4.11, we can find largely reduced maximum sea ice cover in E$oi^{400}$ by 5.6 Mkm$^2$ and 8 Mkm$^2$ respectively for NH and SH as relative to control run. For the minimum sea ice cover,E$oi^{400}$ reduces by 3.7 and 1 Mkm$^2$ respectively for NH and SH. In comparison with PlioMIP1, NH sea ice cover in E$oi^{400}$ reduces by 1.7 Mkm$^2$ and 0.7 Mkm$^2$ respectively for cold and warm season but no difference in SH due to the relative warming between these two experiments.

**Pliocene runs with IPSL-CM5A2.1**

Results in the core experiment E$oi^{400}$_v2.1

Figure4.7 show the anomalies of global mean annual SAT,precipitation rate and SST between E$oi^{400}$_v2.1 and the pre-industrial control with the identical model. The global

mean annual SAT in E$oi^{400}$_v2.1 is about 15.3°C, which is 2.2°C warmer than pre-industrial conditions and the warming in high latitudes is much larger than in the tropics. It should be noted that the absolute SAT in E$oi^{400}$_v2.1 is warmer than that in E$oi^{400}$, while the SAT anomaly in E$oi^{400}$_v2.1 is weaker than E$oi^{400}$. This is due to the bias between these two models: IPSL-CM5A2.1 present a warmer pre-industrial condition by 1.1°C (Sepulchre et al.,in prep) than than with IPSL-CM5A. The global mean annual precipitation rate increased by 0.13 mm/d in E$oi^{400}$_v2.1 ,which is comparable to the results of core experiments with IPSL-CM5A.

In E$oi^{400}$_v2.1, the changes in the ocean conditions relative to its pre-industrial control are similar to E$oi^{400}$.But due to the model bias, the absolute values are different from E$oi^{400}$. The global mean annual SST is 0.7°C warmer than E$oi^{400}$,the AMOC strength (Fig.5) is about 17.9 Sv which is 2.2Sv larger than E$oi^{400}$, while AMOC anomaly is about 4.7 Sv in comparison with its pre-industrial level of 13.2 Sv, which is similar to E$oi^{400}$. The Sea ice cover is also largely decreased due to the warming in high latitudes. Moreover, the decreasing extents of sea ice cover during cold season are always larger than that during warm season for each hemisphere. More details are shown in Table4.3 and in Figure4.11.

The impact of $pCO_2$ uncertainties

Figure4.10 represents the anomalies of global mean annual SAT, precipitation rate and SST between three tire experiments (E$oi^{450}$_v2.1 , E$oi^{350}$_v2.1, E$o^{400}$_v2.1) and core experiments E$oi^{400}$_v2.1 . After augmenting the $pCO_2$ by 50ppmv in E$oi^{450}$_v2.1, the earth is slightly warmed up (0.48°C ) and the warming in high latitudes is more important (0.7°C). However, when abasing $pCO_2$ by 50ppmv in E$oi^{350}$_v2.1, the change of climate is more important than that in E$oi^{450}$_v2.1 , as we observe a global cooling of 0.71°C and cooling of -1.29°C over NH high latitudes. This asymmetric pattern in increasing/decreasing temperatures when augmenting/lowering pCO2 majorly results from the change of surface albedo associated with the snow fall. In E$oi^{450}$_v2.1 , the mean annual snowfall decreases by 6% between 40 N and 80 N when comparing to E$oi^{450}$_v2.1, while E$oi^{350}$_v2.1 represents an increased mean annual snow fall by 30%. The asymmetric pattern between E$oi^{450}$_v2.1 and E$oi^{350}$_v2.1 is also found in the changes of precipitation rates: Global climate gets slightly moister with an increased global precipitation rate by 0.02mm/d (+15%) in E$oi^{450}$_v2.1, while in E$oi^{350}$_v2.1, the global precipitation rate reduces by 0.04mm/d (-31%) and this reduction is more important in the tropical regions. Thus, our results show that the response of IPSL coupling model to the lowering of $pCO_2$ is larger than the in-

creasing of $pCO_2$ in the atmosphere section. But when exploring in the ocean,we find that the increased or decreased extents of SSTs resulting from augmenting or lowering of $pCO_2$ by 50ppmv are likely symmetric. The AMOC strengths are also similar between E$oi^{450}$_v2.1 (17.4Sv) and E$oi^{350}$_v2.1 (17.6Sv). More details are shown in Figure4.9. Nevertheless, the changes of sea ice cover in these two tire experiments are far from each other (Figure4.11). As in E$oi^{450}$_v2.1, the sea ice covers decrease slightly in relative to E$oi^{400}$_v2.1 for both hemisphere (0.2-0.3 $Mkm^2$ during cold season and 0.1-0.6 $Mkm^2$ during warm season), while in E$oi^{350}$_v2.1 , the sea ice covers largely expand for both hemisphere, especially during the warm season and in the SH (1-1.5 $Mkm^2$ during cold season and 2-3 $Mkm^2$ during warm season).

The impact of ice sheet configuration In E$oi^{450}$_v2.1 , the ice sheets in both hemisphere are set as pre-industrial conditions. The relative increased ice sheets modify the atmospheric conditions in high latitudes due to its strong albedo feedback which largely decrease the local incoming radiation then further influence the atmospheric circulation.A decrease of 0.8-1°C is observed in polar regions in both hemisphere.The precipitation rates change slightly in regional scale. Due to the relatively evenly distribution of increased and decreased precipitation rate, the global mean annual precipitation rates are not much perturbed. .SSTs also decreased in high latitudes of NH hemisphere resulting from the air sea interactions. The AMOC strength has slightly increased by 0.5Sv due to the enhanced meridional temperature gradient. In summary, ice sheet boundary conditions takes an important role in the high latitude climates.

**Model data comparison**

Figure4.12 shows the sea surface temperatures with the average of February and August in both core experiments (E$oi^{400}$;E$oi^{400}$_v2.1 ) as well as the PRISM3D proxy-based SST reconstruction during the late Pliocene (Dowsett et al., 2009). The simulated SSTs correlate well with data in representing the reduced meridional temperature gradient and in the mid-to-high latitudes warming. The best overlap between modeling results and data locates in the tropics and lower latitudes.The discords mostly situate in high latitude, especially in the North Hemisphere. Figure4.13 shows the relationship between modeling results and data. Modeling results here are got by extracting the values in the locations where data obtained. In summary, the PlioMIP2 simulated by new version CM5A2.1

(E$oi^{400}$_v2.1) fits better with data than the others due to its warming bias than the old version. The linear correlation between the simulated PlioMIP2 with CM5A and data seems like similar to the PlioMIP1 condition. However, when looking at the moderate SSTs ranges (15-25°C) which mostly represent the mid-to-high latitudes temperatures in the data, the simulated PlioMIP2 (CM5A) usually is warmer than the PlioMIP1, which better fits with the data. On the other hand, the two PlioMIP2 experiments show warmer condition in high latitude continents in which the warming is always underestimated in the PlioMIP1 studies.However, the proxy data PRISM3D (Dowsett et al., 2009) discussed here is not proper for the data-model comparisons, as they are interpreted as the average state of the MPWP, further data-model comparisons are needed to be done when the new precise regional data are prepared (Dowsett et al., 2016).

### 4.3.6 Summary

In this paper, we describe the results of modeled warm interglacial of MIS KM5c (3.205 Ma) located in the interval of the MPWP (3.0-3.3 Ma) with imposing the new boundary conditions of PRISM4 (Dowsett et al., 2016). Two versions of core experiments denoted E$oi^{400}$ and E$oi^{400}$_v2.1 are conducted based on two versions of IPSL coupling model: IPSL-CM5A and IPSL-CM5A2.1. Three tire experiments (E$oi^{450}$_v2.1 , E$oi^{350}$_v2.1 , E$o^{400}$_-v2.1) are conducted based on IPSL-CM5A2.1 to study the roles of the uncertainties of $pCO_2$ and the ice sheet boundary conditions in the warming climate.

The new boundary conditions of PRISM4 adapted in our models produce an enhanced global warming in the MPWP,especially for the mid-to-high latitudes when comparing to the PlioMIP phase 1 results. This modeled meridional surface temperature gradient is similar to the proxy data from PRISM3D. However, the magnitude of the high latitude warming amplification is still underestimated. The enhanced warming can be majorly attributed to the change of high latitude seaways which strengthening AMOC and transport more heat energy to high latitudes and also to the reduced ice sheets and the sea ice covers, which largely decreasing the shortwave radiation. In the core Pliocene experiment, E$oi^{400}$ represents a global warming by 2.3°C (mean annual SAT) and warming amplification in the mid-to-high latitudes with 4.2°C relative to the PI control.E$oi^{400}$_v2.1 represents a relative warmer condition comparing to E$oi^{400}$ due to the model bias but warming anomalies in comparison with its related PI control ( 2.2°C ) is slightly weaker than that

of E$oi^{400}$. The simulated warming in our model is weaker than other studies(Chandan and Peltier, 2017; Kamae et al., 2016).In our two core experiments, AMOC strengths increase remarkably (+4.7 Sv) in comparison with their related PI controls due to the closure of Bering strait and North Canadian Archipelago regions.This result is in agreement with other studies (Hu et al., 2015; Kamae et al., 2016), but the extent of the increase of the AMOC highly depends upon the processes including in the ocean models. The model response to the $pCO_2$ uncertainties (+-50ppmv based on the core simulation) is not symmetric. Based on E$oi^{400}$_v2.1 , the augmenting of $pCO_2$ by 50 ppmv produces warming in the high latitudes (+0.7°C), but the decreasing of $pCO_2$ by 50ppmv leads to much strong cooling in the high latitudes (-1.3°C).This cooling effect is stronger than that produced by the enlarged ice sheets. To conclude, further model intercomparisons and data-model comparisons are needed to better understand the role of new boundary conditions and the internal climatic processes in modeling the Pliocene warming climate.

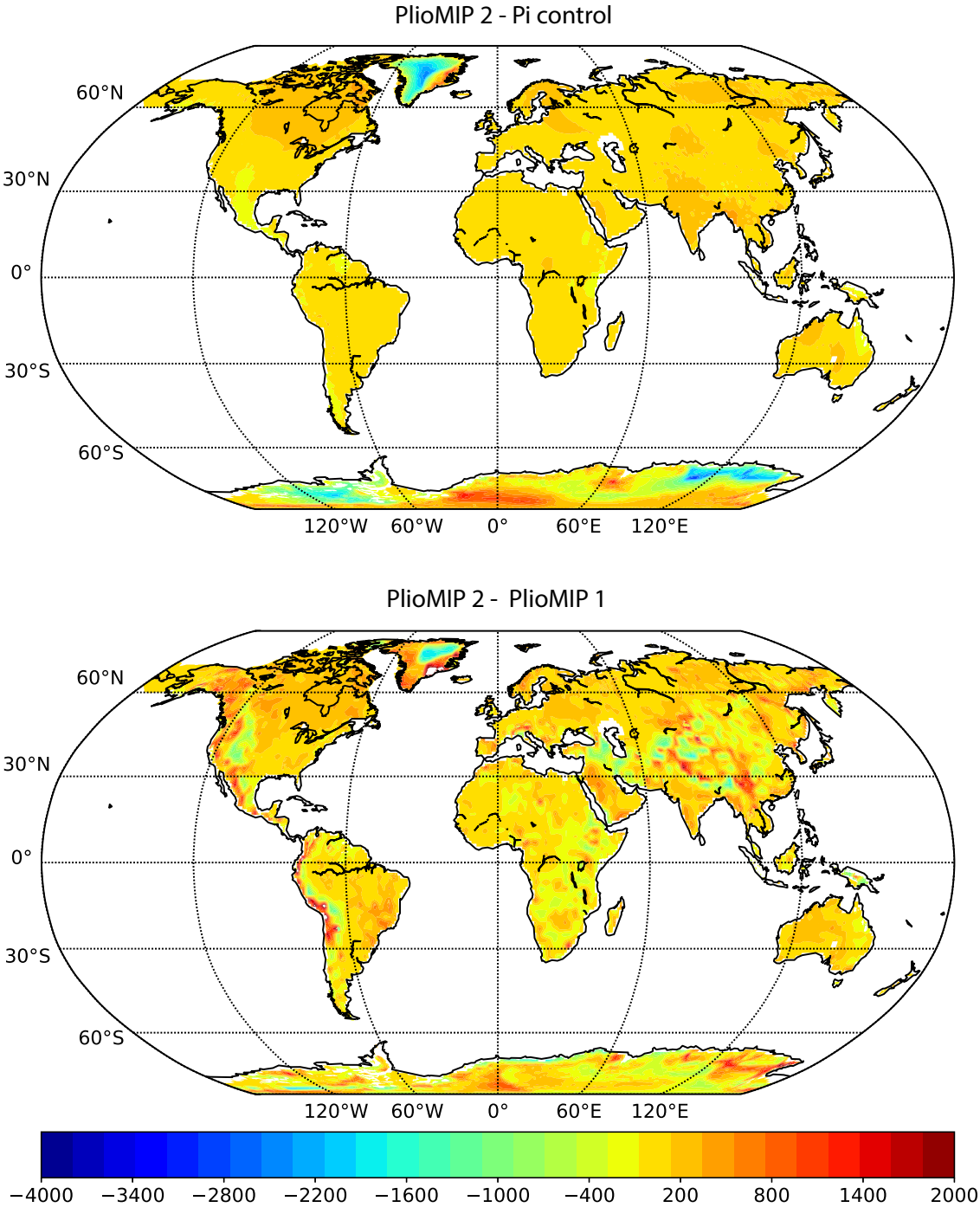


Figure 4.5 – Anomalies prescribed in topography of PlioMIP2 respectively relative to PI control (upper) and PlioMIP1 (lower).

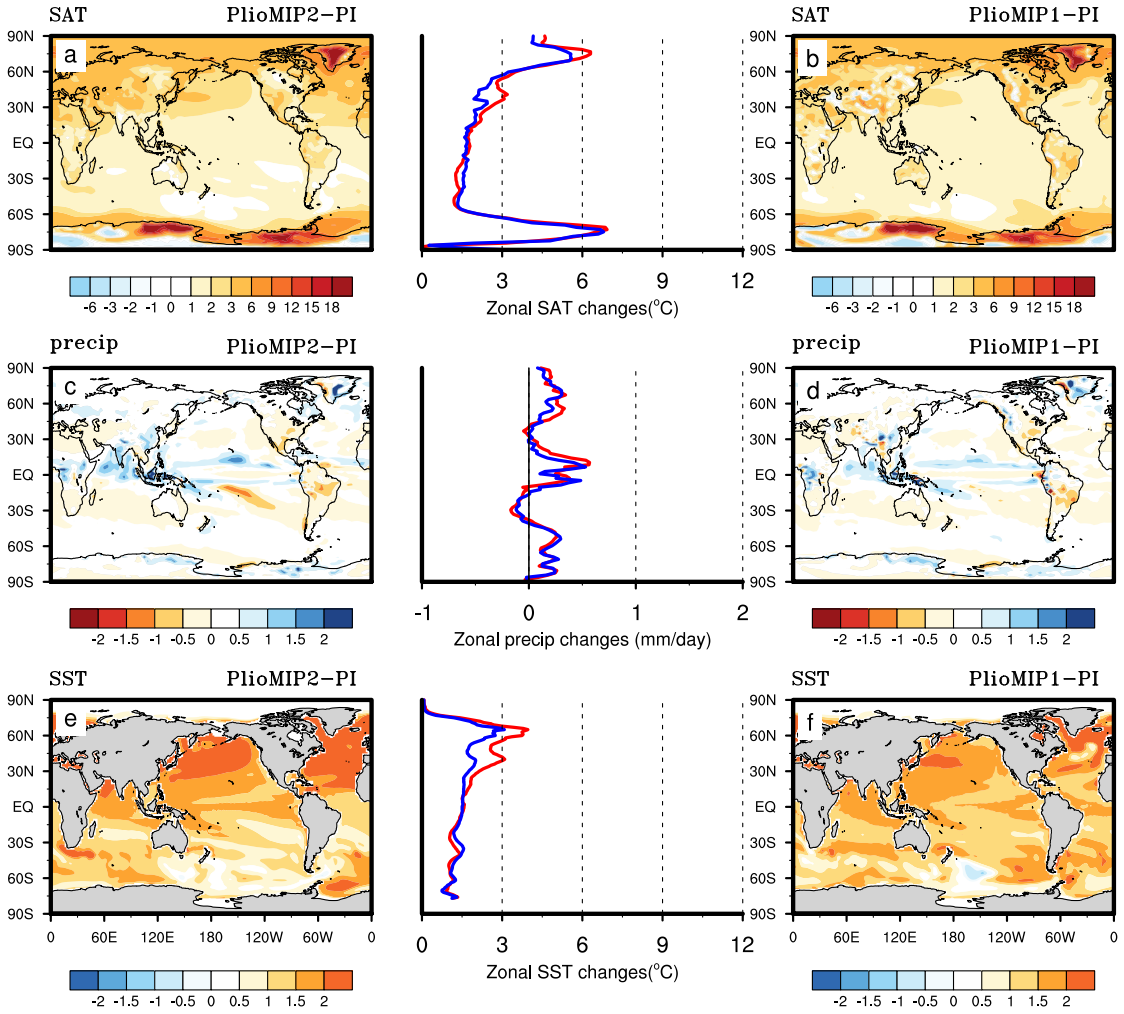


Figure 4.6 – Anomalies of mean annual surface temperature (a;b),mean annual precipitation rates(c;d) and mean annual sea surface temperature for PlioMIP2 (or E$oi^{400}$) and PlioMIP1 conducted with IPSL-CM5A in comparison with associated pre-industrial control experiment. The middle panels represent the zonal mean of related anomalies(PlioMIP2 with red lines and PlioMIP1 with blue lines)

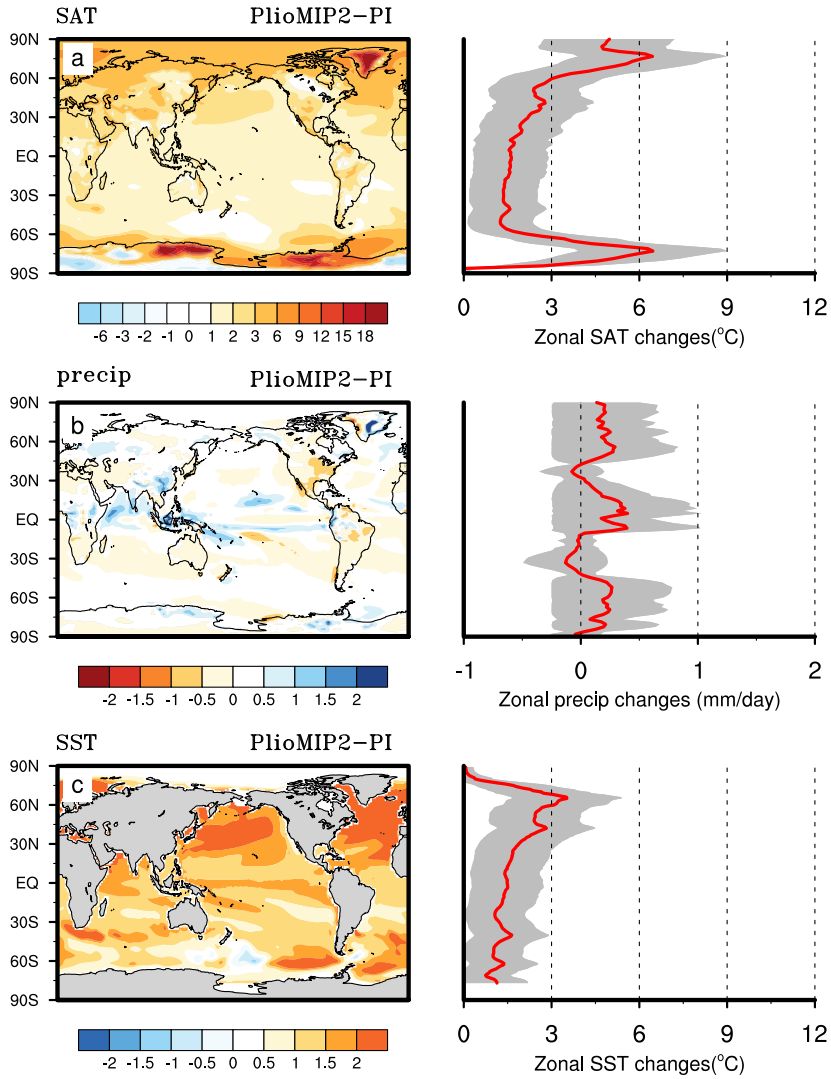


Figure 4.7 – Anomalies of mean annual surface temperature (a;b),mean annual precipitaion (c;d) and mean annual sea surface temperature for PlioMIP2 (or E$oi^{400}$_v2.1 ,) conducted with IPSL-CM5A2.1 in comparison with associated pre-industrial control experiment. The middle panels represent the zonal mean of related anomalies and the associated one sigma standard (shaded region) deviation.

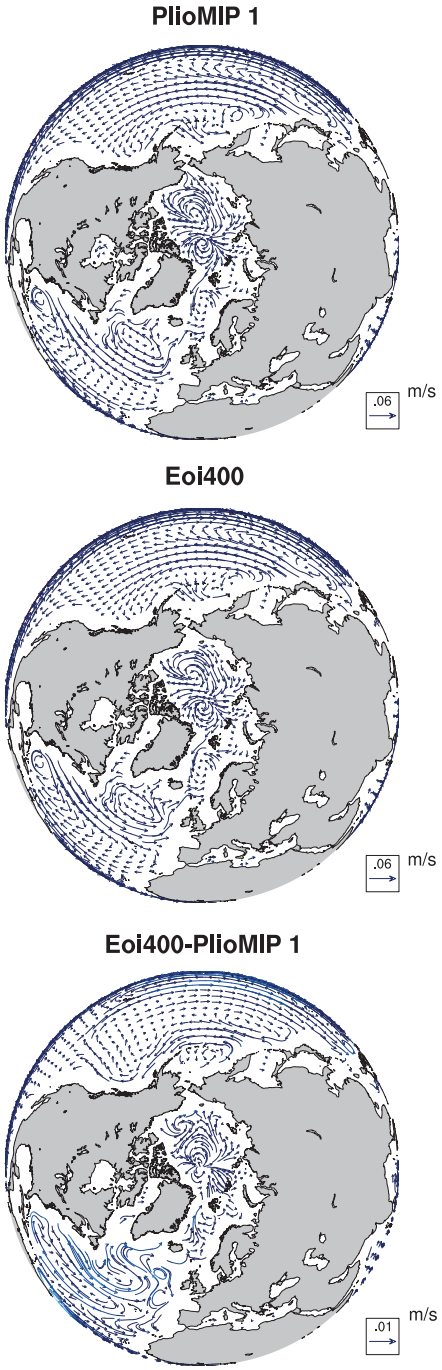


Figure 4.8 – Mean annual Ocean current above 500 meters.

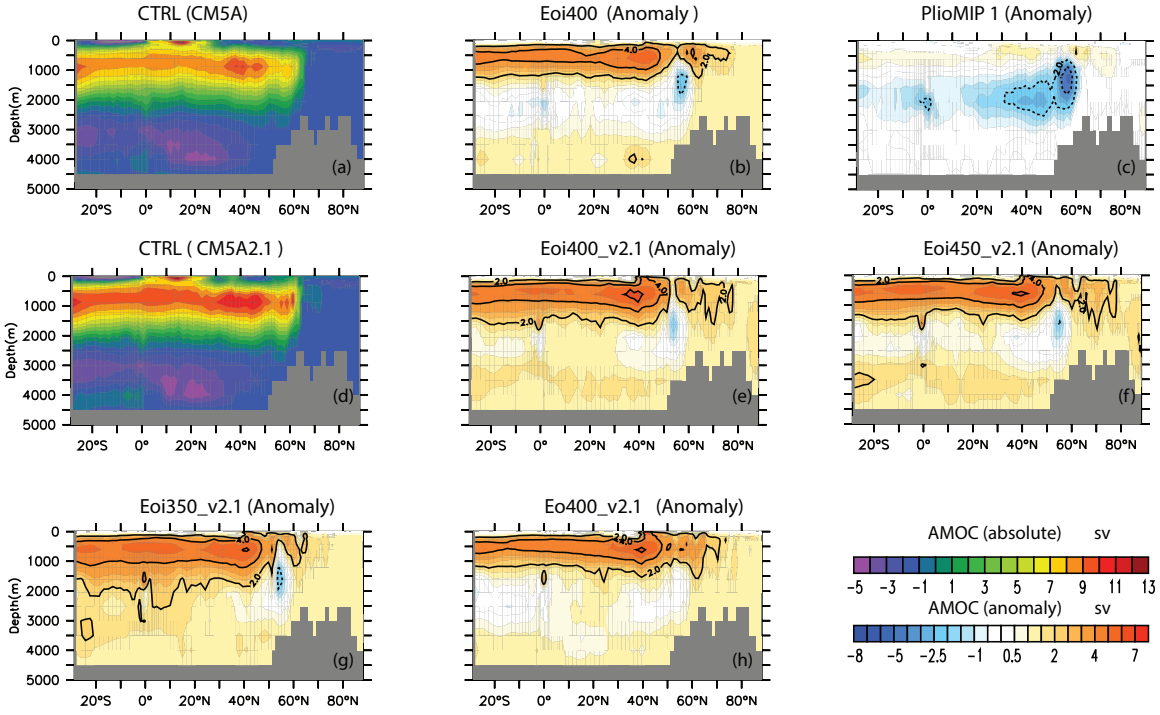


Figure 4.9 – Mean annual AMOC of PI controls (a,d) and AMOC anomalies of each experiment in comparison with their related PI controls.

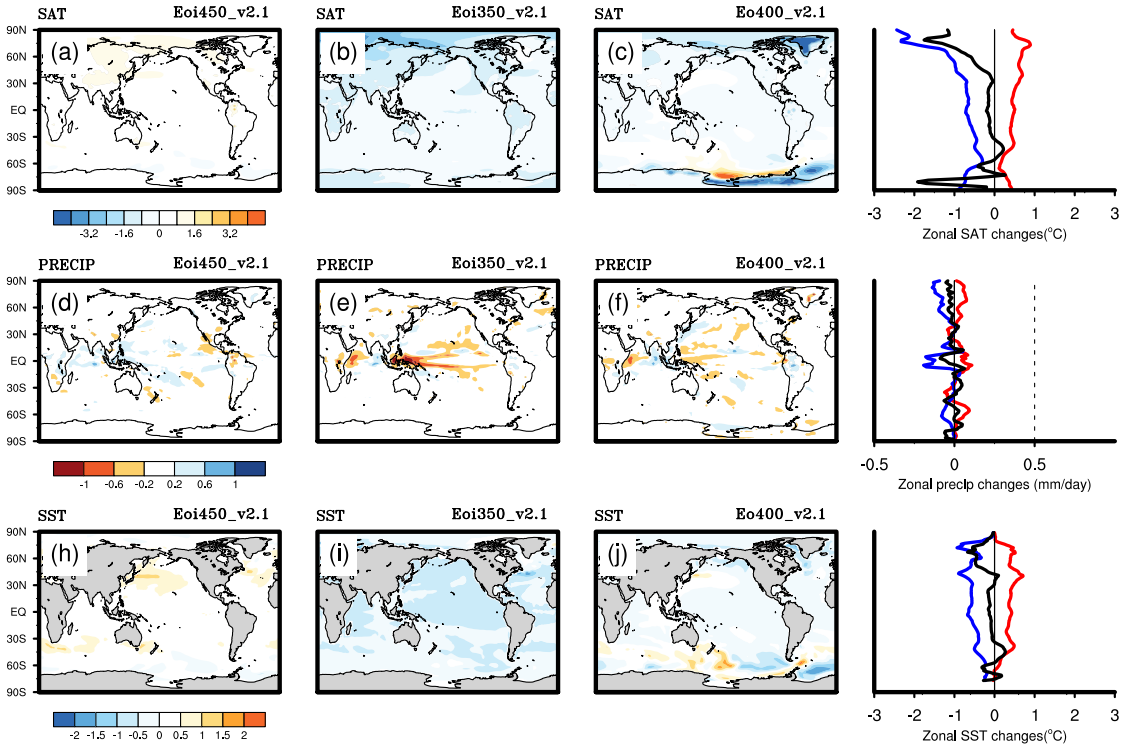


Figure 4.10 – Anomalies of mean annual surface temperatures,mean annual precipitations and mean annual sea surface temperatures in comparison with E$oi^{400}$_v2.1 experiment. The last column represents the zonal mean of related anomalies (red,blue and black lines represent respectively for E$oi^{450}$_v2.1 , E$oi^{350}$_v2.1 and E$o^{400}$_v2.1).

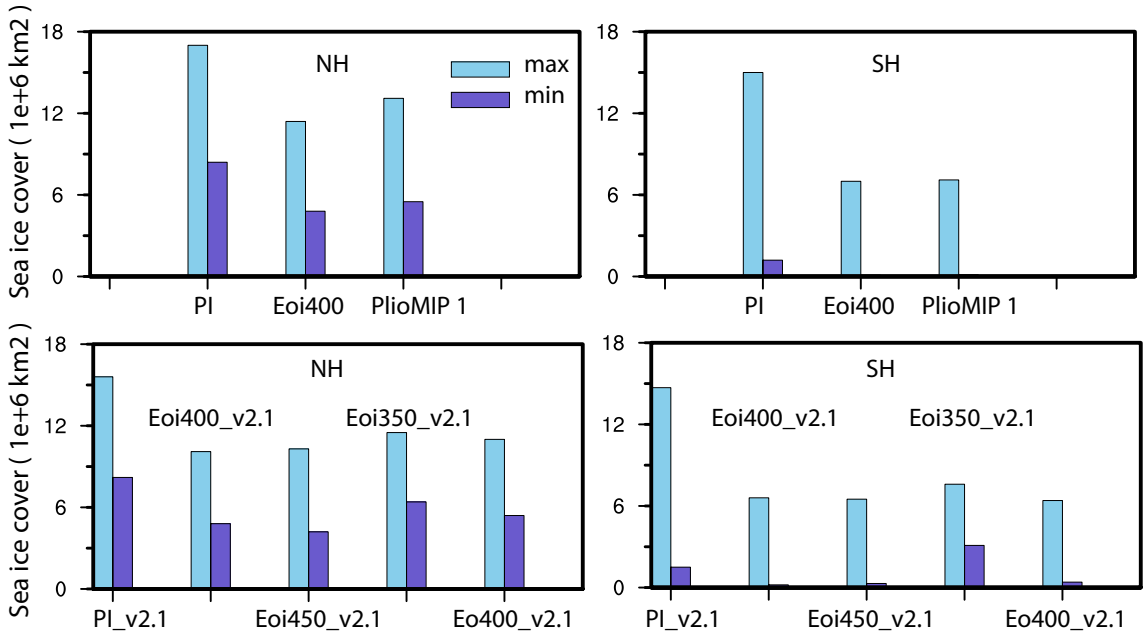


Figure 4.11 – Maximum and Minimum sea ice covers for both hemispheres in each experiment (units: 1E+10$^6$km$^2$ ).

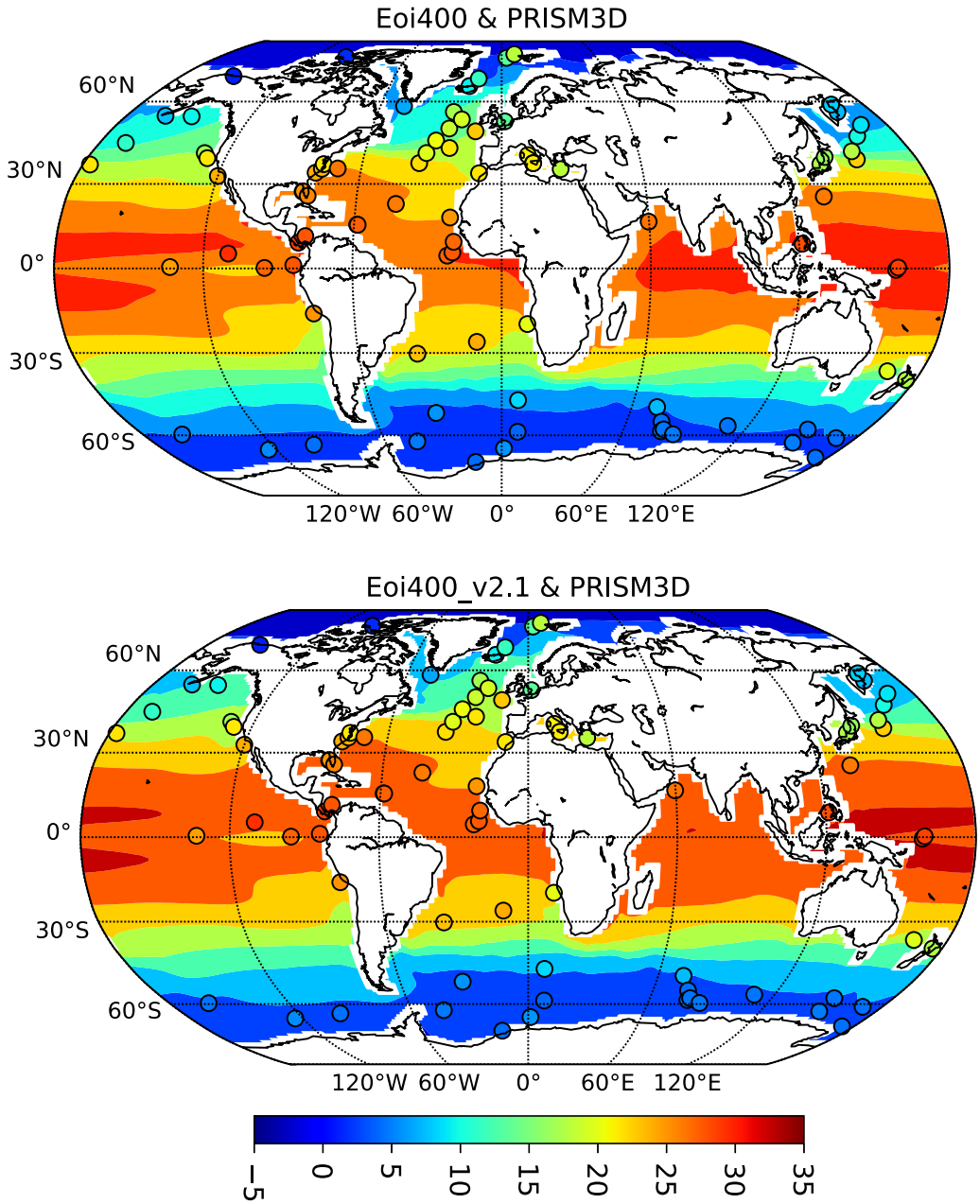


Figure 4.12 – Modeled mean annual (average of February and August) sea surface temperatures and PRISM 3D data (°C).

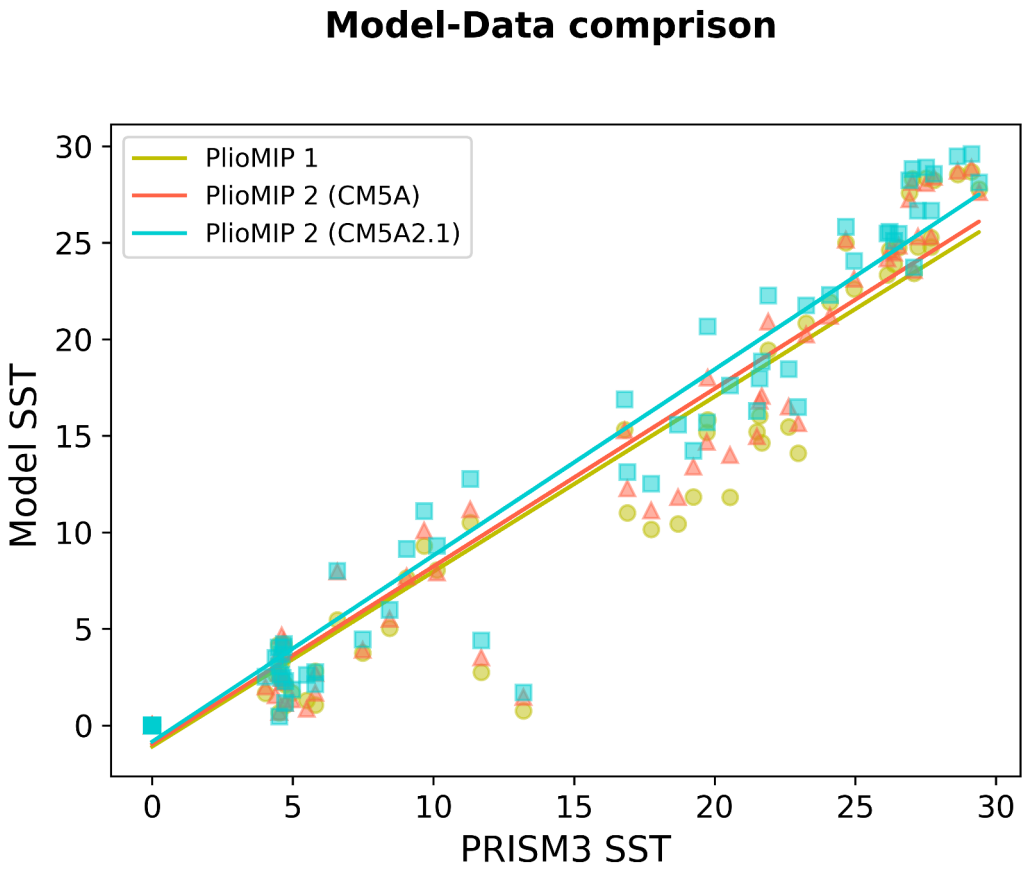


Figure 4.13 – Comparison of modeled mean annual (average of February and August) sea surface temperatures and PRISM 3D data (°C).

## 4.4 Summary and conclusions

In this chapter, we firstly introduced the PlioMIP project and the results of the phase 1 as well as new boundary conditions developped for the phase 2. The paper prepared for the special issue of PlioMIP2 described the models we used for these new boundary conditions. The major interest may be summarized as follows. -We performed with the same AOGCM model (IPSLCM5A) the core simulation designed with the boundary conditions provided by PlioMIP1 and PlioMIP2. The major difference between these experiments is the decrease of the thermal gradient (mainly due to higher temperature for mid and high latitude) due to the Bering strait and Canadian archipelago for PlioMIP2 -Using a new version of the IPSL AOGCM (IPSLCM5A2) for PlioMIP2, which is much faster, we were able to provide sensitivity experiments to CO2 and ice sheet configurations. In our study, the major results are that,the model response to the $pCO_2$ uncertainties (+-50ppmv based on the core simulation) is not symmetric. The decreasing of $pCO_2$ by 50ppmv leads to much strong cooling in the high latitudes. This cooling extent is more important than the warming extent resulting from the increasing of $pCO_2$ as well as is stronger than the cooling extent produced by the enlarged ice sheets.

# Chapter 5

# The Plio-Pleistocene transition and Greenland ice sheet evolution

## Contents

Whereas since late Miocene, there are evidences of sporadic Greenland glaciations (Larsen et al., 1994) that occurred but did not maintain, it is only during Pliocene that pCO2 decrease creates favorable conditions to allow the build-up of GrIS (e.g Lunt et al., 2008). Superimposed to this long term slow decrease of pCO2, changes in summer insolation around 2.7 Ma at high latitudes (Laskar et al., 2004) also played a major role in triggering the onset of GrIS. We will focus here on this major transition from Pliocene to Pleistocene (3.0-2.5 Ma).Following the warming period of the mid-Piacenzian, the earth climate began a long-term cooling phase inferring from the decreasing trend of sea surface temperatures (Herbert et al., 2010; Lawrence et al., 2009; Venti et al., 2013) and land surface temperature (Brigham-Grette et al., 2013). All existed pCO2 records also represent decreasing trends after the MPWP (e.g., Bartoli et al., 2011; Martínez-Botí et al., 2015; Seki et al., 2010). Evident ice-rafted debris (IRD) records are extensively observed around 2.7-2.4Ma (e.g., Flesche Kleiven et al., 2002; Jansen et al., 2000) indicating the establishment of large North Hemisphere Glaciation (Maslin et al., 1998). This long-term cooling phase known as "Plio-Pleistocne transtion" (PPT,3.0-2.5 Ma,Fig.5.2) is an important tipping point in the Earth climate associated with perennial ice sheets in the Northern high latitudes and triggered the glacial-interglacial cycle with a 41-kyrs periodicity. The third part of my thesis work is based on the PPT transition and the study of the Greenland ice-sheet evolution during this period. A summary of this work has been done and already submit to the journals. We provide in Section 5.1 a brief history of Greenland ice sheet evolution from late Miocene.


Figure 5.1 – Map showing Greenland with ice sheet depths. Figure from Wikipedia:*https* : *//en.wikipedia.org/wiki/Greenland*$_i$*ce*$_s$*heet*

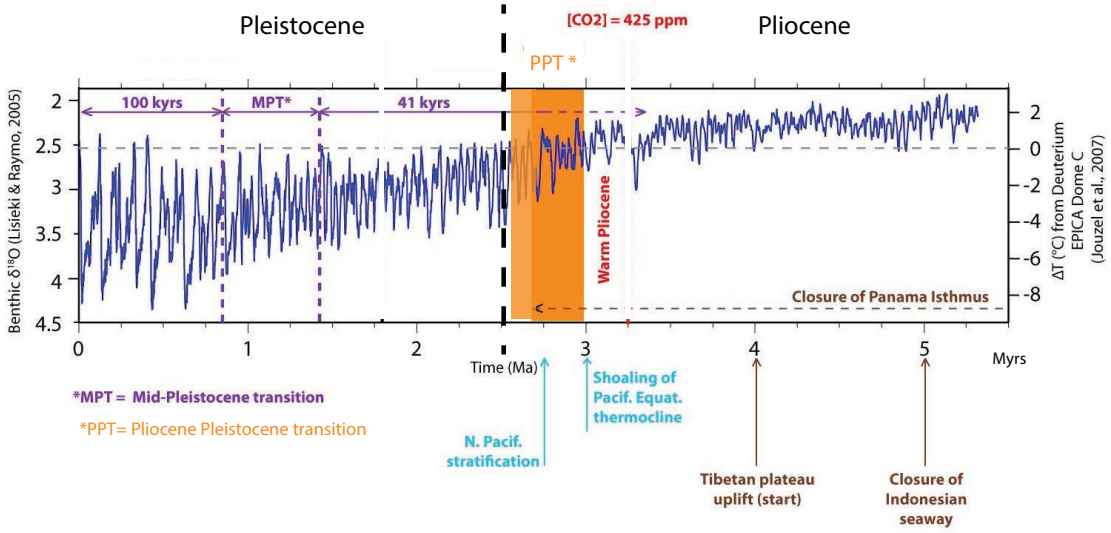


Figure 5.2 – LR04 $\delta^{18}O$ from (Lisiecki and Raymo, 2005) correlated to the temperature anomaly inferred from the deuterium concentration in ice cores from EPICA Dome C, Antarctica (Jouzel et al., 2007)). Figure modified from Colleoni (personal communication)

## 5.1 Greenland ice sheet history

The Greenland ice sheet (GrIS,Fig.5.1), with a volume of 2.99 ± 0.02 ($10^6$ $km^3$) (Morlighem et al., 2017), is the second largest land ice in the world. When this vast land ice totally melts, the seal level will increase by about 7.42 ± 0.05 meters (Morlighem et al., 2017) , which is an important issue in the vulnerability of the climate change. Under the global warming, the rate of ice loss from Greenland is accelerate since 1990s. Studies show that the total ice-sheet loss may result from warming of more than a few degrees above mean 20th century values,but this threshold is poorly defined (2-7°C)(Alley et al., 2010). A long-term history of Greenland ice sheet is very important for us to understand the Greenland ice sheet response to the climate change. Evidences of glaciomarine diamictities and IRDs collected off the shore of southeast show that the Greenland ice sheet has existed as early as the late Miocene (about 7 Ma) (Larsen et al., 1994) and may constrict in the southeast Greenland due to the high topography and precipitation rate. Then another marked signal for the Greenland ice sheet inferring from the IRDs is during the short glacial event of MIS M2 (3.3 Ma,50kyrs) (Jansen et al., 2000) and full Greenland ice sheet likely existed during this period inferring from the estimated sea-level drops (e.g., Miller et al., 2012) and modeling studies (Dolan et al., 2015a; Tan et al., 2017). Following MIS M2, the Greenland ice sheet might largely melt and constrict only in the east Greenland during the MPWP (Dolan et al., 2015b; Koenig et al., 2015). The first perennial Greenland glaciation likely occurred around the 2.7-2.4 Ma along with the intensification of NHG during the PPT, inferring from an abundance of IRD records (e.g., Flesche Kleiven et al., 2002; Jansen et al., 2000). Then after entering the Quaternary, the Greenland glaciation is paced by the glacial-interglacial cycle.

However, there are limitations on the records to understand the long-term history of Greenland ice sheet. For example, based on the ice core records, it is more accurate to reflect on the temperature change rather than the volume of the ice sheet.And the sea-level estimates always include the impact of Antarctic ice sheet, it is difficult to separate the sole impact of the GrIS. Moreover, the marine records of IRD can only predict the existence of large enough GrIS providing continous calving but have no implications for the shrinkage of the GrIS. Thus the constraints on the ice extent during the interglacial period have much uncertainties. For example the estimates of the Greenland ice sheet shrinkage during the last interglacial (130-115 kyrs) gain much debates and are highly

uncertain, which varies from 1 meter to 5.5 meters of sea level equivalent volume based on different studies (e.g., Cuffey and Marshall, 2000).

To understand the long-term history of Greenland ice sheet, the transient climate simulation with coupled climate and cryosphere model may provide an optimal way. However, the cryosphere evolution requires a longer response time (from centruies to millenium) than other climate components. Therefore to simulate long term evolution of both systems, the use of synchronously coupled climate cryosphere is very expensive in terms of computing time especially for a high resolution model representing the local change of Greenland ice sheet.

Till now, very few modeling studies succeeded to simulate the Greenland ice sheet evolution. Willeit et al. (2015) applied a coupled regional climate and cryosphere model to simulate the Greenland ice sheet evolution but with very important parameterization scheme. In our study, we will apply a new physically based method to simulate the Greenland ice sheet evolution which has been already successfully applied to simulate the Antarctic transition by Ladant et al. (2014). More details are shown in the next section.

## 5.2 Paper under review in Nature Communications: Modeling Greenland ice sheet evolution during the Plio-Pleistocene transition:new constraints for pCO2 pathway

### 5.2.1 Abstract

The late Pliocene intensification of Northern Hemisphere glaciation (NHG) with high-amplitude growth and decays of ice sheet has been documented through different observational studies. It is generally considered that the perennial glaciation of Greenland began around 2.7 Ma along with the intensification of NHG, indicated by records of ice rafted debris (IRD). Both data and coupled model studies have demonstrated that a decline in atmospheric pCO2 levels was instrumental in establishing a perennial Greenland ice sheet (GrIS), yet models have generally used simplistic CO2 constraints rather than those derived from data studies. Here, with a new fully physically based forward modelling approach designed for coupling climate and cryosphere models over several 100-kyrs integrations, we simulate the Greenland ice sheet evolution during the Plio-Pleistocene Tran-

sition (PPT, 3.0-2.5 Ma). We demonstrate the pivotal role of specific CO2 pathways, which are confined in a narrow window to trigger and maintain an extended GrIS: values lower than 280 ppmv are needed to produce the major extent of the GrIS at 2.7 Ma, whereas values higher than 320 ppmv, even with favourable insolation conditions, prevent the build-up of a large GrIS. Moreover, this forward method enables us, for the first time, to simulate GrIS evolution with different pCO2 scenarios derived from proxies and model reconstructions. When confronting simulated GrIS evolution to IRD reconstructions, there is a large consistency between IRD reconstructions and GrIS results. Our study emphasizes the crucial role of the pCO2 pathway for the GrIS evolution during PPT, which is particularly relevant in the context of GrIS response to future pCO2 scenarios.

### 5.2.2 Introduction

The long-term trend that led to the initiation of the cyclic Northern Hemisphere glaciations (NHG) can be dated from 3.6 Ma (Mudelsee and Raymo, 2005). A set of globally spread reconstructed SST records (Herbert et al., 2010; Lawrence et al., 2009; Venti et al., 2013) describes a gradual cooling trend for the middle to late Pliocene and early Pleistocene (3.6-2.2 Ma), associated with a progressive increase of benthic foraminiferal $\delta^{18}O$ high peaks (Lisiecki and Raymo, 2005), which can both reflect lower deep-water temperature and increased ice volume. Terrestrial data from Lake El'gygytgyn are also consistent with long-term ocean cooling (Brigham-Grette et al., 2013). During this period, the first marked peak of IRD was found around 3.4-3.3 Ma (MIS MG2 and MIS M2) East of Greenland (ODP site 907, (Jansen et al., 2000)) and is interpreted as evidence for an important glacial event before the establishment of the cyclic NHG around 2.7 Ma (Jansen et al., 2000; Maslin et al., 1998). Significant quantities of IRD were recovered in different ocean drilling sites in the North Atlantic during the PPT (Flesche Kleiven et al., 2002). This deposited IRD likely originated from Greenland, Iceland, North America and Scandinavia, suggesting large land ice expansions to the coast during this interval (Flesche Kleiven et al., 2002; Jansen et al., 2000). The onset of a perennial GrIS and of the cyclic NHG at the end of the PPT stands out as a tipping point in Earth climate evolution. Indeed, it marks the beginning of a low pCO2 world with perennial ice sheets in both hemispheres, which is infrequent in Earth's history (Ramstein, 2011), thereby creating specific geologic and climatic conditions allowing the development of glacial/interglacial cycles. Green-

land, however, may have experienced waxing and waning of ice before the intensification of NHG, as suggested by Eocene, late Miocene and early Pliocene IRD records (Jansen and Sjøholm, 1991; Larsen et al., 1994; Thiede et al., 2011). In particular, the last large glaciation of Northern Hemisphere prior to the major intensification at 2.7 Ma occurred during MIS-M2 (De Schepper et al., 2013; Dolan et al., 2015a; Mudelsee and Raymo, 2005; Tan et al., 2017). This 50 kyrs glaciation was followed by the well-known Mid-Pliocene Warm Period (MPWP) from 3.3 Ma to 3.0 Ma for which numerous observational and modelling studies carried out in the framework of the PlioMIP project (Haywood et al., 2016, 2015) have demonstrated that the warmer conditions led to a reduced GrIS (Hill, 2009; Koenig et al., 2015). The subsequent build-up of a perennial GrIS across the PPT remains poorly constrained from a spatio-temporal point of view because of its minor contribution to the signal in global benthic foraminiferal $\delta^{18}O$ records and of the paucity of direct geological data associated with the GrIS expansion. Models have the potential to provide valuable insights into the GrIS evolution but fully coupled GCM studies of the GrIS onset during the PPT were not yet available. Pioneering studies were carried out under fixed rather than transient climate conditions using snapshot simulations with the exception of the constant CO2 simulations of (DeConto et al., 2008). An important step (Lunt et al., 2008) demonstrated through a series of snapshot experiments of different forcing factors that the pCO2 lowering was the major driver of the GrIS glaciation. However, this result was obtained from equilibrium simulations for 2.7 Ma and using a pre-existent Pliocene GrIS (Hill, 2009). A more recent study (Contoux et al., 2015b)still using snapshot equilibrium simulations at 2.7 Ma suggested that, to maintain Greenland ice sheets after this initial glaciation, CO2 values had to remain low enough when the insolation increased (see Figure5.3b). By contrast, low resolution, conceptual and intermediate complexity models have indeed been useful to realize transient experiments (Berger et al., 1999; De Boer et al., 2010; Stap et al., 2017) but these models remain simplified with respect to many processes and do not have the spatial resolution to focus specifically on Greenland. Willeit et al. (2015) have recently provided the first transient experiment coupling high-resolution regional climate and ice sheet model. However, this study is based on pre-defined pCO2 data and simplified schemes in the method. Therefore, it remains still major challenge to simulate the PPT with a forward physically-based model, that allows for the first time to depict climate and ice sheet evolution over the 3.0-2.5 Ma time span.

### 5.2.3 Methodology

#### Model Description

The climate model used in this study is the IPSL-CM5A GCM (Dufresne et al., 2013).The ice sheet model used in this study is the GRenoble Ice-Shelf and Land-Ice model (GRISLI) (Ritz et al., 2001). More details related to these models are found in the Chapter2.

#### Tri-interpolation method

In the absence of synchronous coupling between GRISLI and IPSLCM5A, we utilise an interpolation that asynchronously couples both models and offers the possibility of carrying long-term numerical integration of the ice sheet model while accounting for the time evolution of main climatic forcings. This method consists in building a matrix of possible climatic states that are generated by IPSLCM5A under various combinations of forcings, which are chosen in the range of possible values taken by said forcings. The ice sheet model GRISLI can then be continuously forced by temperature and precipitation fields obtained by interpolation between the different IPSLCM5A climatic states; interpolation that is based on the time evolution of the forcings. The principle of this method has been described in details in Pollard and DeConto (2009) and an early version of it has been applied to the Eocene-Oligocene Transition (EOT) in Antarctica (DeConto and Pollard, 2003). In this work, we use an improved version of this method that has first been applied to the EO glaciation (Ladant et al., 2014) and that we have adapted to Greenland. Specifically here, we build a three dimensions matrix to account for the three main drivers of an ice sheet evolution, that are: 1) realistic insolation variations, 2) the atmospheric CO2 evolution, and 3) the ice sheet feedbacks on itself. The matrix hence comprises temperature and precipitation fields that are obtained from reference IPSLCM5A runs initialized with different combinations of orbital parameters, CO2 and ice sheet size. In a second step, the temperature and precipitation fields that force GRISLI can be computed by interpolating between the reference IPSLCM5A climatic states, based on the current value taken by the 65°N summer insolation and by the atmospheric pCO2 and on the instantaneous size of the ice sheet in GRISLI. This ensures that the climatic fields passed to GRISLI are appropriately updated at each time step to follow the evolution of both external (insolation and CO2) and internal (ice sheet geometry) forcings.

**Experiment Design**

In this study, we have chosen two orbital configuration that produce respectively the maximal (warm orbit) and the minimal (cold orbit) mean summer insolation at 65°N between 3.0 and 2.5 Ma, according to the astronomical solution calculated by the model of Laskar et al. (2004). At each time step of the ice sheet model simulations for the 3–2.5 Ma periods, the impact of the summer insolation can be included by appropriately interpolating between reference IPSLCM5A runs with warm or cold orbits.

The reference IPSLCM5A runs are initialized with four different CO2 concentrations: 220 ppmv, 280 ppmv, 360 ppmv, and 405 ppmv. Late Pliocene CO2 records indeed document a range of variation of the atmospheric pCO2 comprised between about 200 ppmv and 400 ppmv (See in Figure5.3). Similarly, the instantaneous value of pCO2 over the course of the simulation for the 3–2.5 Ma periods can be interpolated between reference runs with aforementioned pCO2 values. As pCO2 and temperature are linked via a logarithmic relationship, we prescribe a logarithmic interpolation between fixed pCO2 reference runs. Conversely, the interpolation is kept linear for the insolation.

To obtain the reference Greenland ice sheet sizes that are prescribed in the reference IPSLCM5A runs, we carry out a preliminary experiment in which we model the ice sheet development in an offline, one-way regrowth experiment (see (Contoux et al., 2015b) for details). We initialise IPSLCM5A with standard PlioMIP phase 1 conditions Contoux2012, which are then modified to start from an ice-free Greenland and extremely favourable conditions represented by the cold orbit described above and a CO2 concentration of 220 ppmv. GRISLI is then force with constant temperature and precipitation fields from the IPSLCM5A simulation until the ice sheet reaches equilibrium. The ice sheet geometry is then fed back to IPSLCM5A while CO2 and orbital parameters are kept identical. New climatic fields are thus obtained and GRISLI further simulates the ice sheet gain until a new equilibrium is reached. The geometry of the ice sheet can then be again passed to IPSLCM5A. This process is repeated until a new iteration does not markedly increase the ice volume. Here, seven iterations allow us to obtain seven Greenland ice sheet sizes ranging from very small to nearly full size ice sheet (Figure5.4).

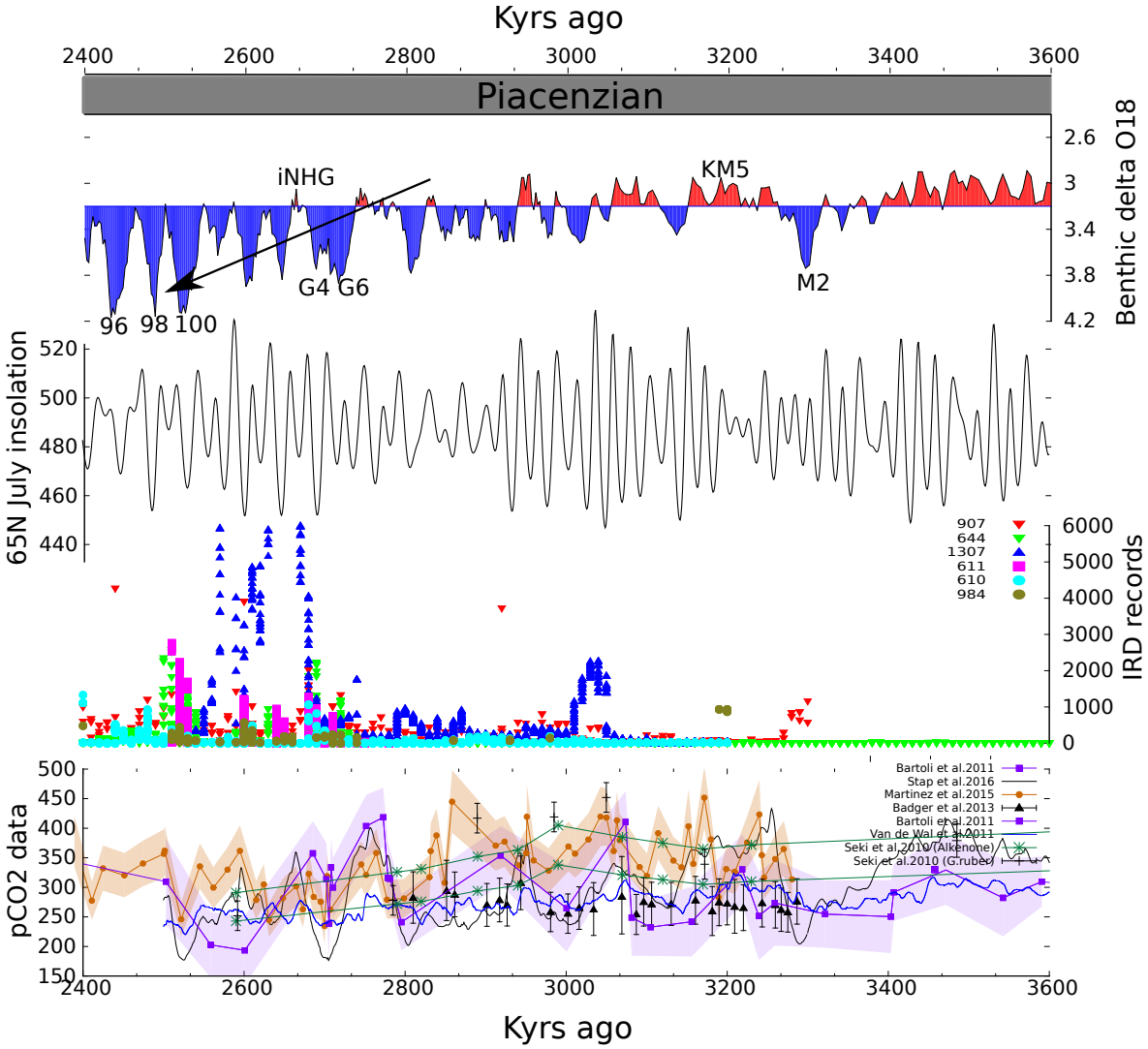


Figure 5.3 – A synthesis of Late Pliocene evolution. (a) LR04 benthic isotope stack (Lisiecki and Raymo, 2005) ; (b) July insolation at 65°N (Laskar et al., 2004); (c) Ice rafted detritus (IRD) records from different studies (DSDP Site 610 (Flesche Kleiven et al., 2002), DSDP Site 611 (Bailey et al., 2013), ODP Site 644 (Jansen and Sjøholm, 1991), ODP Site 907 (Jansen et al., 2000) , ODP Site 984 (Bartoli et al., 2006) and site U1307 (Sarnthein et al.,2009) ); (d) Reconstructed pCO2 records and model inverse data from different studies (Seki et al.,2010; Bartoli et al., 2011; Badger et al., 2013; Martinez-Boti et al., 2015; Van de Wal et al., 2011; Stap et al., 2016).

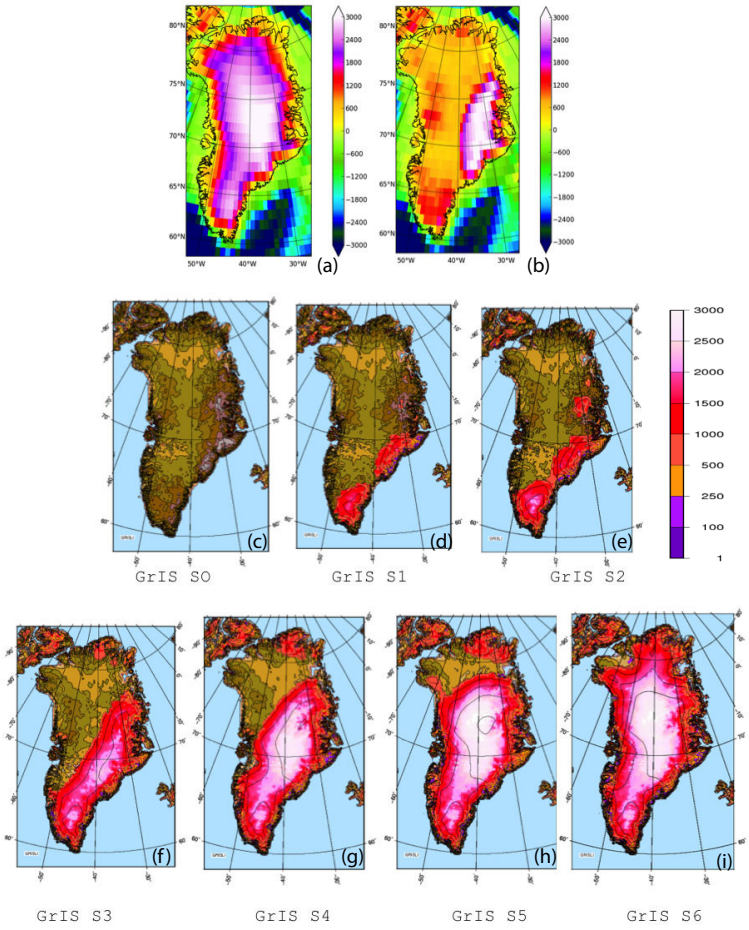


Figure 5.4 – Greenland ice sheet configurations.(a) and (b) present respectively the Pre-industrial and the reconstructed PlioMIP ( 3.2 Ma) Greenland topography (m). (c), (d), (e), (f), (g), (h), (i) present the seven simulated GrIS scenarios in this study which are imposed in the reference AOGCM experiments.

multirow

Table 5.1 – Forcing factors of reference AOGCM experiments

| Orbital Configuration | $pCO_2$ (ppmv) | Vegetation Settings | Prescribed GrIS size |
|---|---|---|---|
| Cold orbit (2.601 Ma) Or Warm orbit (2.589 Ma) | 220 | Cold orbit: PlioMIP modified<br>Warm orbit: PlioMIP | S0,S1,S2...S6 |
| | 280 | Cold orbit: PlioMIP modified<br>Warm orbit: PlioMIP | S0,S1,S2...S6 |
| | 360 | Cold orbit: PlioMIP modified*<br>Warm orbit: PlioMIP | S0,S1,S2...S6 |
| | 405 | Cold orbit: PlioMIP modified*<br>Warm orbit: PlioMIP | S0,S1,S2...S6 |

The matrix of reference IPSLCM5A climatic states is then built using the forcings described above. A total of 2 (for the insolation) x 4 (for CO2) x 7 (for Greenland ice sheet sizes) simulations are run in parallel to provide reference T and P fields that cover the range of possible variations of the three main drivers that are insolation, CO2 and ice sheet size. A continuous T and P forcing can then be calculated based on the prescribed (for insolation and CO2) and emerging (for ice sheet) evolution of these drivers. Although complex and fastidious to implement, this method offers in particular the possibility to test virtually any CO2 scenario without additional GCM runs. It should be noted that vegetation feedbacks linked to vegetation changes under Late Pliocene conditions are taken into account in our IPSLCM5A simulations, since the tundra-taiga feedback has been shown to play a role in the onset of NH glaciation (Koenig et al., 2011). We divide the IPSLCM5A boundary conditions into three types relative to their presumed impact on vegetation: cold, intermediate and warm. The cold conditions are defined by the combination of the cold orbit and either 220 ppmv or 280 ppmv of CO2 concentration. In the reference IPSLCM5A simulations whose boundary conditions fall under the cold criterion, we modify the PlioMIP vegetation map (Salzmann et al., 2008) by specifying tundra north of 50°N. The intermediate conditions are defined by the combination of the cold orbit and either 360ppmv or 405 ppmv of CO2 concentration and the PlioMIP vegetation map is modified by specifying tundra north of 65°N. Finally, the warm conditions are defined by the warm orbit, regardless of the CO2 concentration. Under these conditions, we keep the PlioMIP vegetation map unchanged. All the reference AOGCM experiments are summarized in Table5.1.

## 5.3 Proxy factors and proxy data used to drive and validate our study

### 5.3.1 pCO2 data

In this study, we used three reconstructed pCO2 records as the forcing factors respectively from (e.g., Bartoli et al., 2011; Martínez-Botí et al., 2015; Seki et al., 2010). The former two records are based on the boron isotope composition of the planktic foraminferal species from the ODP site 999, the last records are derived from alkenone estimates. We applied average values and their uncertainties of each data as forcing factors in our simulations. The data from Martinez-Boti et al. and Bartoli et al. include two calculations of uncertainties, and we only applied the smaller errors in the simulation. More details about these data can be found in the reference.

Apart from the direct reconstruction of pCO2 using different proxy records, we also applied three different model-based data of pCO2 in our simulation respectively from Willeit et al.(2015) (3.2 Ma-2.4 Ma), Stap et al.(2016), Van De Wal et al.(2011) (3.5 Ma – 2.5 Ma). The first one are obtained from pre-defined dynamical CO2 function linked with obliquity change based on the available pCO2 records and constrained by the criteria of the both $\delta^{18}O$ and global SST. Here we only choose the best pCO2 scenario to drive our model, which is shown in Figure5.7. The latter two data are obtained from low-resolution coupled climate–ice sheet model, inversely forced by a stacked benthic $\delta^{18}O$ record. The modeled GrIS evolutions with these two pCO2 data are shown in the Figure5.8.

In Willeit's study, the modeled GrIS evolution is from one-way simulation by coupling regional climate and ice-sheet model. The feedback of GrIS change is not incorporated in the global climate. Nevertheless, the approach developed by Wiley remains a first attempt to constrain physically the most possible CO2 pathway, but it includes strong hypothesis and parametrization. In their standard model set-up, the relationship between GrIS size and surface temperature are linearized by an empirical correction: starting from 2 degree for ice free Greenland linearly decreasing to zero degree for a nearly full Greenland ice sheet. More details can be referred to the reference.

### 5.3.2 IRD and SST records

The available IRDs used in this study are obtained respectively from ocean drilling project (ODP) site 907 (Jansen et al., 2000), ODP site 611 (Bailey et al., 2013) and Integrated Ocean Drilling Project (IODP) site U1307 (Sarnthein et al., 2009b).It is important to note that the available IRD datasets differ in temporal resolution, in the method of IRD detection, and the size fraction of mineral grains. The IRD peaks that occur during the PPT are indicative of the presence of dynamic glacial margins. The peaks present in these datasets are general smaller than those observed in Late Pleistocene IRD events which have been considered to indicate the occurrence of large-scale ice sheet collapses (Heinrich, 1988)(Heinrich and Lotti, 1995). They do however represent significant influx of mineral grains from terrestrial provenances into deep marine settings, which in turn indicate the presence glacial margin dynamics. The specific definition of IRD used in the studies references here varies in some details. For ODP Site 907, Jansen et al. (2000) counted all terrestrial non-volcanic mineral grains >125 um as IRD, giving IRD concentration data for their samples. For Site 611, Bailey et al. (2013) counted mineral grains >150 um in size and provide both IRD concentration and flux rate, which are largely in agreement with each other (i.e. there is no significant effect of sedimentation rate on the IRD variability). For IODP Site U1307, Sarnthein et al. (2009) do not provide a clear definition of IRD, simply displaying concentrations. The fact that, despite these differences in IRD definition as well as the different regional settings, significant increases in IRD coincide at 2.7 Ma, gives a clear indication of increased glacial margin dynamics.

According to (Andrews, 2000) an important difference between PPT and more recent (Late Pleistocene) ice rafting may play a role in absolute IRD abundance differences as well. Modern icebergs are relatively clean, containing only small amounts of terrestrial mineral grains, which means that they would provide only small amounts of IRD. Early expansions of the GrIS during the PPT could potentially have contained more mineral grains per iceberg. Bailey et al. (2010) discuss a possible different type of ice sheet behavior (movement of ice sheets over land) during the Pliocene-Pleistocene transition compared to that of large (e.g. modern Greenland) ice sheets, which could potentially lead to changes in IRD signals without large-scale changes in the GrIS volume in the Late Pliocene-Early Pleistocene.

The available SST records used in this study are obtained respectively from ODP site

982 (Lawrence et al., 2009) and from re-drill of Deep Sea Drilling Project (DSDP) site 607 (Naafs et al., 2010). These data are obtained by using the alkenone unsaturation index $U_{37}{}^{k'}$ and show the reconstructed mean annual temperatures at the surface. The referenced SST time series are resolved at orbital time scales (between 2 ka and 4 ka). Other details about these data can be found in the given references. The location of all these sites is shown in Figure5.9a.

### 5.3.3 Results and Discussions

In this study, we use a recent numerical interpolation method (Ladant et al. 2014), which couples climate simulations obtained with the fully coupled IPSL-CM5A model (Dufresne et al. 2013) and the 15-km resolution version of the ice sheet model GRISLI (Ritz et al. 2001), in order to investigate the transient evolution of the GrIS across the PPT under the combined influence of orbital and atmospheric pCO2 variations. The evolution of the 65°N summer insolation is perfectly constrained across the PPT (Laskar et al., 2004) (see Figure5.3b ) but measurements of the CO2 levels for this interval remain poorly constrained because the reconstruction methods have many inherent uncertainties and results are strongly divergent. The major advantage of our approach, however, is the ability to directly test the response of the climate–ice sheet system to different scenarios of the pCO2 evolution in order to then define the plausible pCO2 pathways that led to the GrIS inception and variability. We thus use different reconstructions coming from both proxy records and inverse modelling studies (e.g. Bartoli et al., 2011; Martínez-Botí et al., 2015; Seki et al., 2010; Willeit et al., 2015; Stap et al. 2016, Van de Wal et al. 2011), as well as constant CO2 evolutions.

#### Threshold

We first present six experiments with constant pCO2 ranging from 220 to 405 ppmv using realistic orbital variations (Laskar et al., 2004; Figure5.3b). As shown in Figure5.3c, the evolution of the GrIS clearly shows that under 280 ppmv of pCO2, it is possible to trigger and maintain a large perennial ice sheet over Greenland despite unfavourable orbital condition occurring at 2.6 Ma following after the large extent of GrIS. Between 280 and 320 ppmv, the sensitivity of the GrIS volume to orbital variations is considerable, illustrating the role of the complex interplay between pCO2 and orbital variations in the dynamics

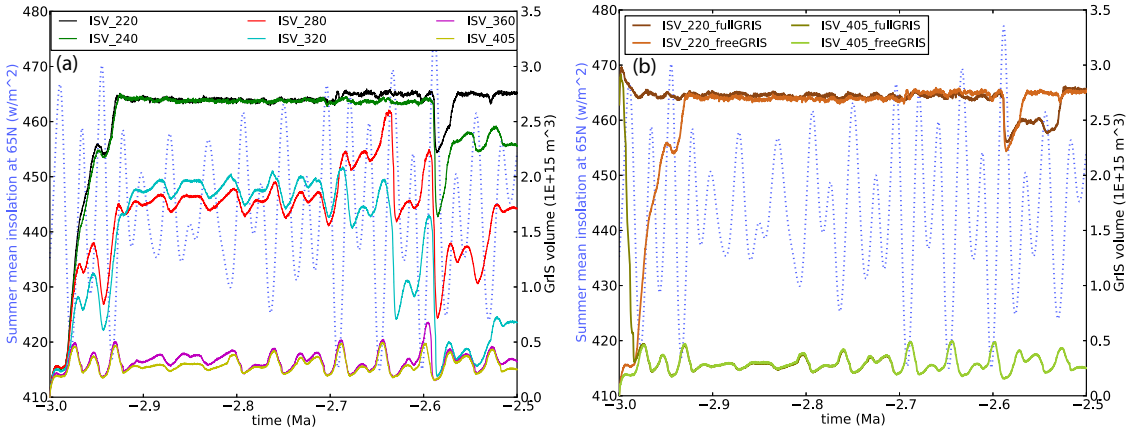


Figure 5.5 – (a) Simulated GrIS volume with different constant CO2 concentrations (220ppmv, 240ppmv, 280ppmv, 320ppmv, 360ppmv, 405ppmv). (b) Simulated GrIS volume with the smallest pCO2 concentration (220ppmv) and the largest one (405ppmv) but using two different initial GrIS configurations: maximum full GrIS corresponding to present day and free GrIS with no ice sheet. Light blue dash lines present the summer mean insolation at 65°N.

of the GrIS, especially after 2.7 Ma when insolation becomes highly variable. Finally for pCO2 levels higher than 320 ppm, we show that the ice sheet can be neither triggered nor maintained after 2.7 Ma. The results of these constant simulations are in good agreement but go one step beyond previous transient experiments at constant CO2 (DeConto et al., 2008) in that we demonstrate that the GrIS possesses dynamics on orbital timescales across the PPT only for a very narrow window of atmospheric pCO2 concentrations ( 50 ppm).

**Initial Conditions**

According to existing knowledge the GrIS ice sheet largely retreated during the MPWP, but the real state of the Greenland ice sheet and topography remain highly uncertain (Dolan et al., 2015b). In order to investigate the impact of different initial GrIS on the threshold of pCO2, we test two different initial GrIS: free GrIS and present GrIS. Our results show that no matter if the pCO2 level is low (220ppmv) or high (405ppmv), the simulated ice sheet evolution does not depend upon the original ice-sheet we begin with at 3.0 Ma. Figure5.5b indicates that for this range of pCO2 values (220 / 405 ppmv) the insolation driven changes are the same regardless of the initial ice sheet size.

**GrIS evolution using pCO2 reconstructions**

In the next step, we forced our setup with published reconstructions of atmospheric pCO2, derived from recent empirical reconstructions (Martinez-Boti et al., 2015; Bartoli et al., 2011; Seki et al., 2010) (Figure5.6) or from inverse modelling (Willet et al., 2015, Stap et al., 2016, Van de Wal et al., 2011) (Figure5.7 and Figure5.8), in order to confront the modelled GrIS evolution to previous work and to IRD records across the PPT. We employed recent pCO2 reconstructions based on alkenones and boron measurements (Martinez-Boti et al., 2015; Bartoli et al., 2011; Seki et al., 2010) (green lines on Figure5.6). These records depict quite different CO2 evolution scenarios, from a mostly linear and low-resolution decrease for the older record (Seki et al. 2010) to high resolution and high pCO2 variations in the more recent record (Martinez-Boti et al., 2015). When forced by the high estimated CO2 levels of Seki et al. 2010, the GrIS evolution confirms the major role of orbital variations when the CO2 levels are confined between 280 ppmv and 320 ppmv (Figure5.6c). While CO2 levels remain above 350 ppm, even large orbital variations do not significantly affect the extension of the GrIS (3.0 to 2.9 Ma). During the 2.9 - 2.7 Ma intervals, the low variability in insolation does not enable the GrIS to grow in spite of CO2 levels decreasing down to 300 ppm. The simulated GrIS evolution then shows a significant increase at 2.7 Ma and a pronounced orbital scale variability between 2.7 and 2.5 Ma, but importantly no full retreat of the GrIS during the insolation maximum after 2.6 Ma because this maximum is associated with low CO2 levels less than 300 ppm (Figure5.6). In contrast, the low estimates of CO2 levels generates a large perennial GrIS as early as 2.9 Ma triggered by the combination of an insolation minimum and low CO2 levels. A similar modelled evolution

of the GrIS is obtained when forced by the Bartoli et al. 2011 CO2 record. Regardless of the uncertainties, the low CO2 levels in this record force an early onset of a perennial GrIS (Figure5.6b). However, because of their low resolution, these two records do not show any CO2 variability on the 10 kyrs timescale contrary to that of Martinez-Boti et al. 2015, who demonstrate that the PPT CO2 evolution is in fact much more variable than previously thought. The uncertainties associated with the estimates of the Martinez-Boti et al. 2015 record show that a completely different evolution of the GrIS can be simulated (Figure5.6a). The high (low) estimates depict an evolution close to that driven by the high (low) estimates of Seki et al. 2010, because CO2 levels during times of insolation extremes (3.0 – 2.9 Ma and 2.7 – 2.6 Ma) are similar. However, the simulation forced with the mean CO2 estimates of Martinez-Boti et al. 2015 (Figure5.6a, solid red line) shows an early attempt of GrIS expansion (2.98 – 2.94 Ma) before a progressive onset from 2.8 Ma onwards with significant increase in GrIS volume at 2.7 Ma and 2.65 Ma during times of coupled low insolation and low CO2 levels. After 2.6 Ma, the GrIS melts rapidly down to small ice caps in the southern and south-eastern margins because of a simultaneous increase in summer insolation and CO2. The ice sheet expansion then resumes at 2.55 Ma. Interestingly, the CO2 records of Martinez-Boti et al. 2015 generate a sharp GrIS volume decrease after 2.6 Ma, regardless of the uncertainties and earlier shape of the expansion of the ice sheet because of an increase in pCO2 values during the insolation maximum. This seems contradictory to a presence of a large and perennial ice sheets from 2.7 Ma onwards but the comparison to IRD records does not invalidate a scenario with a large deglaciation after 2.6 Ma. A comparison to the Willeit et al., (2015) ice sheet evolution provides confidence in the ability of our model to simulate the GrIS evolution across the PPT. Using their monotonously-decreasing and obliquity-modulated best fit CO2 scenario, we find a similar modelled GrIS evolution as Willeit et al., 2015, in particular in that we reproduce the large increases in GrIS volume at 2.7 Ma and 2.55 Ma as well as the large decrease at 2.6 Ma, even though our GrIS volume displays less variability because of a lower sensitivity to the orbital forcing in our fully coupled climate-ice sheet model. Inverse modelling studies (Stap et al., 2016, Van de Wal et al., 2011) have also provided potential CO2 reconstructions for this interval (Figure5.8). However, the low CO2 concentrations throughout most of these reconstructions lead to large perennial GrIS as early as 3.3 Ma, which is inconsistent with a warmer MPWP interval (Haywood et al., 2013).

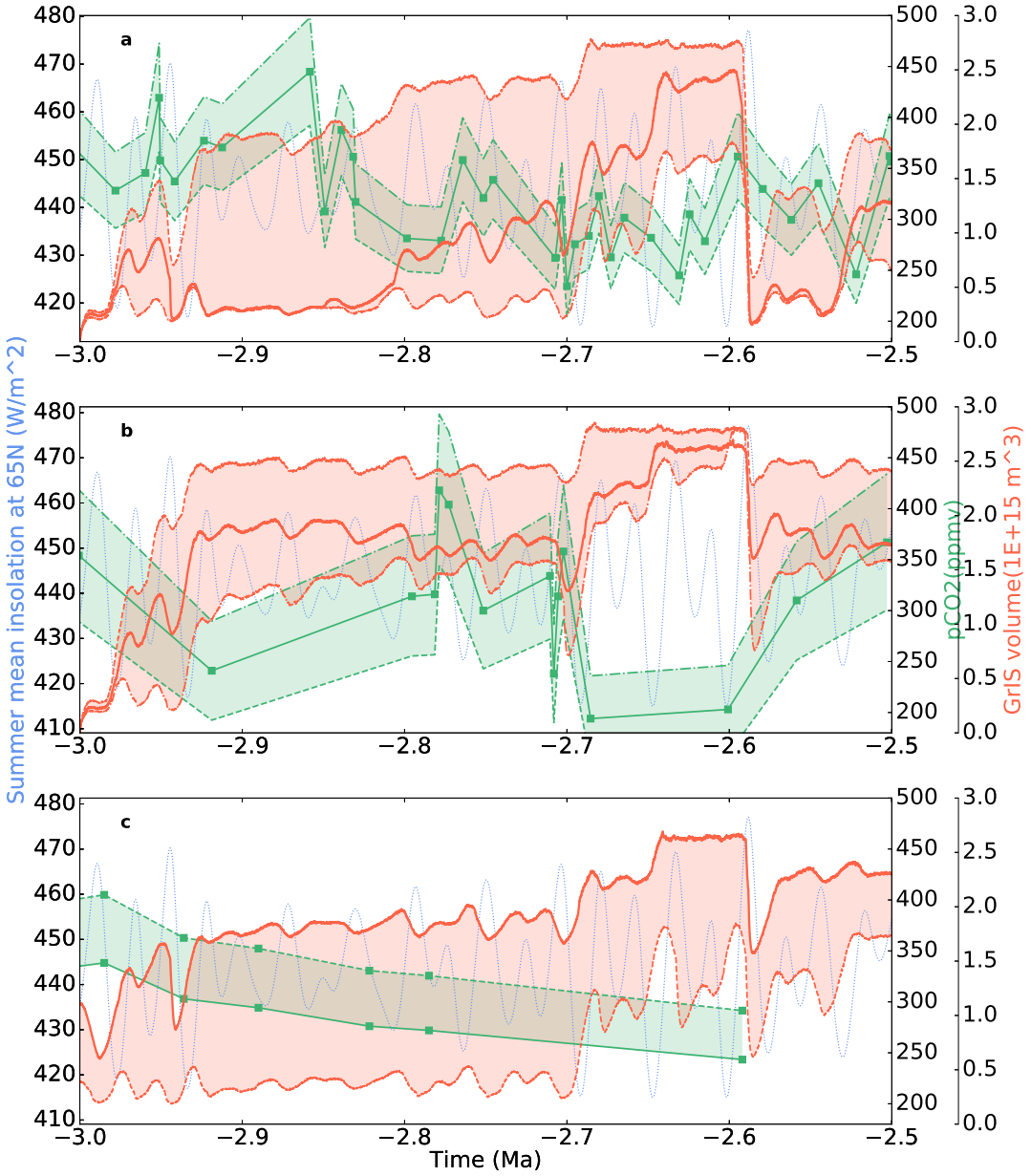


Figure 5.6 – Simulated GrIS volume evolution based on different pCO2 records: (a) Martinez-Boti et al.2015; (b) Bartoli et al. 2010; (c) Seki et al. 2010. In this panel, light blue dash line presents the boreal summer insolation at 65°N; green lines present the pCO2 records and their uncertainties (green shaded region); the orange curves present the simulated GrIS volumes based on pCO2 records and their uncertainties. In (a, b), the middle orange curve present the simulated GrIS volume with the average pCO2 values of each records; the upper and lower shaded orange range present the simulated GrIS with the low and high pCO2 values considering the uncertainties of each records. In (c), the upper and lower shaded orange range respectively present the simulated GrIS volumes with the low and high pCO2 of Seki et al. (2010)

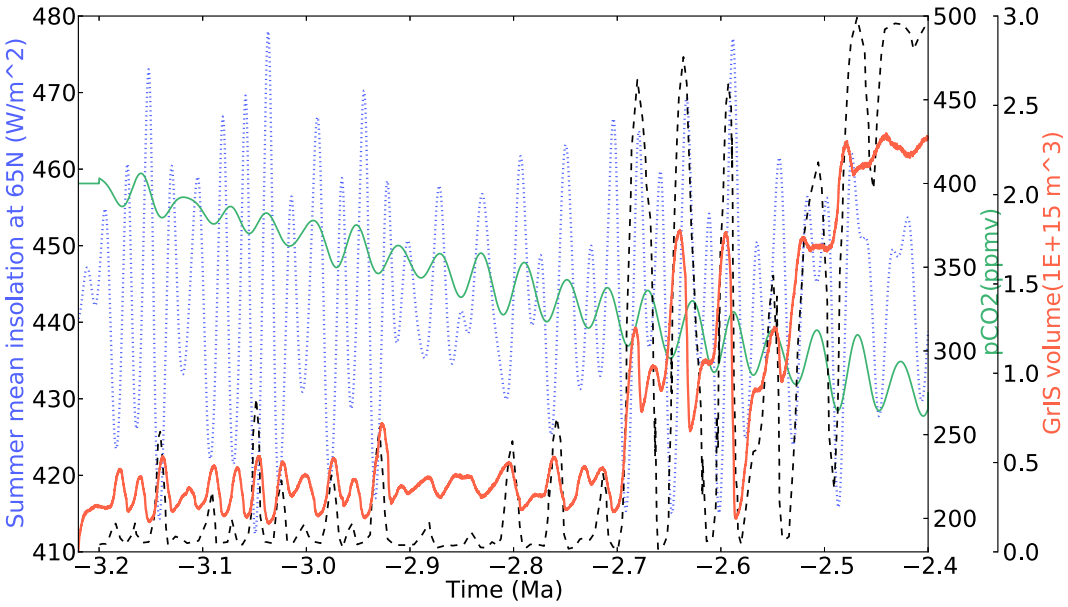


Figure 5.7 – Simulated GrIS volumes with the best scenario of pCO2 built-up by Willeit et al. 2015 (green line). Orange line presents the result of this study, black dash line presents the result of Willeit et al. 2015.

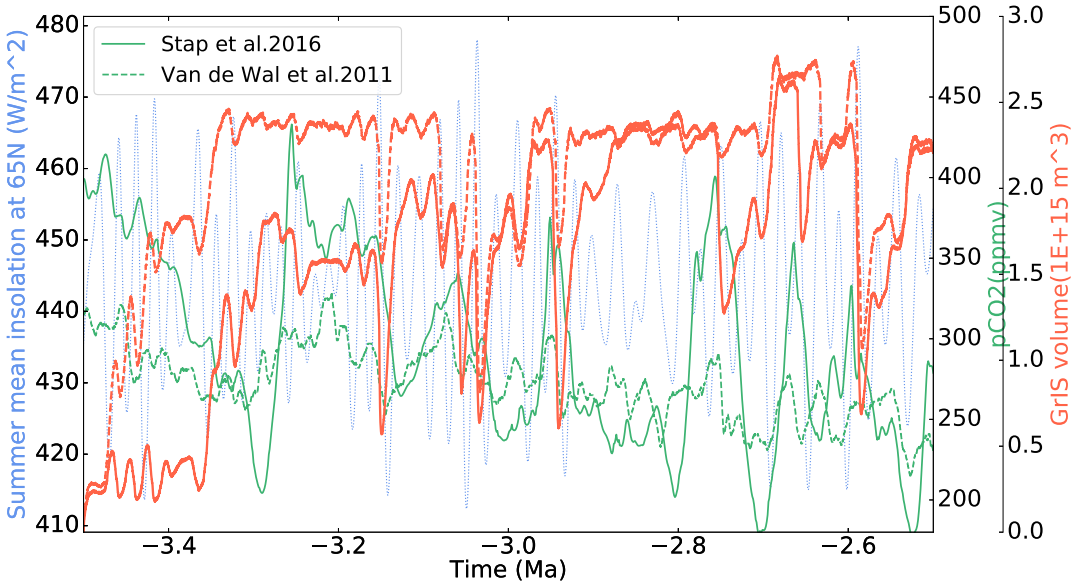


Figure 5.8 – Simulated GrIS volumes during 3.5-2.5 Ma based on two sets of model inverse pCO2 data (Stap et al.2016 and van de Wal et al.2011). Light blue dash line presents the boreal summer insolation at 65°N, Green and orange dash lines present respectively the pCO2 data from van de Wal et al. (2011) and the associated simulated GrIS volume. Green and orange solid lines present respectively the pCO2 data from Stap et al. (2016) and the associated simulated GrIS volume.

**Data-model Comparison**

In this work, we restrict the high-resolution ice sheet modelling to scenario of the evolution of the GrIS across the PPT because Greenland is the primary location for ice nucleation in the North Hemisphere (Larsen et al., 1994), although numerous evidence for ice growth outside Greenland during this period have been reported (Knies et al., 2009, Bailey et al., 2013, Maslin et al., 1998). The limitation to the sole Greenland ice sheet hampers comparisons with 18O and sea level records because the maximum ice volume that can be accommodated over Greenland represents roughly 7 m of equivalent sea level, i.e. in the range of experimental and/or instrumental errors. However, significant insights can be gained from adjacent IRD records (Kleiven et al., 2000) in order to further constrain the possible evolution of the GrIS and of CO2 across the PPT. It must be kept in mind that attempting to constrain the GrIS geometry and volume from IRD records remains speculative because the absence of IRD does not necessarily correlate with the absence of GrIS and because IRD peaks may contain material not only derived from melting Greenland icebergs, iceberg trajectories may change, and the ambient temperature along the iceberg trajectory may influence the melt-out rates of the IRD contained in the icebergs. For instance, variations in North Atlantic SST and/or currents or changes in the sediment contents of the calved icebergs could explain the absence of IRD even though the GrIS maintain a significant iceberg discharge (Andrews 2000; Bailey et al. 2013). In addition, IRD peaks can represent an ice growth phase, during which increasing GrIS volume may lead to increased iceberg discharge, as well as an ice melt phase, during which the warmer climatic conditions may lead to enhanced ice sheet melting and consequently enhanced ice flux at the margin. Despite these uncertainties IRD records comprise a first order insight into ice sheet dynamics, and their relation to orbital variations and coherent behaviour across several core sites indicate that they have a consistency that aid in defining the most probable scenario for GrIS evolution. We used ODP Site 907 (Jansen et al., 2000), IODP Site U1307 (Sarnthein et al., 2009) and ODP Site 611 (Bailey et al.2013) (Details about these data are shown in SI.4;Figure5.9a) because the IRD records from these sites can be confidently assumed to primarily originate from the GrIS (Bailey et al., 2013). Sites U1307 and 907 are located offshore the Greenland margins and show small but continuous IRD deposition in the interval of interest here from as early as 3 Ma (Figure5.9b), with the exception of a single peak at 2.92 Ma at Site 907. Around 2.7 Ma, several IRD peaks in both

records suggest intensification of the iceberg discharge, broadly correlated to North Atlantic sea surface temperatures (SST) cooling events (Figure5.9c). Accordingly, the record from Site 611, located further south from Greenland, shows absence of IRD deposition before 2.72 Ma and several peaks afterwards. There is variable agreement between our reconstructed GrIS volume scenarios and inferred GrIS extension as implied by IRD records. For instance, the GrIS evolution forced by Bartoli et al. (2011) CO2 records agrees poorly with the IRD records because it suggests a large to near complete perennial GrIS as early as 2.98 – 2.95 Ma (Figure5.9b). By 2.9 Ma, a large ice sheet covering the totality of the southern Greenland margin is present without any particular changes above the 3.0 – 2.7 Ma background IRD values at Site U1307. At Site 907, an early increase of a large GrIS could explain the 2.92 IRD peak but in this case, the IRD deposition should have continued on higher levels relative to the pre-glaciation interval. In addition, the absence of any IRD at Site 611 at that time suggests that the GrIS was still of relatively limited size. In contrast to the results from using the Bartoli et al. (2011) CO2 records, the mean and high CO2 estimates of Martinez-Boti et al. (2015) and the high estimate of Seki et al. (2010) generate GrIS evolutions bearing increased consistency with the IRD records. The modelled GrIS using these reconstructions is limited to small ice caps on the southern and south-eastern margins of Greenland during the interval 3.0 – 2.7 Ma, which agrees well with small but continuous IRD inputs at Site 907 and U1307 (Figure5.6a-c and Figure5.9a-b). The sharp increase at 2.7 Ma in IRD deposition is also accounted for by these GrIS evolution scenario. Furthermore, the IRD records of Site 611 (Bailey et al., 2013) displays four IRD peaks (at 2.7 Ma, 2.64 Ma, 2.6 Ma and 2.52 Ma) that are relatively well correlated in time with decreases in North Atlantic SSTs and large modelled GrIS variations (Figure5.9b,c , in particular for the Martinez-Boti et al. (2015) mean and high CO2 scenario. Importantly, the large GrIS volume decrease after 2.6 Ma in these scenarios is not at odds with the IRD records, in that the minimal GrIS state still reaches the southern and south-eastern margins of Greenland, allowing small but uninterrupted iceberg discharge at Site 907. These three pCO2 scenarios (Martinez et al., (2015) high, mean and Seki et al., (2010) high CO2 estimates) therefore seem to correlate relatively well with IRD records because the GrIS expands preferentially from its southern and south-eastern margins and intervals of large GrIS variations are synchronous with IRD peaks. However, the integration of these scenarios into a broader context of NHG intensification reveals that the GrIS evolution driven by the Martinez et al., (2015) mean CO2 estimates is likely the most consistent scenario. In-

deed, evidences for ice sheets outside Greenland are numerous (Bailey et al., 2013; Knies et al., 2009; Lisiecki and Raymo et al., 2005 ) and are more difficult to reconcile with an only partially glaciated Greenland as reconstructed from the Martinez et al., (2015) and Seki et al., (2010) high CO2 estimates.

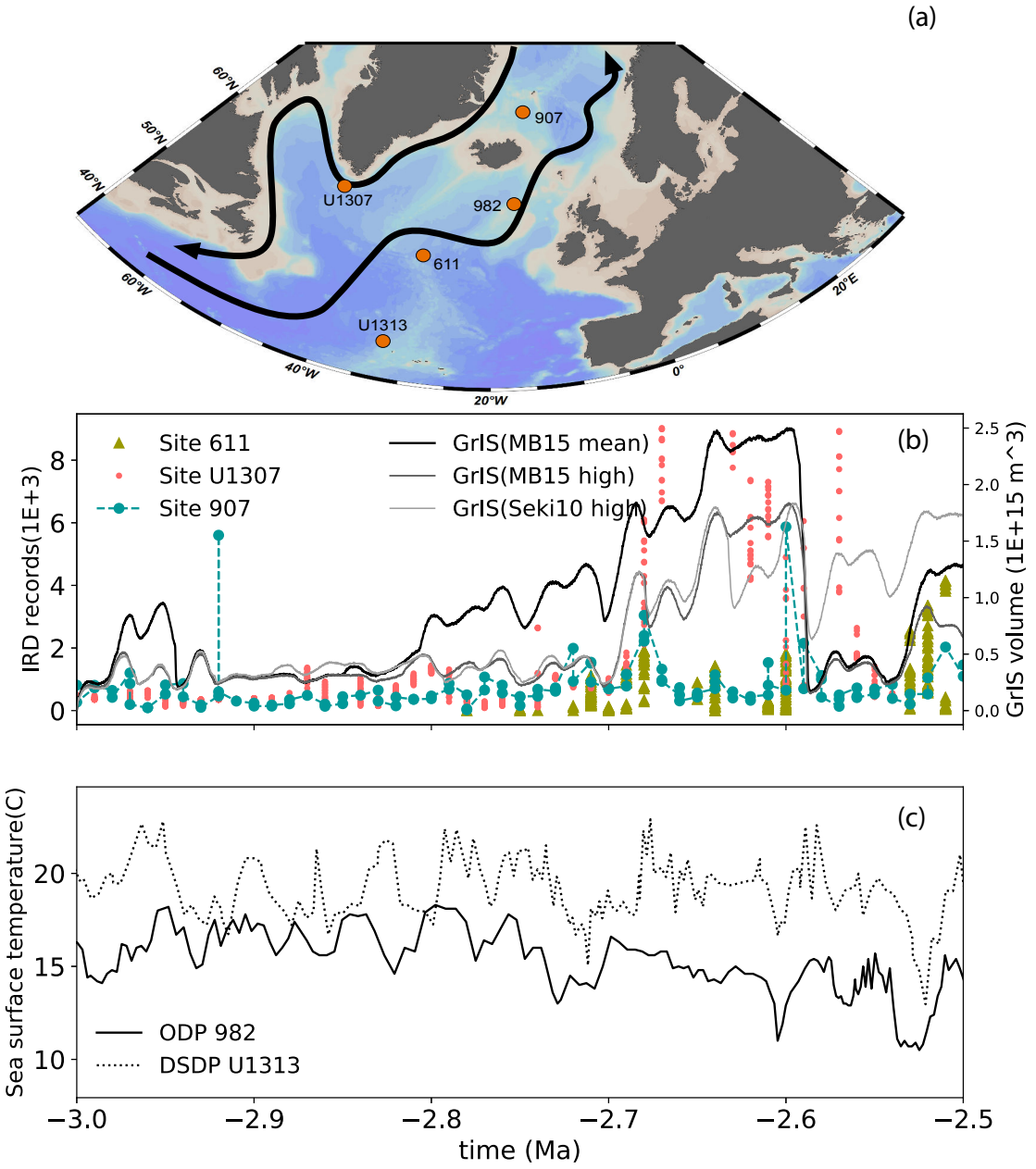


Figure 5.9 – (a) Map showing simplified main ocean currents in NATL and ocean deep drilling sites referenced in this study (Ocean Data View, Schlitze et al.,2012) (b) Related IRD records in the North Atlantic regions: site 907 (Jansen et al., 2000); site U1307 (Sarnthein et al.,2009); site 611 (Bailey et al. 2013) and simulated GrIS volume with the pCO2 reconstructions of Martinez-Boti et al., 2015 mean and high estimates and Seki et al., 2010 high estimate.; (c) Reconstructed sea surface temperature at ODP site 982 by Lawrence et al. (2009) and IODP site U1313 by Naafs et al. (2010).

### 5.3.4 Conclusions

Our forward physically based approach, modelling the GrIS evolution during the PPT, shows that the long lasting paradigm which explained the huge GrIS extension occurring at 2.7 Ma by a minimum summer insolation at 65°N is, by far, too simple. All along the PPT period (3.0-2.5 Ma), the GrIS volume appears very sensitive to CO2 changes. Consequently, our numerical experiments demonstrate that, to trigger and maintain GrIS during the whole period, CO2 pathways have to be confined in a narrow window. Moreover, we show that the GrIS evolution, simulated by using the most recent pCO2 reconstruction (Martinez-Boti et al. 2015 mean estimate), is in good agreement with relevant IRD records. These records depict large variations of GrIS ice-sheet as well as indicating a continuous presence of a GrIS large enough to calve icebergs. This result emphasizes the crucial role of pCO2 pathways during PPT to maintain GrIS, which shapes the framework for the quaternary NH glacial-interglacial cycles. This result is moreover relevant in the context of future GrIS evolution due to different RCP pathways(IPCC AR5 WG1 (2013) ). Indeed, because of its small size and location, GrIS appears to be very sensitive to CO2 variations. In the future there is a strong need for both new marine records and more climate-ice sheet simulations to improve our understanding of the likely CO2 pathways during PPT.Nevertheless, our methodology has indeed also some limitations. A major one is that we hypothesis linear behavior between the phase space of 56 numerical simulations built to nest the evolution of the climate cryosphere system. However, we know that there are also instabilities in the response of the ice sheets (Hodell et al., 2018). These abrupt events are not accounted for in our simulation because very high temporal resolution for pCO2 records for this period are not yet available. Nonetheless, our study contributes to shed light on the first order behavior of climate cryosphere evolution during this key periods when the climate shifted from a asymmetric warm world with high pCO2 to a more symmetric one corresponding to one ice sheet in each hemisphere, colder temperatures and lower pCO2.

# Chapter 6

# General Conclusions and Perspectives

## Contents

## 6.1 General Conclusions

This thesis is devoted to understanding the interaction between cryosphere and climate from the mid Pliocene to the early Quaternary during the onset of Northern Hemisphere Glaciation (NHG). Firstly, we investigate the causes for the development and decay of the large but short living glaciation that occurred during Marine Isotope Stage 2 (M2, 3.264-3.312 Ma); Secondly, in the framework of the international Pliocene Model Intercomparison Project (PLIOMIP2), we study the climate of Mid-Piacenzian Warm Period (MPWP, 3.3-3.0Ma). Thirdly, we explore the Plio-Pleistocene Transition (PPT, 3.0-2.5Ma) with an appropriate asynchronously coupled climate cryosphere model. Through these different periods, we provide a better understanding of the relationship between $pCO_2$, tectonics and climat during the transition from a warm and high-$CO_2$ world to the cold and low-$CO_2$ Quaternary glaciations.

The Marine Isotope Stage M2 (3.264-3.312 Ma) occurred just prior to the well documented warm mid-Pliocene (mPWP). With a 0.5‰benthic foraminiferal $\delta^{18}O$ shift (Lisiecki and Raymo, 2005), MIS M2 is thought to be a glacial comparable period associated with huge but uncertain sea-level records ranging from 20 to 60m being below present level (Naish et al. 2009; Miller et al. 2012; Dwyer et al. 2009). However, the mechanism of M2 initiation and termination are still an enigma, since CO2 records were relatively higher than in the Quaternary glaciation period and the variations of summer insolation during M2 were weaker than other glacial periods. By inferring from marine proxy data, De Schepper (2013) proposed that the shallow open Central American Seaway (CAS) observed during M2 could play as a trigger in M2 initiation, then the closure of this shallow CAS resulting from M2 large ice sheet buildup terminates this glacial period. But this assumption had not been tested by models. In this attempt, we apply IPSL-CM5A Atmosphere-Ocean coupled General Circulation Model (AOGCM) and GRISLI ice sheet model to investigate mechanisms of M2 initiation and termination. We firstly investigate the role of "shallow opening CAS" (De Schepper et al. 2013) on M2 initiation. In the mean time we also take into account the main forcing during M2, which includes astronomical parameters, Greenhouse gases and vegetation. Our results show that shallow opening CAS plays an important role in reducing northward heat transport in Atlantic low latitudes by 0.05-0.1 PW, but it is not a key factor in NH ice sheet build-up; Astronomical parameters and low pCO2 concentration are essential to create a basic global

cooling environment for M2 (cooling by about 3.65 K than mPWP); Cold vegetation replacement amplifies the cooling in north high latitudes by about 8 K, which finally allows large ice sheet building up in Northern Hemisphere (12.25 m sea level drop is simulated with considering ice sheet feedback on the climate) and a large expansion in West Antarctic ice sheet which provides about 4m sea level drop. The simulated ice sheet locations and areas correspond well to the terrestrial ice evidence. The diagnostics in the Atlantic Ocean also suggest a better agreement with data especially in terms of sea surface temperature and North Atlantic Current change. Finally, to explore the relationship between M2 termination and the closure of shallow CAS, we close CAS based on the simulation with large ice sheet built-up scenario. However, after the closure of this shallow CAS, we observed a small change in NH ice sheet which is in the agreement with previous CAS studies (Lunt et al. 2008). Our major finding in this study is therefore the crucial role of pCO2 changes.Future studies should first bring more constrain on carbon climate interaction during MIS M2 and more modeling efforts should be done to simulate this glaciation, notably by exploring potential synergistic effects between the CAS, Bering Strait and Indonesian Seaway (Krebs et al.,2011).

The MPWP following MIS M2 glaciation is well documented and simulated within PLIOMIP framework. Indeed its warming climate associated with similar-to-present pCO2 makes this period very appealing. In the PlioMIP phase 1, the MPWP is simply considered to be a whole warming period, which may make the great influence on the discord between model data comparison. Thus in the PlioMIP phase 2,with the recognition of the climate variability of the MPWP, a specific interglacial period (MIS KM5c, 3.205Ma), in which the orbital parameters are similar, was selected to be the study target and new boundary conditions are accordingly prepared for this new period. This part of the thesis therefore contributes to the PLIOMIP phase 2. In this thesis, we describe the results of modeled warm interglacial of MIS KM5c (3.205 Ma) located in the interval of the MPWP (3.0-3.3 Ma) with imposing the new boundary conditions of PRISM4 (Dowsett et al., 2016). Two versions of core experiments are conducted based on two versions of IPSL coupling model: IPSL-CM5A and IPSL-CM5A2.1. Three tier experiments are conducted based on IPSL-CM5A2.1 to study the roles of the uncertainties of $pCO_2$ and the ice sheet boundary conditions in the warming climate. The new boundary conditions of PRISM4 adapted in our models produce an enhanced global warming in the MPWP,especially for the mid-to-high latitudes when comparing to the PlioMIP phase 1 results. This modeled meridional

surface temperature gradient is similar to the proxy data from PRISM3D. However, the magnitude of the high latitude warming amplification is still underestimated. The enhanced warming can be majorly attributed to the change of high latitude seaways which strengthens the AMOC and transports more heat energy to high latitudes and also to the reduced ice sheets and the sea ice covers. However,the simulated warming in our model is weaker than other studies(Chandan and Peltier, 2017; Kamae et al., 2016).In our two core experiments, AMOC strengths increase remarkably (+4.7 Sv) in comparison with their related PI controls due to the closure of Bering strait and North Canadian Archipelago regions.This result is in agreement with other studies (Hu et al., 2015; Kamae et al., 2016), but the magnitude of the increase of the AMOC highly depends upon the processes included in the ocean models. The model response to the $pCO_2$ uncertainties (+-50ppmv based on the core simulation) is not symmetric. The increase of $pCO_2$ by 50 ppmv produces warming in the high latitudes (+0.7°C), but the decreasing of $pCO_2$ by 50ppmv leads to much stronger cooling in the high latitudes (-1.3°C). The increased snow fall in lower pCO2 experiment associated with stronger albedo is the major influence for this asymmetric pattern. Moreover, this cooling effect in the lowering pCO2 experiment is stronger than that produced by the enlarged ice sheets experiment. To conclude, further model intercomparisons and data-model comparisons are needed to better understand the role of new boundary conditions and the internal climatic processes in modeling the Pliocene warming climate.

The Plio-Pleistocene transition (3.0-2.5 Ma) is an important tipping point in the Earth climate associated with perennial ice sheets in the Northern high latitudes. It is well known that the NHG establishment around 2.7Ma is associated with the long-term decreasing trends of pCO2 and sea surface temperatures. Indeed, the PPT marks the beginning of a low pCO2 world with perennial ice sheets in both hemispheres, which is infrequent in Earth's history (Ramstein 2011), thereby creating specific geologic and climatic conditions allowing the development of glacial/interglacial cycles.The Greenland ice sheet (GrIS) evolution during this transition is difficult to reconstruct due to the paucity of direct geological data and its light delta O18 signal in benthic foraminifera.Our forward physically based approach, modelling the GrIS evolution during the PPT, shows that the long lasting paradigm which explained the huge GrIS extension occurring at 2.7 Ma by a minimum summer insolation at 65°N is, by far, too simple. All along the PPT period (3.0-2.5 Ma), the GrIS volume appears very sensitive to CO2 changes. Consequently, our

numerical experiments demonstrate that, to trigger and maintain GrIS during the whole period, CO2 pathways have to be confined in a narrow window. Moreover, we show that the GrIS evolution, simulated using the most recent pCO2 reconstruction (Martinez-Boti et al. 2015 mean estimate), is in good agreement with relevant IRD records. These records depict large variations of GrIS ice-sheet and indicate a continuous presence of a GrIS large enough to calve icebergs. This result emphasizes the crucial role of pCO2 pathways during PPT to maintain GrIS, which shapes the framework for the quaternary NH glacial-interglacial cycles. Moreover, this result is relevant in the context of future GrIS evolution due to different RCP pathways(IPCC AR5 WG1 (2013) ). Indeed, because of its small size and location, GrIS appears to be very sensitive to CO2 variations. In the future there is a strong need for both new marine records and more climate-ice sheet simulations to improve our understanding of the likely CO2 pathways during PPT.

In summary, this thesis brings new constraints and understanding on the cryosphere and climate interaction from mid-Pliocene to the Quaternary glaciation. Our results points out the necessity to further study the link between ocean dynamics, carbon cycle and climate.

## 6.2 Perspectives

### 6.2.1 Understanding the carbon cycle during the late Pliocene

As discussed before, the reconstructed pCO2 records for the late Pliocene ranged from 200 to 450 ppmv and have large uncertainties. The large variations of pCO2 might be a crucial factor of the climate variability of the late Pliocene. In the MIS M2 study, we have proved the important role of the large lowering of pCO2 in this short but evident glaciation. The Plio-Pleistocene transition is along with the decreasing trend of the pCO2. However, the mechanism underlying the large variations of pCO2 is still unknown for us. The focus on the carbon cycle and link between climate, tectonics,biological and surface processes is strongly needed. Actually there is already some projects aiming at resolving the carbon cycle puzzles for this period. For example, the project launched by Dr. Chamberlain in Standford university, to investigate the terrestrial climate history of the Earth focusing on periods of time in the past that had CO2-levels similar to the present and to future projections and addressing how the chemical weathering of the Earth's crust affects both

the long- and short-term carbon cycle (*https://biox.stanford.edu/about/people/affiliated-faculty/page-chamberlain-professor-environmental-earth-system-science-and*).

### 6.2.2 The relationship between high latitude orography and ocean circulation

In the PlioMIP2 study, we demonstrate a strong effect of the changed orography (closing Bering Strait, North Canadian Archipelago region) on the high latitudes ocean dynamics. Thus we observe an obviously intensified AMOC, which helps to transport more poleward energy and moisture. It is very important for understanding the high latitude warming amplification during the MPWP. Actually, the high latitude gateway changes gain more and more attention recent years, since they are considered to be an very important role for the Cenozoic and Pliocene climate evolution. However, the mechanism underlying the ocean dynamics is poorly understood. Apart from the closure of the Bering strait and North Canadian archipelago regions, the subsidence of Greenland Scotland Ridge (GSR), the exposed Barents Sea are also very important for the ocean circulations, which are included as one of the important objectives in the the Norwegian projects "Ocean Controls on high-latitude Climate sensitivity – a Pliocene case study (OCCP)". In this project, the primary objectives of the OCCP is to resolve the role of the Nordic Seas in determining climate conditions at high northern latitudes during a warmer than present climate state. New and high time-resolved marine proxy data are reconstructed in the Nordic regions and the reconstructions will be combined with results from model experiments designed to investigate the large-scale dynamics of the region. The model results will be used to identify key processes responsible for the observed high latitude climate of the Pliocene and the role of the Nordic Seas “gateway” between the North Atlantic and Arctic. This project will enable us to make substantial progress towards understanding the mechanisms behind the apparent high sensitivity of the Arctic in warm climates, the role of the Nordic Seas in the arctic amplification of Pliocene warming, and will ultimately help constrain the long-term sensitivity of the climate system in a warming world.

### 6.2.3 Low latitude climate systems during the warming Pliocene

This thesis work indeed focused more on the high latitude climate systems, since they are crucial to understand the relationship between climate and cryosphere. However, the low latitude climate systems like the monsoon system, the ENSO pattern, the Hardley circulation etc are very important for understanding the climate variability for the late Pliocene. More studies are strongly needed for understanding the changes of these climate processes in terms of model and data reconstructions. Moreover, the low latitude climate changes link tightly with the dispersal of the hominoids, which is an very interesting topic for recent years. The French project "Human Ancestors Dispersal: the role of Climate (HADoC)" are launched for exploring the relationship between the human ancestors dispersal and the climate change from the early Miocene to the early Pleistocene. This study is also involved in this project. Inferring from the records in the East African by the Paleontologists, the East African regions during the mid Pliocene are likely to be more humid relative to modern conditions. In our model, the simulated climate in the PlioMIP2 can represent a relatively humid environment in these regions. However, in the PlioMIP1 with the identical model, these regions are simulated representing more arid. Since the reconstructed topography are much higher in the East African than present levels. More sensitivity experiments are needed to explore the boundary conditions (topograhpy, vegetation..etc) impact on these regions. Moreover, the dynamics linking the low latitudes and high latitudes climate systems is also very important. As demonstrated by Defrance et al.,2017, strong relationship exists between ice sheet dynamics and tropical atmosphere redistribution of African monsoon in terms of amplitude and location. This mechanism and other fresh water input due to ice sheet instability clearly linked the dynamics of African tropical region of interest in this project to the evolution of northern hemisphere ice sheet at the transition Eocene-Pleistocene.

### 6.2.4 Model intercomparison for the MPWP simulations

For the MPWP studies, we only described the results with our IPSL model hence the results is likely model dependent. As it is the case in the frame of the PlioMIP projects, further model intercomparison work will be intensively conducted. This work is necessary for us to have a less-model-dependent conclusions and to well understand the climate processes during the warm climate as well as the impact of the boundary conditions and

forcing factors change. For example, Our model shows a strong sensitivity of ocean dynamics to the change of high latitude seaways in the MPWP simulations. But this result is not consistent with other models, like the studies of Chandan et al.,2016 and Hu et al.,2015, the change of ocean circulation in response to the modified high latitude seaways is less sensitive than ours. This difference is however expected since the simulated ocean dynamics like AMOC,NADW depends much upon the process and physiques in the ocean model. As shown in the Zhang et al.,2014, although models show consistency in simulating a similar to present AMOC strength in the PlioMP1, the simulated AMOC strength are different among each model, and the IPSL model likely simulate a weakest AMOC strength. Last but not least, all the simulations in the frame of PlioMIP are conducted with a relative rough resolution. When studying the regional climate,like the East African monsoon, a high resolution simulation is needed. Therefore, more efforts can be put into the down-scaling simulations for the future work.

# List of Figures

# List of Tables

# Publications

# Publications

**Tan, N.**, Ramstein, G., Dumas, C., Contoux, C., Ladant, J.-B., Sepulchre, P., Zhang, Z., De Schepper, S., 2017. Exploring the MIS M2 glaciation occurring during a warm and high atmospheric CO2 Pliocene background climate. *Earth Planet. Sci. Lett.* 472, 266-276. *https://doi.org/10.1016/j.epsl.2017.04.050*

**Tan, N.**, Ramstein, G., J-B.,Sepulchre, Dumas, C., Bachem,P. 2018: Modeling Greenland ice sheet evolution during the Plio-Pleistocene transition:new constraints for pCO2 evolution. *Nature Communications.* **Under Revision**

**Tan, N.**, Ramstein, G., Contoux, C., Dumas, C., Sun, Y., Sepulchre, P. 2018. Study on the MIS KM5c interglacial using two versions of IPSL coupled model. **In Prep.**

Zhang, Z., Yan, Q., Farmer, E.J., Li.C., Ramstein, G., Zhang, R., **Tan, N.,** Contoux, C., Dumas, C., Guo, C.C., 2017. Alternation of Northern Hemisphere ice sheet configurations during a glacial. **In prep**

Sun,Y., Ramstein,G., Laurent Z. X. Li, Zhou, T.,J., **Tan, N.,** Wang.Y.,S., Kageyama, M.,2017. Regional meridional cells governing the interannual variability of the Hadley circulation in boreal winter. *Clim, Dynam.* **Accepted**.

# Bibliography

Alley, R. B., Andrews, J., Brigham-Grette, J., Clarke, G., Cuffey, K., Fitzpatrick, J., Funder, S., Marshall, S., Miller, G., Mitrovica, J., Muhs, D., Otto-Bliesner, B., Polyak, L., White, J., 2010. History of the greenland ice sheet: paleoclimatic insights. Quaternary Science Reviews 29 (15), 1728 – 1756, special Theme: Arctic Palaeoclimate Synthesis (PP. 1674-1790).
URL http://www.sciencedirect.com/science/article/pii/S0277379110000399 89

Andrews, J. T., 2000. Icebergs and iceberg rafted detritus (IRD) in the North Atlantic: facts and assumptions. Oceanography 13, 100–108. 99

Bailey, I., Hole, G. M., Foster, G. L., Wilson, P. A., Storey, C. D., Trueman, C. N., Raymo, M. E., 2013. An alternative suggestion for the Pliocene onset of major northern hemisphere glaciation based on the geochemical provenance of North Atlantic Ocean ice-rafted debris. Quaternary Science Reviews 75. 5, 8, 99, 121

Barendregt, R. W., Duk-Rodkin, A., 2011. Chapter 32 - chronology and extent of late cenozoic ice sheets in north america: A magnetostratigraphical assessment 15, 419 – 426.
URL http://www.sciencedirect.com/science/article/pii/B9780444534477000325 4

Bartoli, G., Honisch, B., Zeebe, R. E., 2011. Atmospheric $CO_2$ decline during the Pliocene intensification of Northern Hemisphere glaciations. Paleoceanography 26 (4). 2, 4, 8, 22, 63, 86, 98, 121

Berger, A., Li, X. S., Loutre, M.-F., 1999. Modelling northern hemisphere ice volume over the last 3 Ma. Quaternary Science Reviews 18 (1), 1–11. 92

Braconnot, P., Otto-Bliesner, B., Harrison, S., Joussaume, S., Peterchmitt, J.-Y., Abe-Ouchi, A., Crucifix, M., Driesschaert, E., Fichefet, T., Hewitt, C. D., Kageyama, M., Kitoh, A., Laîné, A., Loutre, M.-F., Marti, O., Merkel, U., Ramstein, G., Valdes, P., Weber, S. L., Yu, Y., Zhao, Y., 2007. Results of pmip2 coupled simulations of the mid-holocene and last glacial maximum ndash; part 1: experiments and large-scale features. Climate of the Past 3 (2), 261–277.
URL https://www.clim-past.net/3/261/2007/ 14

Brierley, C. M., Fedorov, A. V., 2016. Comparing the impacts of Miocene–Pliocene changes in inter-ocean gateways on climate: Central American Seaway, Bering Strait, and Indonesia. Earth and Planetary Science Letters 444, 116–130.
URL http://linkinghub.elsevier.com/retrieve/pii/S0012821X16300978 5

Brierley, C. M., Fedorov, A. V., Liu, Z., Herbert, T. D., Lawrence, K. T., LaRiviere, J. P., 2009. Greatly expanded tropical warm pool and weakened hadley circulation in the early pliocene. Science 323 (5922), 1714–1718.
URL http://science.sciencemag.org/content/323/5922/1714 3

Brigham-Grette, J., Melles, M., Minyuk, P., Andreev, a., Tarasov, P., DeConto, R., Koenig, S., Nowaczyk, N., Wennrich, V., Rosen, P., Haltia, E., Cook, T., Gebhardt, C., Meyer-Jacob, C., Snyder, J., Herzschuh, U., 2013. Pliocene Warmth, Polar Amplification, and Stepped Pleistocene Cooling Recorded in NE Arctic Russia. Science 340 (2013), 1421–1427.
URL http://www.sciencemag.org/cgi/doi/10.1126/science.1233137 63, 86, 91

Cane, M. a., Molnar, P., 2001. Closing of the Indonesian seaway as a precursor to east African aridi ® cation around 3 ± 4 million years ago. Nature 411 (May), 157–162. 5

Chandan, D., Peltier, W. R., 2017. Regional and global climate for the mid-pliocene using the university of toronto version of ccsm4 and pliomip2 boundary conditions. Climate of the Past 13 (7), 919–942.
URL https://www.clim-past.net/13/919/2017/ 74, 116

Contoux, C., Dumas, C., Ramstein, G., Jost, A., Dolan, A. M., 2015a. Modelling Greenland ice sheet inception and sustainability during the Late Pliocene. Earth and Planetary Science Letters 424, 295–305. 5

Contoux, C., Dumas, C., Ramstein, G., Jost, A., Dolan, A. M., 2015b. Modelling Greenland ice sheet inception and sustainability during the Late Pliocene. Earth and Planetary Science Letters 424, 295–305.
URL http://dx.doi.org/10.1016/j.epsl.2015.05.018 92, 94

Contoux, C., Ramstein, G., Jost, A., 2012. Modelling the mid-pliocene warm period climate with the IPSL coupled model and its atmospheric component LMDZ5A. Geoscientific Model Development 5 (3), 903–917. 14, 16, 56, 64, 65, 66, 68

Corvec, S., Fletcher, C. G., 2017. Changes to the tropical circulation in the mid-pliocene and their implications for future climate. Climate of the Past 13 (2), 135–147.
URL https://www.clim-past.net/13/135/2017/ 56

Cravatte, S., Madec, G., Izumo, T., Menkès, C., Bozec, A., 2007. Progress in the 3-D circulation of the eastern equatorial Pacific in a climate ocean model. Ocean Modelling 17, 28–48.
URL http://www.documentation.ird.fr/hor/fdi:010037962 16

Cuffey, K. M., Marshall, S. J., apr 2000. Substantial contribution to sea-level rise during the last interglacial from the Greenland ice sheet. Nature 404, 591.
URL http://dx.doi.org/10.1038/35007053http://10.0.4.14/35007053 90

De Boer, B., de Wal, R. S. W., Bintanja, R., Lourens, L. J., Tuenter, E., 2010. Cenozoic global ice-volume and temperature simulations with 1-D ice-sheet models forced by benthic 18O records. Annals of Glaciology 51 (55), 23–33. 92

De Schepper, S., Gibbard, P. L., Salzmann, U., Ehlers, J., aug 2014. A global synthesis of the marine and terrestrial evidence for glaciation during the Pliocene Epoch. Earth-Science Reviews 135, 83–102.
URL http://linkinghub.elsevier.com/retrieve/pii/S0012825214000713 22

De Schepper, S., Groeneveld, J., Naafs, B. D. a., Van Renterghem, C., Hennissen, J., Head, M. J., Louwye, S., Fabian, K., jan 2013. Northern hemisphere glaciation during the globally warm early Late Pliocene. PloS one 8 (12), e81508.
URL http://www.pubmedcentral.nih.gov/articlerender.fcgi?artid=3861316{&}tool=pmcentrez{&}rendertype=abstract 4, 92

DeConto, R. M., Pollard, D., 2003. Rapid Cenozoic glaciation of Antarctica induced by declining atmospheric CO2. Nature 421 (6920), 245–249. 2, 93

DeConto, R. M., Pollard, D., Wilson, P. a., Pälike, H., Lear, C. H., Pagani, M., oct 2008. Thresholds for Cenozoic bipolar glaciation. Nature 455 (7213), 652–656.
URL http://www.nature.com/doifinder/10.1038/nature07337 92

Dekens, P. S., Christina, R. A., Mccarthy, M. D., 2007. Warm upwelling regions in the pliocene warm period. Paleoceanography 22 (3), –. 3

Dolan, A. M., Haywood, A. M., Hunter, S. J., Tindall, J. C., Dowsett, H. J., Hill, D. J., Pickering, S. J., 2015a. Modelling the enigmatic Late Pliocene Glacial Event - Marine Isotope Stage M2. Global and Planetary Change 128, 47–60.
URL http://linkinghub.elsevier.com/retrieve/pii/S0921818115000399 3, 89, 92

Dolan, A. M., Hunter, S. J., Hill, D. J., Haywood, A. M., Koenig, S. J., Otto-Bliesner, B. L., Abe-Ouchi, A., Bragg, F., Chan, W.-L., Chandler, M. A., Contoux, C., Jost, A., Kamae, Y., Lohmann, G., Lunt, D. J., Ramstein, G., Rosenbloom, N. A., Sohl, L., Stepanek, C., Ueda, H., Yan, Q., Zhang, Z., 2015b. Using results from the pliomip ensemble to investigate the greenland ice sheet during the mid-pliocene warm period. Climate of the Past 11 (3), 403–424.
URL https://www.clim-past.net/11/403/2015/ 22, 63, 89, 102

Dowsett, H., Dolan, A., Rowley, D., Pound, M., Salzmann, U., Robinson, M., Chandler, M., Foley, K., Haywood, A., 2016. The PRISM4 (mid-Piacenzian) palaeoenvironmental reconstruction. Climate of the Past Discussions 4 (March), 1–39.
URL http://www.clim-past-discuss.net/cp-2016-33/ 57, 60, 64, 66, 73, 115

Dowsett, H. J., Chandler, M. a., Robinson, M. M., jan 2009. Surface temperatures of the Mid-Pliocene North Atlantic Ocean: implications for future climate. Philosophical transactions. Series A, Mathematical, physical, and engineering sciences 367 (1886), 69–84.
URL http://www.ncbi.nlm.nih.gov/pubmed/18852090 3, 63, 72, 73

Dowsett, H. J., Foley, K. M., Stoll, D. K., Chandler, M. A., Sohl, L. E., Bentsen, M., Otto-Bliesner, B. L., Bragg, F. J., Chan, W.-L., Contoux, C., Dolan, A. M., Haywood, A. M.,

Jonas, J. A., Jost, A., Kamae, Y., Lohmann, G., Lunt, D. J., Nisancioglu, K. H., Abe-Ouchi, A., Ramstein, G., Riesselman, C. R., Robinson, M. M., Rosenbloom, N. A., Salzmann, U., Stepanek, C., Strother, S. L., Ueda, H., Yan, Q., Zhang, Z., jun 2013. Sea Surface Temperature of the mid-Piacenzian Ocean: A Data-Model Comparison. Scientific Reports 3, 2013.
URL http://dx.doi.org/10.1038/srep02013http://10.0.4.14/srep02013https://www.nature.com/articles/srep02013{#}supplementary-information 57, 59, 122

Dowsett, H. J., Robinson, M. M., Haywood, A. M., Hill, D. J., Dolan, A. M., Stoll, D. K., Chan, W.-L., Abe-Ouchi, A., Chandler, M. A., Rosenbloom, N. A., Otto-Bliesner, B. L., Bragg, F. J., Lunt, D. J., Foley, K. M., Riesselman, C. R., 2012. Assessing confidence in Pliocene sea surface temperatures to evaluate predictive models. Nature Clim. Change 2 (5), 365–371. 3, 22, 64

Ducoudré, N. I., Laval, K., Perrier, A., 1993. Sechiba, a new set of parameterizations of the hydrologic exchanges at the land- atmosphere interface within the lmd atmospheric general circulation model. J.Climate 6, 248–273. 16

Dufresne, J.-L., Foujols, M.-a., Denvil, S., Caubel, a., Marti, O., Aumont, O., Balkanski, Y., Bekki, S., Bellenger, H., Benshila, R., Bony, S., Bopp, L., Braconnot, P., Brockmann, P., Cadule, P., Cheruy, F., Codron, F., Cozic, a., Cugnet, D., Noblet, N., Duvel, J.-P., Ethé, C., Fairhead, L., Fichefet, T., Flavoni, S., Friedlingstein, P., Grandpeix, J.-Y., Guez, L., Guilyardi, E., Hauglustaine, D., Hourdin, F., Idelkadi, a., Ghattas, J., Joussaume, S., Kageyama, M., Krinner, G., Labetoulle, S., Lahellec, a., Lefebvre, M.-P., Lefevre, F., Levy, C., Li, Z. X., Lloyd, J., Lott, F., Madec, G., Mancip, M., Marchand, M., Masson, S., Meurdesoif, Y., Mignot, J., Musat, I., Parouty, S., Polcher, J., Rio, C., Schulz, M., Swingedouw, D., Szopa, S., Talandier, C., Terray, P., Viovy, N., Vuichard, N., feb 2013. Climate change projections using the IPSL-CM5 Earth System Model: from CMIP3 to CMIP5. Climate Dynamics 40, 2123–2165.
URL http://link.springer.com/10.1007/s00382-012-1636-1 14, 15, 17, 65, 93, 121

Dwyer, G. S., Chandler, M. a., 2008. Mid-Pliocene sea level and continental ice volume based on coupled benthic Mg/Ca palaeotemperatures and oxygen isotopes. Philo-

sophical transactions. Series A, Mathematical, physical, and engineering sciences 367 (1886), 157–168. 4

Dwyer, G. S., Chandler, M. A., 2009. Mid-pliocene sea level and continental ice volume based on coupled benthic mg/ca palaeotemperatures and oxygen isotopes. Philosophical Transactions of the Royal Society of London A: Mathematical, Physical and Engineering Sciences 367 (1886), 157–168.
URL http://rsta.royalsocietypublishing.org/content/367/1886/157 22

Fausto, R. S., Ahlstrøm, A. P., Van As, D., Bøggild, C. E., Johnsen, S. J., 2009. A new present-day temperature parameterization for Greenland. Journal of Glaciology 55 (189), 95–105. 18

Flesche Kleiven, H., Jansen, E., Fronval, T., Smith, T. M., 2002. Intensification of Northern Hemisphere glaciations in the circum Atlantic region (3.5-2.4 Ma) - Ice-rafted detritus evidence. Palaeogeography, Palaeoclimatology, Palaeoecology 184 (3-4), 213–223. 2, 4, 8, 86, 89, 91, 121

Groeneveld, J., Hathorne, E., Steinke, S., DeBey, H., Mackensen, a., Tiedemann, R., oct 2014. Glacial induced closure of the Panamanian Gateway during Marine Isotope Stages (MIS) 95–100 (<mml:math altimg="si1.gif" overflow="scroll" xmlns:xocs="http://www.elsevier.com/xml/xocs/dtd" xmlns:xs="http://www.w3.org/2001/XMLSchema" xmlns:xsi="http://www.w. Earth and Planetary Science Letters 404, 296–306.
URL http://linkinghub.elsevier.com/retrieve/pii/S0012821X14005056 27, 28, 121

Haug, G. H., Tiedemann, R., 1998. Effect of the formation of the Isthmus of Panama on Atlantic Ocean thermohaline circulation. Nature 393 (6686), 673–676.
URL http://dx.doi.org/10.1038/31447{%}5Cnhttp://www.nature.com/nature/journal/v393/n6686/abs/393673a0.html{%}5Cnhttp://www.nature.com/doifinder/10.1038/31447 5, 25, 28

Haywood, A. M., Dolan, A. M., Pickering, S. J., Dowsett, H. J., McClymont, E. L., Prescott, C. L., Salzmann, U., Hill, D. J., Hunter, S. J., Lunt, D. J., Pope, J. O., Valdes, P. J., 2013. On the identification of a Pliocene time slice for data-model comparison. Philosophical

transactions. Series A, Mathematical, physical, and engineering sciences 371 (2001). 56, 64

Haywood, A. M., Dowsett, H. J., Dolan, A. M., 2016. Integrating geological archives and climate models for the mid-Pliocene warm period. Nature Communications 7 (May 2015), 10646.
URL http://www.nature.com/doifinder/10.1038/ncomms10646 22, 55, 58, 64, 92, 122

Haywood, a. M., Dowsett, H. J., Dolan, a. M., Rowley, D., Abe-Ouchi, a., Otto-Bliesner, B., Chandler, M. a., Hunter, S. J., Lunt, D. J., Pound, M., Salzmann, U., 2015. Pliocene Model Intercomparison (PlioMIP) Phase 2: scientific objectives and experimental design. Climate of the Past Discussions 11, 4003–4038.
URL http://www.clim-past-discuss.net/11/4003/2015/ 57, 60, 61, 64, 65, 66, 92, 122

Haywood, a. M., Dowsett, H. J., Otto-Bliesner, B., Chandler, M. a., Dolan, a. M., Hill, D. J., Lunt, D. J., Robinson, M. M., Rosenbloom, N., Salzmann, U., Sohl, L. E., mar 2010. Pliocene Model Intercomparison Project (PlioMIP): experimental design and boundary conditions (Experiment 1). Geoscientific Model Development 3 (1), 227–242.
URL http://www.geosci-model-dev.net/3/227/2010/ 3

Haywood, A. M., Valdes, P. J., 2004. Modelling pliocene warmth: contribution of atmosphere, oceans and cryosphere. Earth Planetary Science Letters 218 (3), 363–377. 2, 3

Heinrich, H., 1988. Origin and consequences of cyclic ice rafting in the northeast atlantic ocean during the past 130,000 years. Quaternary research 2 (29), 142–152. 99

Heinrich, H., Lotti, R., 1995. ceberg discharges into the north atlantic on millennial time scales during the last glaciation. Science-AAAS-Weekly Paper Edition 5200 (267), 1005–1009. 99

Herbert, T. D., Peterson, L. C., Lawrence, K. T., Liu, Z., 2010. Tropical Ocean Temperatures Over the Past 3.5 Million Years. Science 328 (June), 1530–1535. 86, 91

Hill, D. J., 2009. Modelling earth's cryosphere during pliocene warm peak. Ph.D.thesis,University of Bristol, United Kingdom, 368. 3, 63, 92

Hodell, D. A., Channell, J. E. T., Curtis, J. H., Romero, O. E., Röhl, U., 2018. Onset of "hudson strait" heinrich events in the eastern north atlantic at the end of the middle pleistocene transition (640 ka)? Paleoceanography and Paleoclimatology 23 (4).
URL https://agupubs.onlinelibrary.wiley.com/doi/abs/10.1029/2008PA001591 111

Hourdin, F., Foujols, M.-A., Codron, F., Guemas, V., Dufresne, J.-L., Bony, S., Denvil, S., Guez, L., Lott, F., Ghattas, J., Braconnot, P., Marti, O., Meurdesoif, Y., Bopp, L., May 2013. Impact of the lmdz atmospheric grid configuration on the climate and sensitivity of the ipsl-cm5a coupled model. Climate Dynamics 40 (9), 2167–2192.
URL https://doi.org/10.1007/s00382-012-1411-3 15

Hourdin, F., Musat, I., Bony, S., Braconnot, P., Codron, F., Dufresne, J.-L., Fairhead, L., Filiberti, M.-A., Friedlingstein, P., Grandpeix, J.-Y., Krinner, G., LeVan, P., Li, Z.-X., Lott, F., 2006. The LMDZ4 general circulation model: climate performance and sensitivity to parametrized physics with emphasis on tropical convection. Climate Dynamics 27 (7), 787–813.
URL http://dx.doi.org/10.1007/s00382-006-0158-0 15

Howell, F. W., Haywood, A. M., Otto-Bliesner, B. L., Bragg, F., Chan, W.-L., Chandler, M. A., Contoux, C., Kamae, Y., Abe-Ouchi, A., Rosenbloom, N. A., Stepanek, C., Zhang, Z., 2016. Arctic sea ice in the pliomip ensemble. Clim. Past 12, 749–767. 3

Hu, A., Meehl, G. A., Han, W., Otto-Bliestner, B., Abe-Ouchi, A., Rosenbloom, N., 2015. Effects of the bering strait closure on amoc and global climate under different background climates. Progress in Oceanography 132, 174 – 196, oceanography of the Arctic and North Atlantic Basins.
URL http://www.sciencedirect.com/science/article/pii/S0079661114000172 74, 116

Jansen, E., Fronval, T., Rack, F., Channell, J. E. T., 2000. Pliocene-pleistocene ice rafting history and cyclicity in the nordic seas during the last 3.5 myr. Paleoceanography 15 (6), 709–721.
URL http://dx.doi.org/10.1029/1999PA000435 8, 86, 89, 91, 121

Jansen, E., Sjøholm, J., 1991. Reconstruction of glaciation over the past 6 Myr from ice-borne deposits in the Norwegian Sea. Nature 349 (6310), 600–603.

URL http://www.scopus.com/inward/record.url?eid=2-s2.0-0025585221{&}partnerID=tZOtx3y1 8, 92, 121

Jost, A., Fauquette, S., Kageyama, M., Krinner, G., Ramstein, G., Suc, J.-P., Violette, S., 2009. High resolution climate and vegetation simulations of the late pliocene, a model-data comparison over western europe and the mediterranean region. Climate of the Past 5 (4), 585–606.
URL https://www.clim-past.net/5/585/2009/ 16

Jouzel, J., Masson-Delmotte, V., Cattani, O., Dreyfus, G., Falourd, S., Hoffmann, G., Minster, B., Nouet, J., Barnola, J. M., Chappellaz, J., Fischer, H., Gallet, J. C., Johnsen, S., Leuenberger, M., Loulergue, L., Luethi, D., Oerter, H., Parrenin, F., Raisbeck, G., Raynaud, D., Schilt, a., Schwander, J., Selmo, E., Souchez, R., Spahni, R., Stauffer, B., Steffensen, J. P., Stenni, B., Stocker, T. F., Tison, J. L., Werner, M., Wolff, E. W., aug 2007. Orbital and millennial Antarctic climate variability over the past 800,000 years. Science (New York, N.Y.) 317 (5839), 793–6.
URL http://www.ncbi.nlm.nih.gov/pubmed/17615306 88, 123

Kageyama, M., Braconnot, P., Bopp, L., Caubel, A., Foujols, M.-A., Guilyardi, E., Khodri, M., Lloyd, J., Lombard, F., Mariotti, V., Marti, O., Roy, T., Woillez, M.-N., 2013. Mid-Holocene and Last Glacial Maximum climate simulations with the IPSL model—part I: comparing IPSL_CM5A to IPSL_CM4. Climate Dynamics 40 (9), 2447–2468.
URL http://dx.doi.org/10.1007/s00382-012-1488-8 14, 65

Kamae, Y., Yoshida, K., Ueda, H., 2016. Sensitivity of pliocene climate simulations in mri-cgcm2.3 to respective boundary conditions. Climate of the Past 12 (8), 1619–1634.
URL https://www.clim-past.net/12/1619/2016/ 74, 116

Kasahara, A., 1977. Computational aspects of numerical models for weather prediction and climate simulation, in: Methods in com- putational physics,. Journal of the Atmospheric Science, 173–197. 15

KEIGWIN, L., jul 1982. Isotopic Paleoceanography of the Caribbean and East Pacific: Role of Panama Uplift in Late Neogene Time. Science 217 (4557), 350–353.
URL http://science.sciencemag.org/content/217/4557/350.abstract 5, 25

Knies, J., Matthiessen, J., Vogt, C., Sverre, J., Hjelstuen, B. O., Smelror, M., Larsen, E., Andreassen, K., Eidvin, T., Vorren, T. O., 2009. The Plio-Pleistocene glaciation of the Barents Sea – Svalbard region : a new model based on revised chronostratigraphy. Quaternary Science Reviews, 1–18.
URL http://dx.doi.org/10.1016/j.quascirev.2008.12.002 4

Koenig, S. J., DeConto, R. M., Pollard, D., 2011. Late Pliocene to Pleistocene sensitivity of the Greenland Ice Sheet in response to external forcing and internal feedbacks. Climate Dynamics 37, 1247–1268. 97

Koenig, S. J., Dolan, A. M., de Boer, B., Stone, E. J., Hill, D. J., DeConto, R. M., Abe-Ouchi, A., Lunt, D. J., Pollard, D., Quiquet, A., Saito, F., Savage, J., van de Wal, R., 2015. Ice sheet model dependency of the simulated greenland ice sheet in the mid-pliocene. Climate of the Past 11 (3), 369–381.
URL https://www.clim-past.net/11/369/2015/ 63, 89, 92

Krinner, G., Viovy, N., de Noblet-Ducoudre, N., Ogee, J., Polcher, J.and Friedlingstein, F., Ciais, P., Sitch, S., Prentice, I. C., 2005. A dynamic global vegetation model for studies of the coupled atmosphere-biosphere system. Global Biogeochem. Cy. 19 (GB1015). 16

Ladant, J.-B., Donnadieu, Y., Lefebvre, V., Dumas, C., aug 2014. The respective role of atmospheric carbon dioxide and orbital parameters on ice sheet evolution at the Eocene-Oligocene transition. Paleoceanography 29 (8), 810–823.
URL http://doi.wiley.com/10.1002/2013PA002593 2, 90, 93

Larsen, H. C., Saunders, A. D., Clift, P. D., Wei, W., 1994. Seven Million Years of Glaciation in Greenland. Science 264, 952–955. 86, 89, 92

Laskar, J., Robutel, P., Joutel, F., Gastineau, M., Correia, a. C. M., Levrard, B., dec 2004. A long-term numerical solution for the insolation quantities oftheEarth. Astronomy and Astrophysics 428 (1), 261–285.
URL http://www.edpsciences.org/10.1051/0004-6361:20041335 8, 9, 55, 86, 94, 121, 122

Lawrence, K. T., Herbert, T. D., Brown, C. M., Raymo, M. E., Haywood, A. M., 2009. High-amplitude variations in north atlantic sea surface temperature during the early pliocene warm period. Paleoceanography 24 (2), 1–15. 2, 5, 86, 91, 100

Lévy, M., Estublier, A., Madec, G., 2001. Choice of an advection scheme for biogeochemical models. Geophysical Research Letters 28 (19), 3725–3728.
URL http://dx.doi.org/10.1029/2001GL012947 16

Lisiecki, L. E., Raymo, M. E., mar 2005. A Pliocene-Pleistocene stack of 57 globally distributed benthic δ 18 O records. Paleoceanography 20 (1), n/a–n/a.
URL http://doi.wiley.com/10.1029/2004PA001071 2, 4, 5, 8, 55, 88, 91, 121, 122, 123

Lunt, D. J., Foster, G. L., Haywood, A. M., Stone, E. J., 2008. Late Pliocene Greenland glaciation controlled by a decline in atmospheric CO2 levels. Nature 454 (August), 1102–5.
URL http://www.ncbi.nlm.nih.gov/pubmed/18756254 3, 5, 86, 92

Lunt, D. J., Haywood, A. M., Schmidt, G. A., Salzmann, U., Valdes, P. J., Dowsett, H. J., 2010. Earth system sensitivity inferred from pliocene modelling and data. Nature Geoscience 3 (1), 60–64. 3

MacAyeal, D. R., 1989. Large-scale ice flow over a viscous basal sediment: Theory and application to ice stream B, Antarctica. 18

Madec, G., 2008. Technical note, ipsl, available at: http://www.nemo-ocean.eu/about-nemo/reference-manuals, nemo book v3 4.pdf. NEMO book. 16

Madec, G., Imbard, M., 1996. A global ocean mesh to overcome the North Pole singularity. Climate Dynamics 12 (6), 381–388. 16

Martínez-Botí, M. a., Foster, G. L., Chalk, T. B., Rohling, E. J., Sexton, P. F., Lunt, D. J., Pancost, R. D., Badger, M. P. S., Schmidt, D. N., 2015. Plio-Pleistocene climate sensitivity evaluated using high-resolution CO2 records. Nature 518, 49–54.
URL http://dx.doi.org/10.1038/nature14145 2, 4, 8, 22, 63, 86, 98, 121

Maslin, M. a., Li, X. S., Loutre, M. F., Berger, a., 1998. The contribution of orbital forcing to the progressive intensification of Northern Hemisphere glaciation. Quaternary Science Reviews 17 (97), 411–426. 2, 5, 86, 91

Miller, K. G., Wright, J. D., Browning, J. V., Kulpecz, A., Kominz, M., Naish, T. R., Cramer, B. S., Rosenthal, Y., Peltier, W. R., Sosdian, S., 2012. High tide of the warm pliocene: Implications of global sea level for antarctic deglaciation. Geology 40 (5), 407.
URL +http://dx.doi.org/10.1130/G32869.1 2, 3, 4, 22, 63, 89

Molnar, P., jun 2008. Closing of the Central American Seaway and the Ice Age: A critical review. Paleoceanography 23 (2), n/a–n/a.
URL http://doi.wiley.com/10.1029/2007PA001574 25

Moran, K., Backman, J., Brinkhuis, H., Clemens, S. C., Cronin, T., Dickens, G. R., Eynaud, F., Gattacceca, J., Jakobsson, M., Jordan, R. W., 2006. The cenozoic palaeoenvironment of the arctic ocean. Nature 441 (7093), 601–5. 4

Morland, L. W., 1984. Thermomechanical balances of ice sheet flows. Geophysical & Astrophysical Fluid Dynamics 29 (1-4), 237–266.
URL http://dx.doi.org/10.1080/03091928408248191{%}5Cnhttp://www.tandfonline.com/doi/abs/10.1080/03091928408248191 18

Morlighem, M., Williams, C. N., Rignot, E., An, L., Arndt, J. E., Bamber, J. L., Catania, G., Chauché, N., Dowdeswell, J. A., Dorschel, B., Fenty, I., Hogan, K., Howat, I., Hubbard, A., Jakobsson, M., Jordan, T. M., Kjeldsen, K. K., Millan, R., Mayer, L., Mouginot, J., Noël, B. P. Y., O'Cofaigh, C., Palmer, S., Rysgaard, S., Seroussi, H., Siegert, M. J., Slabon, P., Straneo, F., van den Broeke, M. R., Weinrebe, W., Wood, M., Zinglersen, K. B., 2017. Bedmachine v3: Complete bed topography and ocean bathymetry mapping of greenland from multibeam echo sounding combined with mass conservation. Geophysical Research Letters 44 (21), 11,051–11,061.
URL https://agupubs.onlinelibrary.wiley.com/doi/abs/10.1002/2017GL074954 89

Mudelsee, M., Raymo, M. E., 2005. Slow dynamics of the Northern Hemisphere glaciation. Paleoceanography 20. 5, 91, 92

Naafs, B. D. A., Stein, R., Hefter, J., Khélifi, N., De Schepper, S., Haug, G. H., 2010. Late Pliocene changes in the North Atlantic Current. Earth and Planetary Science Letters 298 (3-4), 434–442. 100

Naish, T. R., Wilson, G. S., 2009. Constraints on the amplitude of Mid-Pliocene (3.6-2.4Ma) eustatic sea-level fluctuations from the New Zealand shallow-marine sediment record. Philosophical transactions. Series A, Mathematical, physical, and engineering sciences 367 (1886), 169–87.
URL http://www.ncbi.nlm.nih.gov/pubmed/18852088 3, 4, 22

Pagani, M., Liu, Z., LaRiviere, J., Ravelo, A. C., 2010. High Earth-system climate sensitivity determined from Pliocene carbon dioxide concentrations. Nature Geoscience 3 (1), 27–30.
URL http://dx.doi.org/10.1038/ngeo724 4, 22, 63

Pagani, M., Zachos, J., Freeman, K., Tripple, B., Bohaty, S., 2005. Marked decline in Atmospheric Carbon Dioxide Concentrations during the Paleocene. Science 309 (5734), 600–603. 2

Passchier, S., 2011. Linkages between east antarctic ice sheet extent and southern ocean temperatures based on a pliocene highresolution record of icerafted debris off prydz bay, east antarctica. Paleoceanography 26 (4), –. 4

Petit, R. J., Raynaud, D., Basile, I., Chappellaz, J., Ritz, C., Delmotte, M., Legrand, M., Lorius, C., Pe, L., 1999. Climate and atmospheric history of the past 420,000 years from the Vostok ice core, Antarctica. Nature 399, 429–413. 14

Peyaud, V., Ritz, C., Krinner, G., 2007. Modelling the Early Weichselian Eurasian Ice Sheets: role of ice shelves and influence of ice-dammed lakes. Climate of the Past Discussions 3 (1), 221–247. 18

Pollard, D., DeConto, R. M., 2009. Modelling West Antarctic ice sheet growth and collapse through the past five million years. Nature 458 (7236), 329–332.
URL http://dx.doi.org/10.1038/nature07809 3, 93

Pound, M., Tindall, J., Pickering, S., Haywood, A., Dowsett, H., Salzmann, U., 2014. Late pliocene lakes and soils: a global data set for the analysis of climate feedbacks in a warmer world. Climate of the Past 10 (1), 167–180. 64

Ramstein, G., 2011. Climates of the earth and cryosphere evolution. Earth's Cryosphere and Sea Level Change, Surveys in Geophysics 32 (issue 4), 329–350. 91

Raymo, M. E., 1991. Geochemical evidence supporting t. c. chamberlin's theory of glaciation. Geology 19 (4), 344. 5

Ritz, C., Rommelaere, V., Dumas, C., 2001. Modeling the evolution of Antarctic ice sheet over the last 420,000 years: Implications for altitude changes in the Vostok region. Journal of Geophysical Research 106, 31943. 18, 93

Ruddiman, W. F., Raymo, M. E., Lamb, H. H., Andrews, J. T., 1988. Northern hemisphere climate regimes during the past 3 ma: Possible tectonic connections [and discussion]. Philosophical Transactions of the Royal Society B Biological Sciences 318 (318), 429–430. 5

Rybczynski, N., Gosse, J. C., Harington, C. R., Wogelius, R. A., Hidy, A. J., Buckley, M., 2013. Mid-pliocene warm-period deposits in the high arctic yield insight into camel evolution. Nature communications 4, 1550. 63

Sadourny, R., Laval, K., 1984. January and july performance of the lmd general circulation model, in: New perspectives in climate modeling. edited by: Berger, A. and Nicolis, C., Elsevier, Amsterdam, 173–197. 15

Salzmann, U., Haywood, A. M., Lunt, D. J., Valdes, P. J., Hill, D. J., 2008. A new global biome reconstruction and data-model comparison for the Middle Pliocene. Global Ecology and Biogeography 17 (3), 432–447. 3, 16, 22, 63, 97

Salzmann, U., Williams, M., Haywood, A. M., Johnson, A. L. A., Kender, S., Zalasiewicz, J., 2011. Climate and environment of a Pliocene warm world. Palaeogeography, Palaeoclimatology, Palaeoecology 309 (1-2), 1–8.
URL http://dx.doi.org/10.1016/j.palaeo.2011.05.044 57

Sarnthein, M., Prange, M., Schmittner, a., Schneider, B., Weinelt, M., 2009a. Mid-Pliocene shifts in ocean overturning circulation and the onset of Quaternary-style climates*. Climate of the Past Discussions 5 (1), 251–285. 4, 8, 121

Sarnthein, M., Prange, M., Schmittner, a., Schneider, B., Weinelt, M., 2009b. Mid-Pliocene shifts in ocean overturning circulation and the onset of Quaternary-style climates*. Climate of the Past Discussions 5, 251–285. 99

Seki, O., Foster, G. L., Schmidt, D. N., Mackensen, A., Kawamura, K., Pancost, R. D., 2010. Alkenone and boron-based Pliocene pCO2 records. Earth and Planetary Science Letters 292 (1-2), 201–211. 2, 4, 8, 22, 63, 86, 98, 121

Sitch, S., Smith, B., Prentice, C., Arneth, A., Bondeau, A., Cramer, W., Kaplan, J. O., Levis, S., Lucht, W., Sykes, M. T., Thonicke, K., 2003. Evaluation of ecosystem dynamics, plant geography and terrestrial carbon cycling in the lpj dynamic vegetation model. Glob. Change Biol. 9, 161–185. 16

Stap, L. B., van de Wal, R. S. W., de Boer, B., Bintanja, R., Lourens, L. J., 2017. The influence of ice sheets on temperature during the past 38 million years inferred from a one-dimensional ice sheet–climate model. Climate of the Past 13 (9), 1243–1257.
URL https://www.clim-past.net/13/1243/2017/ 8, 92, 121

Tan, N., Ramstein, G., Dumas, C., Contoux, C., Ladant, J.-B., Sepulchre, P., Zhang, Z., De Schepper, S., 2017. Exploring the MIS M2 glaciation occurring during a warm and high atmospheric CO 2 Pliocene background climate. Earth and Planetary Science Letters. 89, 92

Thiede, J., Jessen, C., Knutz, P., Kuijpers, A., Mikkelsen, N., Nørgaard-Pedersen, N., Spielhagen, R. F., 2011. Million years of Greenland Ice Sheet history recorded in ocean sediments. Polarforschung 80 (3), 141–149. 92

Treut, H. L., Somerville, R., Cubasch, U., 2007. 2007: Historical overview of climate change. Oecd Org 45 (4), XXXVII–XXXVIII. 10, 121

Valcke, S., 2006. OASIS3 user guide (prism 2-5). PRISM-Support Initiative Report No 3 (3), 64. 16

Van De Wal, R. S. W., De Boer, B., Lourens, L. J., Köhler, P., Bintanja, R., 2011. Reconstruction of a continuous high-resolution CO 2 record over the past 20 million years. Climate of the Past 7 (Milankovitch 1941), 1459–1469. 8, 121

Venti, N. L., Billups, K., Herbert, T. D., 2013. Increased sensitivity of the plio-pleistocene northwest pacific to obliquity forcing. Earth and Planetary Science Letters 384, 121–131.
URL https://doi.org/10.1016/j.epsl.2013.10.007 86, 91

Willeit, M., Ganopolski, A., Calov, R., Robinson, A., Maslin, M., 2015. The role of CO2 decline for the onset of Northern Hemisphere glaciation. Quaternary Science Reviews 119, 22–34. 90, 92

Wright, J. D., Miller, K. G., 1996. Control of north atlantic deep water circulation by the greenland-scotland ridge. Paleoceanography 11 (2), 157–170. 5

Zachos, J., Pagani, M., Sloan, L., Thomas, E., Billups, K., 2001. Trends, rhythms, and aberrations in global climate 65 Ma to present. Science 292 (5517), 686–693.

URL http://www.ncbi.nlm.nih.gov/pubmed/11326091{%}5Cn{%}3CGotoISI{%}3E://000168478300041 2

Zhang, Z.-S., Nisancioglu, K. H., Chandler, M. a., Haywood, a. M., Otto-Bliesner, B. L., Ramstein, G., Stepanek, C., Abe-Ouchi, a., Chan, W.-L., Bragg, F. J., Contoux, C., Dolan, a. M., Hill, D. J., Jost, a., Kamae, Y., Lohmann, G., Lunt, D. J., Rosenbloom, N. a., Sohl, L. E., Ueda, H., jul 2013. Mid-pliocene Atlantic Meridional Overturning Circulation not unlike modern. Climate of the Past 9 (4), 1495–1504.
URL http://www.clim-past.net/9/1495/2013/ 3, 56, 64

Áslaug Geirsdóttir, 2011. Chapter 16 - pliocene and pleistocene glaciations of iceland: A brief overview of the glacial history 15, 199 – 210.
URL http://www.sciencedirect.com/science/article/pii/B9780444534477000167 4